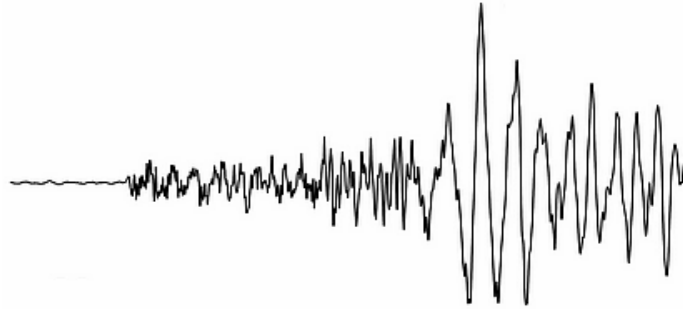# Earthquake analysis
# of quay walls

- Seismic analysis -

Date
11 July 2011

Author
J.W. Liang

Master Programme
Civil Engineering and Geo Sciences,
Specialisation Hydraulic Structures

Graduation Committee

Prof.drs.ir. J.K. Vrijling	Delft University of Technology
Prof.Ir. A.C.W.M. Vrouwenvelder	Delft University of Technology
Dr.ir. J.G. de Gijt	TU Delft / Public Works Rotterdam
Ir. W.J.M. Peperkamp	Delft University of Technology
Ir. A.A. Roubos	Public Works Rotterdam

TUDelft

Delft University of Technology

Gemeentewerken
Gemeente Rotterdam

Preface

This thesis is part of the Hydraulic Engineering MSc program at the faculty of Civil Engineering and Geosciences of the Technical University of Delft (TUD). It has been performed in cooperation and under the supervision of Engineering Department Public Works of Rotterdam (IGWR). The subject of this thesis deals with analysing the behaviour of different types of quay wall structures during earthquakes at the Euromax terminal situated on port of Rotterdam.

I would like to thank all the members of my graduation committee for their critical advice, guidance and advices. Especially Dr.Ir.J.G. de Gijt and Ir. A.A. Roubos.

I also would like to thank all the colleagues at Public Works Rotterdam who helped me and gave me their support during my thesis work, special thanks to Mr. Brassinga and Miss. Oung.

Furthermore, i would like to thank Dennis Grotegoed, Trude maas, Job Kool, Paolo Gatta and Axel Booij for their company during the breaks and the interesting discussions we have had.

Finally I want to thank my family and friends and especially my parents for their support.

Rotterdam, june 2011,

Jaw Wah Liang

TUDelft
Delft University of Technology

Earthquake analysis of quay walls
- Seismic Analysis-

Gemeentewerken
Gemeente Rotterdam

Table of contents

TUDelft
Delft University of Technology

Earthquake analysis of quay walls
- Seismic Analysis-

Gemeentewerken
Gemeente Rotterdam

Summary

In the life cycle of port structures, devastation by an earthquake might be a rare event. However, once it occurs, the magnitude of the consequences might be so large that the effects of earthquakes can be a major issue of national interest. The vulnerability of port waterfront structures to seismic ground motions of moderate intensity has been demonstrated during numerous recent earthquakes around the world. In most cases the damage to quay walls was manifested to limited deformations, as opposed to catastrophic failures or the collapse of structures. Although these permanent deformations are often repairable, the economic loss sustained by the ports due to trade interruption during repair and reconstruction is commonly viewed as unacceptable by many port authorities.

In this thesis the impact of an earthquake on quay walls located at the Euromax terminal of the Port of Rotterdam is analyzed. A quay wall is a soil retaining structure where ships can moore and transfer goods. Seismic behaviour of two different types of quay walls are investigated and compared by performing a seismic analysis on the Euromax terminal. The first quay wall is the existing quay wall of the Euromax terminal which is a diaphragm quay wall with relieving structure as shown in Figure 1. To make a good comparison a disapproved preliminary caisson quay wall design (see figure 2) is used which is based on the same requirements and boundary conditions as the diaphragm quay wall. The seismic analysis is based on three steps which will include assessment of the regional seismicity, the geologic hazards and soil-structure interaction analysis.
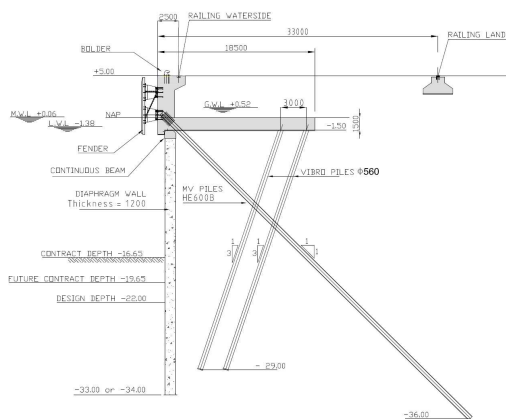
Figure 1 Cross- section diaphragm quay wall
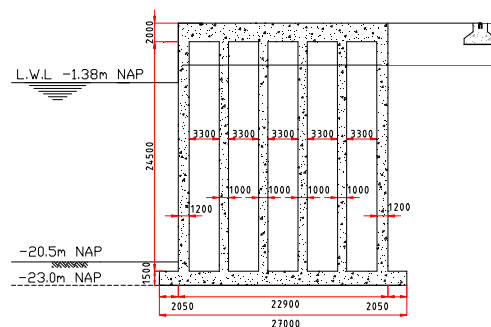
Figure 2 Cross- section caisson quay wall

The first step is to define the earthquake motion and its magnitude for the Euromax terminal. This is done by making a seismic hazard analysis which is based on geologic, tectonic and historical seismicity data available for the Netherlands. The major faults are located in the south-eastern of Netherlands. Therefore, majority of earthquakes in the Netherlands have been observed near this location. For the Euromax terminal which is located at south-western Netherlands, no earthquake has been observed. The probability of occurrence of a high earthquake magnitude at the Euromax terminal is very low due to the fact that no major faults are located near the terminal.

The second step is to define the dynamic soil response of the Euromax terminal. This is accomplished by making a liquefaction analysis to determine the liquefaction resistance of the near surface soils and the associated potential for ground failure. The Euromax terminal is located on a reclaimed area of the Port of Rotterdam which indicates that the soil deposit is young. This will increases the susceptibility to liquefaction because younger soil deposits are generally more susceptible to liquefaction than older deposits. Besides the age of the soil deposit, soil liquefaction is also influenced by its state. The tendency of a soil to contract or densify under cyclic loading condition is influenced by both density and effective stress. Loose soils are much more susceptible to liquefaction than dense soils. The soil deposit at the eastern side of the terminal consists of several layers of loose sand which made this the most sensitive section to liquefaction. Liquefaction at this location occurs at earthquake magnitude of $M_W = 6,2$ which corresponds with a horizontal peak ground acceleration of $a_H = 3$ m/s^2 and a return period of 751000 years.

The final step is to make a seismic analysis of the quay wall structure including seismic forces acting on the two different quay walls. A literature study shows that once an earthquake hits the Euromax terminal causing the ground to shake may result in three major disadvantageous consequences for a quay wall structure. First the driving forces acting on the quay wall will increase. Secondly, shear resistance may decrease due to excess pore water generation resulting in softening of the soil and resonance may develop when the earthquake frequency reaches the fundamental frequency of the structure. The three consequences may result in strength, stability and displacement failure of a quay wall structure.

The seismic behaviour of the quay walls are determined with two different methods which is the pseudo static approach and a finite element method. The pseudo static approach is using the Mononobe-Okabe method and the Westergaard solution to determine dynamic earth and water pressures respectively. It is proven that this approach is not capable to determine the seismic behaviours of the quay wall because no accurate displacements and stresses of the quay wall could be determined. On the contrary, the finite element method gives more reliable seismic behaviours of quay walls because the program that is used has a dynamic module which incorporated earthquakes. Based on the results achieved from the finite element calculation three typical failure mechanisms for each quay wall type are analyzed. It appeared that the critical failure mechanism of the diaphragm quay wall is caused by the insufficient bending capacity of the diaphragm wall resulting in breaking of the diaphragm wall. For the caisson quay wall the critical situation relates to large deformations of the landside crane track causing the cranes not to function properly. Both failure mechanisms are triggered around the same order of earthquake magnitude which is a local magnitude of $M_L \approx 5,1$ with a return period of approximate 2500 years.

Over all it can be concluded that the probability of occurrence of high magnitude earthquakes are very low. When an earthquake does strike the Euromax terminal the diaphragm quay walls and a caisson quay walls fail in a different way. Nevertheless, both failure mechanisms occur at the same order of earthquake magnitude. This indicates that both quay walls have the same order of resistance against earthquake. However, the consequences of the diaphragm quay wall failure and probably also for the combined walls will be much higher compared to that of the caisson. Seismic failure of the diaphragm quay wall will always result in a total destruction of the quay wall while seismic failure of the caisson quay wall can be repaired. For this reason, the caisson quay wall is a better solution against earthquakes compared to the diaphragm wall.

List of symbols

α	slope inclination [degree]
α_{pfl}	angle of the planar failure surface respect to horizontal [degree]
β	inclination of back of wall to vertical [degrees]
$\dfrac{1}{\beta}$	Length of equivalent fixity wall below ground [m]
γ_{dry}	Volumetric weight of dry soil [kN/m^3]
$\gamma_{eff,1}$	effective volumetric weight of soil with excess pore pressure [kN/m^3]
γ_{w}	Volumic weight of water [kN/m^3]
γ_{wet}	Volumetric weight of saturated soil [kN/m^3]
$\gamma_{0.7}$	Shear strain at 72% of the reference shear modulus at very small strains [-]
δ	Wall friction angle [degree]
ε	Strain (of the soil) [percentage]
φ	Internal friction angle [degree]
ω_{max}	Maximum reinforcement rario [-]
ω_{min}	Minimum reinforcement rario [-]
σ'_{vo}	Vertical effective stress [kPa]
σ_{vo}	Vertical total stress [kPa]
ϑ_{2}	angle of displacement [degree]
ψ	Dilatancy angle [degree]
ψ_{1}	seismic inertia angle with excess pore pressure [degree]
v	Poisson ratio [-]
A	Cross sectional area [m^2]
a_{H}, a_{max}, a_{pga}	peak horizontal ground acceleration [m/s^2]
c	Cohesion [kPa]
CPT	Cone penetration test [-]
CRR	Cyclic resistance ratio [-]
CRR$_{7.5}$	Cyclic resistance ratio for a 7.5 magnitude earthquake [-]
CSR	Cyclic stress ratio [-]
e	Void ratio [-]
E	Young's modulus for linear elastic material [kPa]
EI	Flexural rigidity wall [in kNm^2]
E$_{50}$	Young's modulus at 50 % of failure load [kPa]
E$_{ur}$	Unloading-reloading stiffness [kPa]
F	Force acting on wall [kN]
F	Normalized friction ratio [percentage]
f$_{caisson}$	Horizontal fundamental frequency of caisson [Hz]
f$_{n}$	Fundamental frequency [Hz]

TUDelft
Delft University of Technology

Earthquake analysis of quay walls
- Seismic Analysis-

Gemeentewerken
Gemeente Rotterdam

f_s	Sleeve friction [kPa]
F_{pre}	Prestressing force in anchor strands [kN]
FS	Factor of safety [-]
g	acceleration due to gravity [m/s^2]
G	Shear modulus of soil [kPa]
G_0^{ref}	Shear modulus at very small strains at a reference pressure of 100 kPa [kPa]
h	water depth [m]
h_{total}	total depth of the pool of water [m]
I_p	Plasticity index [percentage]
k	stiffness of the spring [N/m]
K_c	Correction factor that is a function of grain characteristics of the soil [-]
K_{dw}	Stiffness of diaphragm wall [N/m]
k_h	Seismic coefficient of horizontal acceleration [m/s^2]
k_v	Seismic coefficient of vertical acceleleration [m/s^2]
k_1	Modulus of subgrade reaction between 0 and 50% mobilisation [kN/m^2]
k_2	Modulus of subgrade reaction between 50 and 80% mobilisation [kN/m^2]
k_3	Modulus of subgrade reaction between 80 and 100% mobilisation [kN/m^2]
k_0	Lateral earth pressure ratio at rest [-]
k_a	Lateral earth pressure ratio at active yielding [-]
k_{ae}	Seismic lateral earth pressure ratio at active yielding [-]
$K_{caisson}$	Stiffness of caisson [N/m]
K_{mv}	Stiffness of MV pile [N/m]
k_p	Lateral earth pressure ratio at passive yielding [-]
k_{pe}	Seismic lateral earth pressure ratio at passive yielding [-]
k_{sub}	Coefficient of subgrade reaction [MPa/m]
K_{dw}	Stiffness of vibro pile [N/m]
$LF_{hydrostatic}$	Equivalent heavy fluid hydrostatic pressure [kN]
$LF_{hydrodynamic}$	Equivalent heavy fluid hydrodynamic pressure [kN]
l_{anchor}	Length of the anchor strands [m]
I_c	Soil behavior type index [-]
I_{MM}	Modified Mercalli intensity [-]
I_0	the maximum observed epicentral intensity of an earthquake [-]
$l_{spacing}$	Center to center distance of the anchors [m]
m	mass of system [in kN/m]
M	Moment acting on wall [kNm]
M_L	Local magnitude [-]
M_s	Surface wave magnitude [-]
MSF	Magnitude scaling factor [-]
M_b	Body wave magnitude [-]
M_o	Seismic moment [-]

M_w	Moment magnitude [-]
N	the annual number of events with magnitude equal to or larger than M_L [-]
P	Earth pressure thrust [kN]
P_L	Probability of liquefaction [-]
p^{ref}	Reference pressure for stiffness parameters, usually 100 kPa [kPa]
p_{wd}	hydrodynamic pressure distribution [kN]
q	Surcharge load [kN/m2]
Q	Normalized CPT penetration resistance
q_c	Cone resistance [MPa]
q_{c1N}	Normalized CPT penetration resistance [MPa]
$(q_{c1N})_{cs}$	Clean sand normalized cone penetration resistance [MPa]
q_v	Tip resistance [kPa]
r	Factor depending on the type of retaining structure [-]
r_d	Shear stress reduction factor [-]
Re	Relative density [percentage]
R_{inter}	Reduction parameter for the strength in the interface [-]
S	Soil factor [-]
u_{anchor}	Horizontal displacement at the center of the anchor wall [mm]
U_{dyn}	Resultant hydrodynamic thrust [kN]
$U_{stat,back}$	Steady state pore water pressure force [kN]
$U_{stat,sea,front}$	Hydrostatic water pressure [kN]
$U_{stat,ground,front}$	Steady state pore water pressure force [in kN]
$U_{dyn,sea,front}$	Hydrodynamic water pressure force [kN]
$U_{dyn,ground,}$	Hydrodynamic water pressure force of the pore water [kN]
$U_{dyn,epwp}$	Excess pore water pressure [kN]
W	Mass of the sliding wedge [kg]
w_2	Displacement [in m]

TUDelft
Delft University of Technology

Earthquake analysis of quay walls
- Seismic Analysis-

Gemeentewerken
Gemeente Rotterdam

1. Introduction

1.1 General introduction

Since the dawn of history people have been fascinated by the possibility of travelling on water. Driven by the desire for conquest or economic gain, the explorers and traders sailed the world's seas to extend their opportunities. In places where their ships could moor, villages and towns grew up. Mooring places grew up into quays and developed into seaports and trading places. These seaports have served as a crucial economic lifeline by bringing goods and services to people around the world for centuries. Today, seaports remain a critical component of the nation's economy. Not only do seaports deliver goods to consumers and export products overseas, they create millions of jobs. They serve as the gateway to national and international trade, connecting large and small businesses to the global market. The Port of Rotterdam is one of these seaports and the largest logistic and industrial hubs of Europe (see figure 1-1). It is located at the city Rotterdam, in the south-west of the Netherlands. With an annual throughput of 430 million tons of cargo in 2010, Rotterdam has the largest seaport of Europe and forms a gateway to the European market for more than 500 million consumers. To become and stay a world leading seaport an expansion of harbour territory was needed for the Port of Rotterdam. This was done by reclaiming land of the North Sea. Due to the increase in shipping the Port of Rotterdam had to be repeatedly deepened and the port area moved further seaward as shown in figure 1-1.

Figure 1-1 Port of Rotterdam [www.portofrotterdam.nl]

In the design of the new reclaimed harbour area and port infrastructure (quay walls), dimensions of ships play an important role. The last decennia the dimensions, consequently the load capacity of the ships, have increased dramatically. This affects the water depth in front of the quay wall, length of the berths and width of the port basins. Most recent build port infrastructures in the Netherlands/Rotterdam were not designed to resist seismic loadings due to the fact that earthquake were seldom recorded in the past. Therefore, earthquake was assumed not to occur or too small to do any harm to port structures. Only at places where high risks are involved, seismic design was performed. This assumption is not totally correct because there is always a chance in occurrence of earthquake with a random magnitude. This random magnitude is attended with consequential damage. This consequential damage also depends on the adjacent port infrastructure. Therefore, good insight in the behaviour of port structures during earthquake is needed to determine whether seismic loading should be included during the design or not.

In foreign countries located at seismic regions, where earthquakes occur more frequently and with a higher magnitude compared to the Netherlands, seismic designing needs to be performed according to their national standards. The vulnerability of port waterfront structures to seismic ground motions of moderate intensity has been demonstrated during numerous recent earthquakes around the world. In most cases the damage to quay walls was manifested to limited deformations, as opposed to catastrophic failures or the collapse of structures. Although these permanent deformations are often repairable, the economic loss sustained by the ports due to trade interruption during repair and reconstruction is commonly viewed as unacceptable by many port authorities.

An example is a severe port damage of the Kobe port located in Japan. This historical event shows us that earthquakes can cause a seaport stop operating resulting in billions of euros damage. During the Hyogoken Nanmbu earthquake in Japan 1995, an earthquake with a local (Richters) magnitude of 7,2 hit Kobe port. This earthquake caused severe damage and destroyed more than 90% of the waterfront structures (see Figure 1-2). The displacements of the quay walls during the earthquake were among the largest recorded in the history of port facilities in Japan. Maximum seaward movement of the wall

recorded was 5 meters and the maximum tilting recorded was 4 degrees towards sea. About the same order of magnitude of settlement was induced in the soil backfill behind the walls due to strong earthquake motion. During and after this earthquake, Kobe port stopped operating and reparations were needed. Besides the loss of income, the port suffered a direct loss of €4.3 billion and an indirect loss of €4.7 billion for only the first year. After this event, Kobe port couldn't become the port as it was ones before.

Knowing the impact of earthquakes and the major influence the Port of Rotterdam has to the local and/or worldwide economy, insight into the behaviour of port structure during earthquake is recommended. New visions can be obtained concerning the measures needs to be taken if earthquakes do occur. This thesis can also contribute to constructive considerations during the design of a quay wall structure.

Figure 1-2 Kobe Port immediately after being struck by the hyogoken Nanbu Earthquake in 1995 [www.pari.go.jp]

1.2 Problem description

No insights and research into the probability of occurrence of earthquakes at the Port of Rotterdam and the consequence of these earthquakes to the seaport infrastructure are presented yet at this moment. Therefore the consequences for the seaport trade caused by earthquakes are still vague.

Knowing the impact an earthquake can cause (Kobe port 1995), insight into the seismic behaviour of existing Euromax quay is interesting to know. Especially to a world seaport like Port of Rotterdam, were the port is a critical component of the nation's economy.

1.3 Research questions

The main question throughout this report is:

How do different types of quay wall structures at the Euromax terminal (maasvlakte) behave during high magnitude earthquakes?

At first, some sub-questions should be formulated in order to be able to answer the main question:

a) What is the probability of occurrence of an earthquake at the Maasvlakte?
b) What are the effects of an earthquake to a quay wall in general?
c) Which earthquake magnitude will cause the current Euromax quay wall (diaphragm wall) to fail and what is the failure mechanism?
d) How will a gravity quay wall behave at the Euromax terminal to earthquakes?

1.4 Main objective

The main objective of this master thesis is to gain insight in the behaviour and failure mechanisms of different types of quay wall structures near the Euromax Terminal during earthquakes.

Based on results of the above mentioned studies, perhaps a conclusion can be made which type of quay wall structure at the Euromax terminal is the least sensitive too earthquakes. Maybe an answer can be found whether is makes sense to include earthquake analysis into the designing of port structures for the Port of Rotterdam.

TUDelft
Delft University of Technology

Earthquake analysis of quay walls
- Seismic Analysis-

Gemeentewerken
Gemeente Rotterdam

1.5 Layout of this report

First an introduction to the Port of Rotterdam, the Euromax terminal and its quay wall will be presented. Hereafter an overview of requirement, boundary conditions and assumptions that were made during this thesis is given. From these requirements and assumptions the normative earthquake acceleration can be determined which probably cause the Euromax quay wall to fail.

General information about triggering, wave propagation and measurement of earthquakes are given in chapter 4. This background knowledge can be used to get a better understanding of the phenomena earthquake and its ground motion.

In chapter 5 many different types of quay wall designs are presented, followed up by the seismic effect on these quay walls. Also some failure mechanisms due earthquake in general will be presented in this chapter.

To investigate the behaviour of the Euromax quay wall during earthquake, a seismic analysis will be preformed. This will be based on three steps which will include assessment of the regional seismicity, the geologic hazards and soil-structure interaction analysis.

1. The first step is to define the earthquake motion and its magnitude by making a seismic hazard analysis which is based on geologic, tectonic and historical seismicity data available for the Netherlands (chapter 6).
2. The second step is determining the dynamic soil response. This has been accomplished by making a liquefaction analysis to determine the liquefaction resistance of the near surface soils and the associated potential for ground failure (chapter 7).
3. The third step is to make a seismic analysis of the quay wall structure including seismic forces on the quay wall. This was done for 2 different types of quay wall: diaphragm quay wall (chapter 8), Caisson quay wall (chapter 9).

Finally the conclusions of this thesis will be presented and recommendations will be given.

2. The Port of Rotterdam

2.1 Generally about the port

The Port of Rotterdam is the biggest sea port in Europe. The total area of the port is 10.556 hectares out of which 5.299 hectares are infrastructure and area of water and 5.257 hectares is industrial part. It has got a long but short territory as shown in Figure 1-1. The length of the port is about 40 km and it is linked to the Rhine River. Direct connection with the most industrial areas of Western Europe (Rhineland and the Ruhr) was made through the Rhine River and the Meuse river. Due to this, different terminals are situated on the banks of the Rhine River and the coast of the North Sea. The depth of water in the port enables navigation for bulk carriers and container ships (Post Panamax and Super Post Panamax) which transport containers from/to Asia and America [2.1].

The first part of the port was built in the city centre of Rotterdam. The port has expanded from the city centre to the coast of the North Sea due to the increase of transfer of cargo and the size of the vessels. Most of containers which come to/from the Port of Rotterdam are transferred in Maasvlakte 1. This part of the port was built in the 1960s by reclaiming land from the North Sea through dykes and sand filling. In the 1980s Europe Container Terminal (ECT) started to build terminals at the Maasvlakte 1. There are three container terminals build at the Maasvlakte 1: Euromax, APM terminal Rotterdam and ECT. Nowadays the Port of Rotterdam is reaching its limit and has not got enough free area for its expanding where new terminals could be built. In September 2008 the construction of a new part of the port Maasvlakte 2 (see Figure 2-1) started to carry out next to Maasvlakte 1. A new artificial peninsula has been built so far by reclaiming the land from the North Sea. The total area of this peninsula is 2,000 hectares which will increase the land of the port by 20%. By extending the Yangtzehaven situated at Maasvlakte 1, an entrance has been created to the Maasvlakte 2 (see Figure 2-1). There will be container terminals for a new generation of container ships, areas for chemical industry and distribution. Expectations are that the first container terminal at the Maasvlakte 2 will be opened in 2013 and reaching it full occupancy as late as 2033 [2.2].
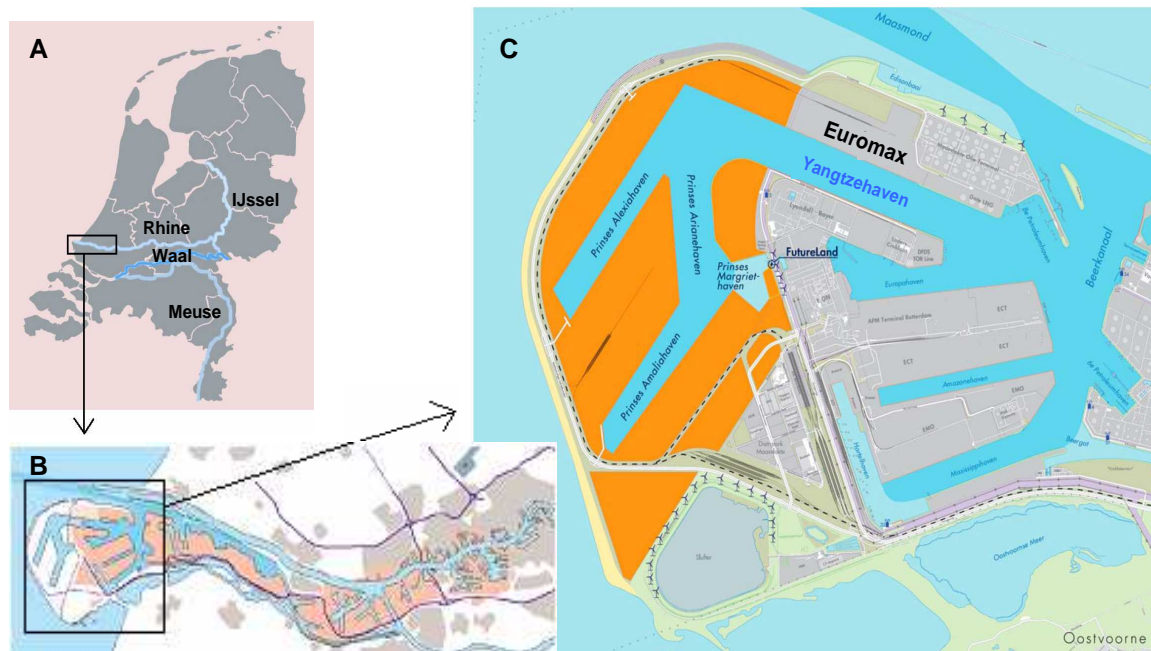

Figure 2-1 A: Map of the Netherlands and some rivers
      B: Port of Rotterdam
      C: Maasvlakte 1 (grey), Maasvlakte 2 (orange) and the Euromax terminal

2.2 Euromax terminal

The Euromax Terminal in the Port of Rotterdam is a high sophisticated container handling centre. High performance, flexibility, safety, efficiency and low costs are all key criteria in relation to the terminal's design, construction and operations. The terminal has a capacity of 5 million TEU (Twenty-foot equivalent unit, standardized dimensions of container). Goal of the Euromax Terminal is to be capable of handling ultra large vessels 24 hours a day and without any restriction. It is situated at the north-westerly corner of the Maasvlakte 1 next to the oil terminal, just around the corner from the entrance to the Port of Rotterdam, see Figure 2-1 . The terminal lie against the Yangtzehaven, which in the future will function as the entrance and exit of the new reclaimed port area called Maasvlakte 2. From the North Sea, container vessels can be moored at the new container terminal and shipping traffic is not hampered by any restrictions whatsoever. With its depth of 16.65 metres, the Yangtzehaven can easily accommodate even the largest fully laden container vessels. However, the terminal was made for vessels capable of carrying 12.500 TEU (Southhampton++/ suezmax class). Transhipments of these containers are taken place by transport over road, rail and water. Quay wall structures were build to make these large vessels to berth in a save way. With a quay length of 1980 metres, the quay wall is accommodated with 23 cranes in total to make the transhipment as fast as possible [2.3].

Commissioned by the Port of Rotterdam the new terminal has been build in favor of P&O/Nedlloyd-ECT. Public Works Rotterdam made a feasibility study for various alternatives. Subsequently the Euromax quay wall was set in the market as a Design & Construct project. The design of BAM, a Dutch contractor, was chosen and the quay wall is constructed with a diaphragm wall.

2.3 Euromax quay wall

Quay walls (earth retaining structures) where built to make sure that container vessels can easily berth and tranship their goods. They are equipped with bollards to provide mooring and fendering systems to absorb the impacts of the vessels. Cranes or other heavy equipment that moves alongside the ship makes sure that transhipment of goods will be as fast and as save as possible.

For the quay wall a diaphragm wall with a relieving platform, tension piles and bearing piles was chosen as shown in Figure 2-2 [2.5]. This design obtained the highest score in risk management, quality management, maintenance and innovation based on the review done by Engineering Department Public Works of Rotterdam [2.4]. It is innovative due to the fact that a quay with diaphragm wall was never built before in the Port of Rotterdam. The diaphragm wall of the Euromax Terminal, which at some places goes 34 meters into the ground, have been designed with a further deepening of the port to 19.65 meters in mind. With the bed protection in mind, the design depth becomes NAP – 22m. The mean sea water level is located at NAP + 0,06m and the surface level behind the quay is located at NAP + 5m. The ground water level is controlled by a drainage system and is located at NAP + 0,52m.

The quay wall has to withstand many external forces acting on the structure. These forces are shown in Apendix E. Forces caused by the rail-mounted cranes are being supported by crane foundations. For the chosen design, the waterside crane rail is situated at the relieving platform above the diaphragm wall, hence the foundation of the waterside crane rail is integrated with the quay wall structure. For the landside crane rail an independent foundation (continuous reinforced beam) was used as shown in Figure 2-2 .

The quay wall consists of several quay elements (Figure 2-2). Most important ones are listed below:

- Relieving platform: concrete superstructure on top of the foundation which will reduce the horizontal force on the diaphragm wall. Vertical forces on top of the superstructure will be directly transferred to the deeper soil layers by the bearing elements as axial forces.
- Diaphragm wall: soil retaining wall made from reinforced concrete with a thickness of 1,2 meters. In some section it reaches a depth of NAP – 34 m.
- MV pile: tensile piles formed by introducing a layer of grout around the steel pile during the driving process with the aid of a floor plate or tray welded onto the point of the pile. These tension piles have a HE600B profile, centre to centre distance of 5,6 metres and reach a depth of NAP – 36 m. The MV pile is fixed to the relieving platform with an angle 1:1.

TUDelft
Delft University of Technology

Earthquake analysis of quay walls
- Seismic Analysis-

Gemeentewerken
Gemeente Rotterdam

- Vibro pile: Concrete reinforced bearing piles which are cast in place by driving steel tubular piles through the sand strata and pulled back when reinforcement and concrete are placed. These bearing piles have a diameter of 0,56 metres, centre to centre distance of 2,8 metres and reach a depth of NAP – 29 m. These piles are fixed to the relieving platform with an angle of 1:3.

- Continuous beam: On top of the diaphragm wall a continuous beam made of concrete was placed to support the upper structure. The relieving platform is simply supported to the continuous beam with rubber supporting strips in between. These strips ensure a good contact between the two elements and prevent collision damage between the two elements.

- Landside beam: A beam was placed behind the relieving structure to support the cranes moving alongside the quays. Railings where placed on top of these beams. Bearing capacity of the soil strata underneath the beam is sufficient enough to absorb the forces on the beam. Therefore no piles where needed to support this beam.
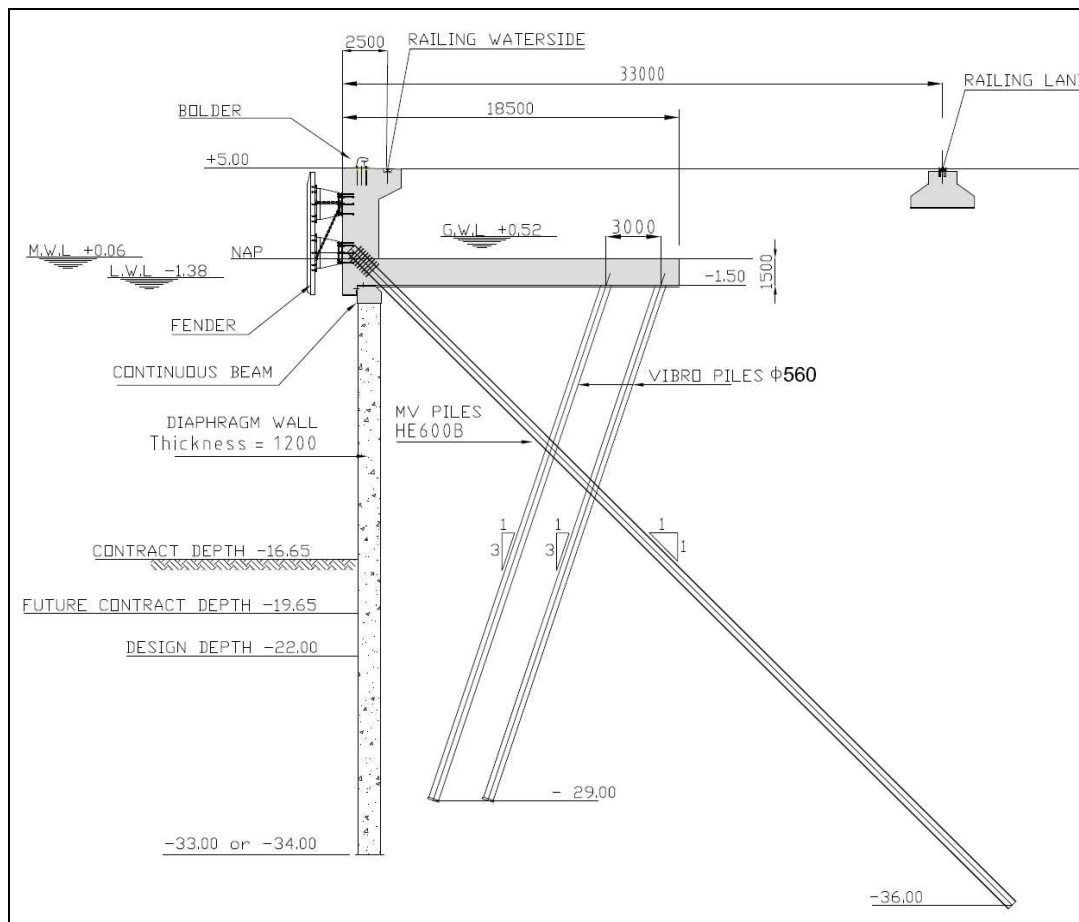
Figure 2-2 Quay wall design Euromax Terminal: Relieving platform with diaphragm wall, tension and bearing piles

2.4 References

[2.1]   www.portofrotterdam.com , 06-2010
[2.2]   www.maasvlakte2.com , 06-2010
[2.3]   www.ect.nl , 06-2010
[2.4]   Gemeentewerken Rotterdam, Kadeconstructie Euromax - Beoordelingsrapportage t.b.v. design & construct en optioneel maintenance contract, 12-2004
[2.5]   BAM, Tekening nummer O-T-004, "Kadeconstructie Euromax ", 06-2005

TUDelft
Delft University of Technology

Earthquake analysis of quay walls
- Seismic Analysis-

Gemeentewerken
Gemeente Rotterdam

3. Boundary conditions, Requirements and Assumptions

3.1 Introduction

Under the Authority of the Port of Rotterdam a list of requirements and boundary conditions is composed. It shows an overview of all aspects which have to be taken into account for the engineering of the quay wall in the Euromax Terminal. It involves boundary conditions which are imposed by the surroundings and requirements from the Port of Rotterdam. The overview presented in this chapter is composed with help of the List of Requirements by Public Works Rotterdam [3.1]. An overview of some important assumptions that were made during this thesis is followed up thereafter.

3.2 Boundary conditions

3.2.1 Hydraulic boundary conditions

Water levels are not given in the report with the List of requirements [3.1]. They have to be determined by the contractor that designs and builds the quay wall. This depends on the seawater level and the drainage system they use behind the quay wall. Wave impact is negligible for this type of structure since it is located inside the port protected by flood defenses.

3.2.2 Geotechnical boundary conditions

Geotechnical research is executed by the engineering department of Public Works of Rotterdam, IGWR (Ingenieursbureau Gemeentewerken Rotterdam). For orientation many cone penetration tests have been done at the location of the Euromax quay wall. BAM has used these cone penetration tests to determine the soil profile of the Euromax quay wall. This results in many different soil profiles, because the quay wall has a length of 1955 m. Out of this, 14 different soil profiles which represent the total quay length of 1955 m was determined [3.2] which will be used in this master thesis. Appendix A shows an overview of these soil profiles.

3.3 Requirements

3.3.1 Technical requirements

- Technical lifetime: 50 years
- Concrete cover: 50 mm for concrete above soil
  100 mm for concrete in the soil
- Front of quay wall must be a vertical, flat wall from NAP +5,00 m to NAP -2,00 m. Over the length it may vary with jumps in favor of fender structures.

3.3.2 Loads

- Between front of quay wall and crane rail on landside: 40 kN/m^2
- Outside waterfront cargo handling area behind crane rail landside: 60 kN/m^2
- Traffic loads: Traffic class 60
- Mooring loads: 2400 kN per bollard horizontal and normal to the quay wall. Bollard couples c.t.c. distance 15,00 m, c.t.c. bollards 2,70 m
- Toggles: 300 kN per toggle
  c.t.c. distance 15,00 m at NAP +1,90 m
- Crane loads: See section 3.3.7

3.3.3 Retaining requirements

- Total length quay wall: 1900 m
- Contract depth: NAP -16,65 m
- Future depth: NAP -19,65 m
- Construction depth: NAP -22,00 m
- Top of structure: NAP +5,00 m

3.3.4 Nautical requirements

- Sea vessel: Southhamptons ++ class   12.500 TEU
  Length (overall):   382,0 m
  Width: 57,0 m
  Draught: 17,0 m
  Water displacement: 215.000 metric tons
  Mooring angle: 5°
  Mooring velocity: 0,15 m/s
- Inland vessel: Length: 220,0 m
  Mooring angle: 15°
  Mooring velocity: 0,25 m/s

3.3.5 Berthing facilities

- Fenders maximum center to center distance: 15,0 m
- Safety factor mooring energy: 1,5

3.3.6 Crane details

- Container crane on 2,5 m from the waterside
- C.t.c. distance of crane tracks: 30,48 m
- C.t.c. distance wheelbases: 17,25 m
- 8 wheels per leg, c.t.c. 1,05 m, so crane loads acts on 7x1,05=7,35 m
- Distance between buffer: 27,20 m
- Average operational wind speed: 25 m/s
- Maximum allowable displacement deviations between crane railing normal to quay wall:
  Vertical: 80 mm
  Horizontal: 60 mm for contract depth NAP -16,65 m
  80 mm for future contract depth NAP -22,0 m

3.3.7 Crane loads

	Per wheel [kN]	Load on corner [kN]	Load per m [kN/m]
Landside in operation	2.500	20.000	2.721
Waterside in operation	2.000	16.000	2.177
Landside during storm	2.000	16.000	2.177
Waterside during storm	1.400	11.200	1.524
Tie-down load during storm	1.700 per lash		

Table 3-1: Representative vertical loads of crane

	Per wheel [kN]	Load on corner [kN]	Load per m [kN/m]
Landside in operation	45	350	48
Waterside in operation	45	350	48
Landside during storm	170	1350	184
Waterside during storm	170	1350	184

Table 3-2: Representative horizontal load of crane, normal to the crane rail

	Per wheel [kN]	Load on corner [kN]	Load per m [kN/m]
Landside in operation	35	280	38
Waterside in operation	50	400	54
Landside during storm	187.5	1500	204
Waterside during storm	187.5	1500	204

Table 3-3: Representative horizontal load of crane, parallel to the crane rail

TUDelft
Delft University of Technology

Earthquake analysis of quay walls
- Seismic Analysis-

Gemeentewerken
Gemeente Rotterdam

3.4 Assumptions

The important assumptions that are made during this thesis are given in this section. They will follow the order to the chapters in the thesis.

3.4.1 Seismic hazard analysis

Empirical relations are used to determine the earthquake parameters like magnitude, acceleration and return period. However, these relations are only valid for the south-eastern part of the Netherlands. No specific research on earthquake parameters relations has been performed near the Euromax terminal due to the few earthquake observations. Based on the seismic zoning map created by de Crook (1996) a relation is assumed between the earthquake parameters at the Euromax terminal and the south east of the Netherlands. The assumed relation has a ratio of 4,55. This means that the horizontal peak ground acceleration at south eastern part of the Netherlands is 4,55 times higher than that of the Euromax terminal.

During this analysis another assumption is made, that is that the maximum observed epicentral intensity of an earthquake is located at the Euromax terminal itself ($I_0 = I_{MM}$). This means that the epicenter of the earthquake is located at the Euromax terminal. This assumption is very conservative because the farther the epicenter from the quay wall the less impact the earthquake will have on the quay wall. Due to the lack of information about the surrounding soil profile, the propagation and epicenter of the earthquake have made it is very difficult to determine the relation between I_0 and I_{MM}.

3.4.2 Liquefaction analysis

Methods based on measurements of in situ soil strength and observations of field performance in previous earthquakes are used to predict the probability of liquefaction of the soil strata located at the Euromax Terminal. Assumed during this analysis was that liquefaction will occur if the probability of liquefaction is equal or higher than 0,6. Influences of liquefiable layers to each other are not included in this analysis. Assumed was that a liquefiable layer will not trigger other layers to liquefy at an earlier stage. This assumption is not totally correct because a frictional material like sand will get influenced by their surrounding. This assumption was taken due to the state of the art of this phenomenon.

3.4.3 Cross sections

The existing Euromax quay wall with a total quay length of 1955 meters is analyzed during this thesis. As a representative cross section for the entire quay wall, the first 100 meters of the east section is used (denoted in this thesis as section 1) since here it was determined that the soil profile is the most suitable for occurrence of liquefaction. The occurrence of liquefaction will have adverse consequences on the quay wall which is mentioned in section 5.4.1.

3.4.4 Seismic Loads

Pseudo static analysis was performed to get a first impression how the quay wall will react on seismic loadings. Assumptions that are made to determine these seismic forces are given below.

Seismic coefficient
For the purpose of the pseudo static analysis, the seismic action is represented by a set of horizontal and vertical static forces equal to the product of the gravity forces and a seismic coefficient. Due to the absence of seismic studies near the project location, the horizontal and vertical seismic coefficients (k_h and k_v) affecting all the masses shall be taken according to the Eurocode 8 [3.3]. No national annex for this Eurocode is available for the Netherlands because of the few earthquakes that occur and the low seismicity of the earthquakes. Therefore, a response spectrum with a soil factor of 1.35 was adopted as recommended by the Eurocode 8. This results in a $k_h=0,067$ and $k_v=0,022$ for an earthquake acceleration of 0,5 m/s^2.

Dynamic earth pressure

Dynamic earth pressures in a pseudo static approach caused by an earthquake are determined using the Mononobe-Okabe method. This method is an extension of the Coulomb sliding wedge theory taking into account horizontal and vertical inertial forces acting on the soil. The following assumptions are made during the determination of the dynamic earth pressure using the Mononobe-Okabe method.

- The structure is free to yield sufficiently to enable full soil strength or active pressure conditions to be mobilized. In reality the ground will not always yield freely which make this a conservative assumption.
- Planar failure surface is assumed, which only approximates the actual curved slip surface.

Dynamic water pressure

Under free pore water conditions, the dynamic water pressure results from the dynamic response of a body of water is assumed to be 70% of the free standing water which can be determined using Westergaard's solution. This amount of percentage is also suggested by Matsuo and Ohara (1965).

Excess pore water pressure generation

Development of excess pore water during earthquake shaking can be determined making use of cyclic triaxial testing. However, this kind of testing is not available and therefore assumptions are made. Knowing that excess pore pressure is not able to develop in very dense and clayey soils, it is assumed that excess pore water generation will only occur at loose sand layers. The development from no excess pore pressure to full liquefaction is assumed linear.

3.4.5 Failure mechanisms

Three possible mechanisms that could cause the diaphragm quay wall to fail are analyzed, which is diaphragm wall failure, MV-pile failure and displacement failure of the crane railings. Based on the observations from the past, these three failure mechanisms are assumed to be normative and therefore no other failure mechanisms are checked.

Just like the diaphragm wall three assumed normative failure mechanism are checked for the caisson quay wall: Wall failure, Stability failure (sliding overturning) and displacement failure of crane railings.

3.5 References

[3.1] Public Works Rotterdam, Project code HH1169, "Programma van Eisen", Version as-built, 2007
[3.2] Delta Marine Consultants bv, Rapport nummer O-R-013, "Kadeconstructie:ontwerpbasis", 06-2005
[3.3] Eurocede 8

TUDelft
Delft University of Technology

Earthquake analysis of quay walls
- Seismic Analysis-

Gemeentewerken
Gemeente Rotterdam

4. Earthquake ground motion

4.1 General introduction

The basic data of earthquake engineering are the recordings of ground accelerations during earthquakes. Knowledge of the ground motion is essential to an understanding of the earthquake behaviour of structures. Recorded ground motions contain valuable characteristics and information that are used directly, or indirectly, in seismic analysis and design. Parameters such as peak ground motion values (acceleration, velocity and displacement), measures of the frequency content of the ground motion, duration of strong shaking and various intensity measures play important roles in seismic evaluation of existing structures and design of new systems.

This chapter presents general information about earthquakes and some background information about some seismic ground motion properties.

4.2 Earthquakes in general

Earthquake is a sudden movements/shaking of the ground. It can cause massive damage and destruction to structures. There are many types of earthquakes occurring in the soil body. The type of earthquake depends on the location where it occurs and the geological conditions. They can be divided in the following types:

- Tectonic earthquakes; occur due to tectonic plates of the earth crust moving along each other
- Volcanic earthquakes; occur due to volcanic activity
- Collapse earthquakes; occur due to the collapse of mines and caverns
- Explosion earthquakes; occur due to explosion of chemical and nuclear devices

The most common earthquake around the world is the tectonic earthquake. In comparison with the other earthquake types, tectonic earthquakes have relatively a higher magnitude and a longer duration. That's why tectonic earthquakes are the most important earthquakes when building in the underground. This chapter will only explain the phenomena tectonic earthquake because the other earthquake types don't occur near the Euromax terminal.

Earth consists of multiple tectonic plates which move freely from each other according to the plate theory (Figure 4-1) [4.1]. Plate boundaries occur at the location where the tectonic plates meet. Large faults within the Earth's crust are formed due to the tectonic forces near these plate boundaries.

The types of fault are (Figure 4-2):
- Strike slip fault; where slip on the fault plane is approximately vertical
- Dip slip fault; where the slip is approximately horizontal
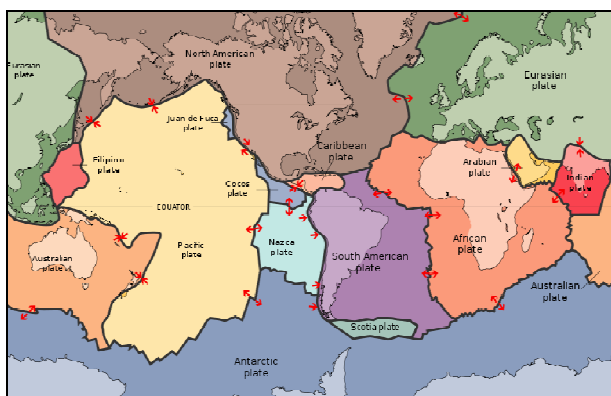- Oblique fault; has non-zero components of both strike and dip slip

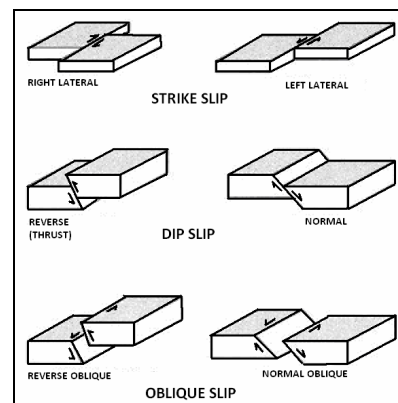*Figure 4-1 Tectonic plates around the world and its movement*

Figure 4-2 Different types of faulting

The mechanical aspects of geological faults are the key factors in understanding the generation of strong seismic motions. Within these faults, stresses are being built up, during movement. When the stresses exceed the resistance between two plates, the accumulated stress or energy will be released in the form of ground shaking. Notion must be made that faulting can also occur in the middle of the plates, particularly in the continents.

4.3 Propagation of seismic waves

When the seismic ground motions in solid rock or soil are not too extreme, the waves involved can be explained in terms of linear elastic theory [4.2]. In this case two basic types of elastic waves make up the shaking that is felt:

- Body waves: waves that's propagate through the earth's interior
- Surface waves: waves restricted to the earth surface

Body waves

Body waves can be subdivided into two types of waves, P-waves and S-waves. Celerity of these waves depends on the density of the material. The faster of these body waves is appropriately called the P-wave. The propagation of a P-wave is caused by a pressure difference. Subjected to a P-wave, particles move in the same direction as the propagation of the wave as illustrated in Figure 4-3 [4.3]. These P-waves are able to travel through both solid rock and liquid material. P-waves are also known as compression wave, because of the pushing and pulling they do.

S-waves are transverse or shear waves; this means that the movement of the ground is perpendicular to the direction of the wave propagation direction, as shown in Figure 4-3. It can produce a vertical and horizontal motion. The propagation of the wave is caused by shear stresses. This is why S-waves propagate only through solids, because fluids and gasses do not support shear forces.
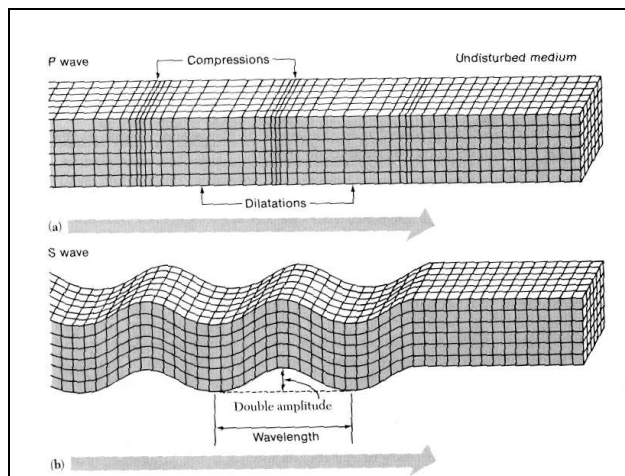
Figure 4-3 Propagation of body waves
(a) P-wave
(b) S-wave

As body waves move through layers of rock in the crust they are reflected or refracted at the interfaces between rock types. Whenever either one is reflected or refracted, some of the energy of one type is converted to waves of the other type. When the elastic module differ from one layer to another, the layers act as wave filters that amplify the waves at some frequencies and de-amplify them at others. Marked resonance effects occur at certain frequencies. When P and S-waves reach the surface of the ground, most of their energy is reflected back into the crust, so that the surface is affected almost simultaneously by upward and downward moving waves. This surface amplification enhances the shaking damage produced at the surface of the Earth.

Surface waves

Motions of surface waves are restricted to near the earth surface. Such waves correspond to ocean waves that do not disturb the water at depth. Similarly, as the depth below the ground surface increases, the soil or rock displacement decreases. Surface waves in earthquakes are of two types. The first is called the love wave. It moves the ground side to side in a horizontal plane parallel to the

TUDelft
Delft University of Technology

Earthquake analysis of quay walls
- Seismic Analysis-

Gemeentewerken
Gemeente Rotterdam

Earth's surface, but at right angles to the direction of propagation. No vertical displacement is involved during its propagation (Figure 4-4) [4.3].

The second type of surface wave is called the Rayleigh wave. Like ocean waves, the particles of rock displaced by a Rayleigh wave move both vertically and horizontally in a vertical plan oriented in the direction in which the waves are traveling. Each point in the rock moves in an ellipse as the wave passes (Figure 4-4) [4.3].
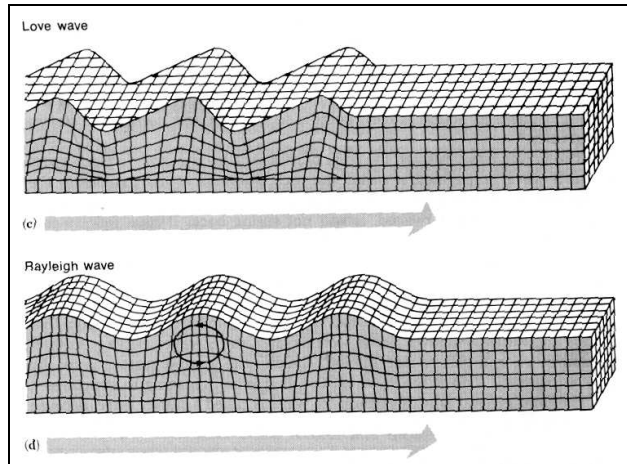
Figure 4-4 propagation of surface waves
(c) love wave
(d) Rayleigh wave

Seismic waves of all types are progressively damped as they travel because of the non-elastic properties of the rocks and soils. The attenuation of S-waves is greater than that of P-waves, but for both types attenuation increases as wave frequency increases. Distinction must be made between shallow earthquakes and deep earthquakes which depend on the depth of the epicentre. When deep earthquakes and shallow earthquakes have the same magnitude, deep earthquakes will cause less ground motion at the surface compared to shallow earthquakes because of the difference in travelling distance of the seismic waves. As mentioned above, these waves are progressively damped by the soil and therefore will not continue forever.

The frequency range of seismic waves is large, from as high as the audible range (greater than 20 hertz) to as low as the frequencies of the free oscillations of the whole Earth ($3*10^{-4}$ hertz). Attenuation of the waves in rock imposes high-frequency limits, and in small to moderate earthquakes the dominant frequencies extend in surface waves from about 1 to 0.1 hertz.

The amplitude range of seismic waves is also great in most earthquakes. Displacement of the ground ranges from 10^{-10} to 10^{-1} meter. In the greatest earthquakes the ground amplitude of the predominant P-waves may be several centimeters at periods of two to five seconds.

Mechanical properties of the rocks, such as incompressibility, rigidity, and density, play a role in the speed with which the waves travel and the shape and duration of the wave. The layering of the rocks and the physical properties of surface soil also affect wave characteristics. In most cases, elastic behaviour occurs in earthquakes, but strong shaking of surface soils from the incident seismic waves sometimes results in non-elastic behaviour, including the downward and outward movement of unconsolidated material and the liquefaction of sandy soil.

4.4 Ground acceleration

For engineering practice, it is advantageous to record directly either the ground accelerations or the ground displacement. Seismic forces against structures are related to the ground acceleration or ground displacement caused by earthquakes. The horizontal motion was assumed to be normative, which has been extensively studied and considered in the design process. The vertical component of the ground motion has generally been neglected in design and hardly studied from hazard point of view. Also most of the prevailing building codes worldwide assume the vertical component of the ground motion to be ½ to ⅔ of the horizontal component. However, in recent destructive earthquakes such as the 1989 Loma Prieta, 1994 Northridge, 1995 Kobe and 1999 Chi-Chi, it was found that vertical ground motion may equal or even significantly exceed the local horizontal ground motion.

Ground motion recorded at different sites and in different earthquakes will vary significantly due to several factors, including earthquake source, local site condition, and depth of sediments. Measuring Earthquakes range broadly in size. The size of earthquakes is commonly expressed in two ways: magnitude and intensity. Magnitude is a measure of the total energy released during an earthquake (section 4.4.2). It is determined from a seismogram which plots the ground motion produced by seismic waves. Because the magnitude does not describe the extent of the damage, its usefulness is limited to an approximation of wether the earthquake is large, small or medium sized. The destructiveness of an earthquake is a complex matter related to the geology, population density and cultural features of a specific area at a specific distance from the epicenter.

Seismologists and geologists also describe earthquakes by their intensity. Measured on a numerical scale, intensity is the degree of damage or the observable effects caused by an earthquake at a particular location. An earthquake of a particular magnitude will produce different intensities at different places, according to geology, population density, cultural features, and distance from the epicentre. The most widely used intensity scale, the Modified Mercalli Scale, is divided into 12 degrees, each identified by a Roman numeral (see section 4.4.1).

Magnitude and intensity measure different characteristics of an earthquake. Relation between the two is difficult to determine because the intensity is location dependent and the fact that the magnitude will decrease once the distance to epicentre becomes larger. A rough estimation of the relation between the two measurements is shown in Table 4-3 [4.4].

4.4.1 The modified Mercalli intensity scale

The effect of an earthquake on the Earth's surface is called the intensity. The intensity scale consists of a series of certain key responses such as people awakening, movement of furniture, damage to chimneys, and finally - total destruction. This scale, composed of 12 increasing levels of intensity that range from imperceptible shaking to catastrophic destruction, is designated by Roman numerals. It does not have a mathematical basis; instead it is an arbitrary ranking based on observed effects. The lower numbers of the intensity scale generally deal with the manner in which the earthquake is felt by people. The higher numbers of the scale are based on observed structural damage as shown in Table 4-1. Structural engineers usually contribute information for assigning intensity values of VIII or above.

Modified Mercalli scale	Evaluation by Mercalli
I	Instrumental: only registered by seismographs
II	Feeble, only felt at good circumstances
III	Slight: vibrations as passing traffic
IV	Moderate: felt by many, trembling doors & windows, like heavy traffic
V	Rather strong: felt at home, moving objects ganging at the wall
VI	Strong: Objects at home tumble, damage to less solid houses
VII	Very strong: cracking of walls, chimneys break off
VIII	Destructive: chimneys fall and there is some damage buildings
IX	Ruinous: ground begins to crack, houses begin to collapse and pipes break
X	Disastrous: ground badly cracked and many buildings are destroyed, there are some landslides
XI	Catastrophic: few buildings remain standing; bridges and railways destroyed; water, gas, electricity and telephones out of action
XII	Devastating: total destruction; all buildings destroyed, much heaving, shaking and distorted of the ground

Table 4-1 Modified Mercalli scale

TUDelft
Delft University of Technology

Earthquake analysis of quay walls
- Seismic Analysis-

Gemeentewerken
Gemeente Rotterdam

The Modified Mercalli Intensity value assigned to a specific site after an earthquake has a more meaningful measure of severity to the nonscientist than the magnitude because intensity refers to the effects actually experienced at that place.

4.4.2 Earthquake magnitudes

Scientists use the magnitude of an earthquake to characterize its size located at the epicenter. Magnitude tells nothing about the damage it may cause at the surface because this damage also depends on the depth of the epicenter. Due to damping of the seismic waves, earthquakes with a deeper epicenter will result in less ground movements at the surface compared to shallow earthquakes and therefore causing less damage on structures.

Since 1900 all over the world earthquakes have been measured by various seismographs. The well known Richter magnitude scale refers to a number of ways to assign a single number to quantify the energy contained in an earthquake. In all cases, the magnitude is a base-10 logarithmic scale obtained by calculating the logarithm of the amplitude of waves measured by a seismograph. An earthquake that measures 5,0 on the Richter scale has a shaking amplitude 10 times larger than one that measures 4,0.

There are several scales which have historically described as the Richter scale, especially the local magnitude, M_L, and the surface wave magnitude, M_s. In addition, the body wave magnitude, M_b, and the moment magnitude, M_W, have been widely used for decades, and a couple of new techniques to measure magnitude are in the development stage.

All magnitude scales have been designed to be compatible. The reason for so many different ways to measure the same thing is that at different distances for different hypocentral depths and for different earthquake sizes, the amplitudes of different types of elastic waves must be measured. To translate the measurements into an analytic value, the above mentioned magnitudes are listed in Table 4-2.

Symbol	Name	Formula
M_L	Local magnitude	$M_L = \log A_L - \log A_0$ where: A_L = maximum trace amplitude in millimetres recorded on a standard short-period seismometer $\log A_o$ = standard value as a function of distance (≤ 600 km)
M_s	Surface wave magnitude	$M_s = \log A_s + 1{,}66 \log \Delta + 2{,}0$ where: A_s = the maximum ground amplitude in micrometers Δ = the epicentral distance of the seismometer measured in degrees
M_b	Body wave magnitude (P-wave)	$M_b = \log (A_b / T) + \sigma (D,h)$ where: A_b = maximum amplitude of the P wave in micrometers T = period of measurement σ = Calibration term that depends on distance D and event h
M_o	Seismic moment	$M_o = \mu A_o \overline{D}$ where: μ = rupture strength A_o = rupture area $\overline{D}$ = average amount of slip
M_w	Moment magnitude	$M_w = \dfrac{\log M_o}{1.5} - 10.7$ where: M_o = seismic moment

Table 4-2 Different types of earthquake magnitude

The surface magnitude is most commonly used to describe the size of shallow (less than about 70 km focal depth) earthquake with a moderate to large distance (farther than about 1000km). The body wave magnitude (Gutenberg, 1945) is a worldwide magnitude scale based on the amplitude of the first few cycles of p-waves which are not strongly influenced by the focal depth.

For strong earthquakes, the measured ground-shaking characteristics become less sensitive to the size of the earthquake than for smaller earthquakes. This phenomenon is called "saturation". The moment Magnitude is the only magnitude that is not subjected to saturation. Therefore it is a good magnitude to apply to very strong earthquake. In practice all magnitudes are used. Depending on the earthquake or the phenomenon which is of importance a magnitude has to be chosen. E.g. the released energy during an earthquake doesn't have to be proportional to the maximum acceleration of an earthquake. For relatively small earthquakes, the Richter magnitude is being used. For strong magnitudes commonly the moment magnitude is used.

Modified Mercalli Intensity	Magnitude (M_L)	Modified Mercalli Intensity	Magnitude (M_L)
I	2	VII	5.5
II	2.5	VIII	6
III	3	IX	6.7
IV	3.7	X	7.3
V	4.3	XI	8
VI	5	XII	8.5

Table 4-3 Rough estimation between relation of Modified Mercalli Intensity and Local magnitude.
intensities that are typically observed at locations near the epicenter of earthquakes of different

4.5 References

[4.1]   www.usgs.gov, 05-2010
[4.2]   Y. Bozorgnia, V.V. Bertero, Earthquake engineering – From engineering seismology to performance-based engineering, CRC press, Washington D.C., 2004
[4.3]   www.pnsn.org, 05-2010
[4.4]   S. van Baars, Lecture note - Soil dynamics, TU Delft, 2009
[4.5]   http://en.wikipedia.org/wiki/Richter_magnitude_scale

TUDelft
Delft University of Technology

Earthquake analysis of quay walls
- Seismic Analysis-

Gemeentewerken
Gemeente Rotterdam

5. Seismic effects on quay walls

5.1 Introduction

In the life cycle of port structures, devastation by an earthquake might be a rare event. However, once it occurs, the magnitude of the consequences will be so large that the effect of earthquakes can be a major issue of national interest. Earthquakes thus pose low probability and high consequence threats to port structures. To reduce these threats, first need to find out what these need to be known threats are. A better estimation in seismic behaviour for the Euromax quay wall can be made by getting more insight of the seismic soil behaviour.

During an earthquake, ground starts shaking which result in movement of soil particles. These particles are subjected to acceleration. According Newton's second law, acceleration is accompanied with a force. This earthquake induced force will act like an additional force on the quay wall structure. Also strength and strain reduction of the soil layer will appear when liquefaction occurs. This chapter presents some information about quay walls in general (section 5.2), primary forces acting on a quay wall (section 5.3), more detailed information about force addition and strength reduction caused by earthquake (section 5.4) and some failure mechanisms that may occur due to these seismic forces (section 5.5). Finally a rough risk estimation is performed in section 0.

5.2 Quay wall in general

Characteristic of quay walls is that it retains soil and that ships can berth alongside. This is space saving compared to situations where there is a slope. Cranes, trucks and trains can get close to the ship and it is comparatively easy to handle the freight. Overview of main functions for a quay is listed below:

- Soil retaining
- Water retaining
- Berthing of ships
- Transhipment of goods

Many different types of quay wall have been designed and build nowadays [5.1]. The choice depends on the location of the port, geological conditions of the soil strata and requirements the quay wall must fulfil. These requirements will vary according to the users. For the Euromax terminal the requirements are presented in section 3.3.

5.2.1 Gravity walls

Early types of quays were gravity walls. As the name indicates, the soil retaining function of the gravity wall is derived from the self-weight of the wall that is so heavy that sufficient resistance to shearing is generated in the soil and it cannot tilt or slide. Gravity walls often consist of prefabricated elements. These structures all have natural foundations. This means that the subsoil must have sufficient bearing capacity or that the bearing layer does not lie too far below the level of the bottom of the harbour and that extensive soil improvement is not necessary. Nowadays, gravity walls are still being built at places where bearing capacity of the subsoil is large enough and places where the subsoil is not suitable for a sheet pile wall because it consists of rock or very firm sand. Also at seismic region, gravity walls are common in use. A caisson type gravity wall is shown in Figure 5-1 [5.1].
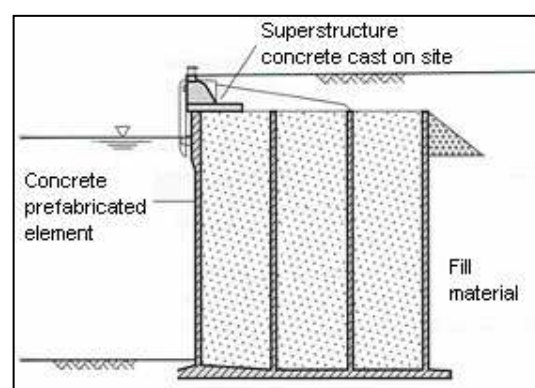

Figure 5-1 Caisson type gravity wall

T̃UDelft
Delft University of Technology

Earthquake analysis of quay walls
- Seismic Analysis-

Gemeentewerken
Gemeente Rotterdam

5.2.2 Sheet pile walls

At coast lines with weak soils sheet pile walls have been developed. They get their soil retaining function and stability from the fixation capacity of the soil. The sheet pile wall then is a cantilever beam elastically fixed in the ground (Figure 5-2). With increasing height the deflections at the top become too large so that the top needs to be anchored (Figure 5-2). Once more the fixation capacity of the soil is the stabilization element for the anchors. The most important requirement to use sheet pile walls is that the ground can be easily penetrated.

Early sheet pile structures had been made from wooden elements, connected by groove and tongue. The anchors were chains leading to anchor plates back behind of the structure. In case of weak soils forming the upper soil strata the walls have been anchored by inclined piles or by pile racks. Later the wall elements were U-shaped steel profiles, connected together with bolted on Z-profiles. These elements combined a higher stiffness with a length depending to the construction height. For quay walls with high retaining height that must bear considerable loads, heavy structures that may consist of various types of combined walls are needed. A combined wall consists of heavy primary elements that are deeply embedded in the subsoil at a set distance from each other. The primary elements transfer the forces to the subsoil and the anchoring system. A seal composed of standard steel sheet piles that are welded to each other is installed between the primary elements. These intermediate sheet piles are shorter than the primary elements because the soil pressure is transferred to the primary elements by arch action.
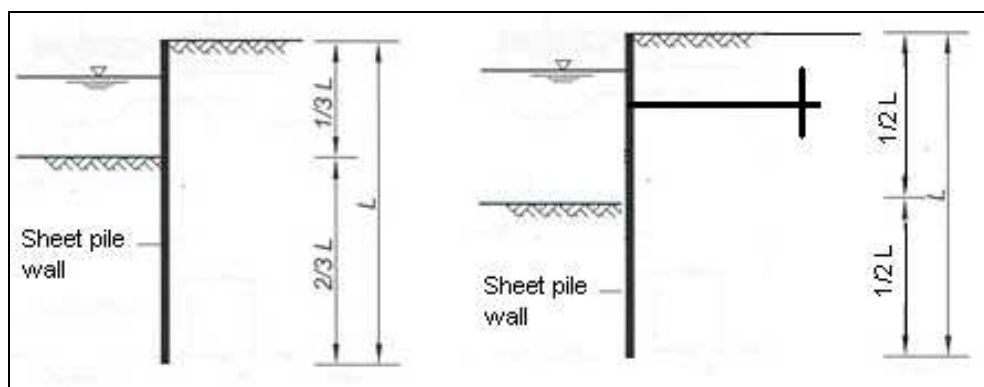
Figure 5-2 Principle of sheet pile walls without and with anchor

Another type of sheet pile wall that is used nowadays is called diaphragm wall. A diaphragm wall is a reinforced concrete wall that is made in situ. The wall has high bearing capacity and is stiff so the deformations are minimal. However, one disadvantage is that the width of the panels is limited and this can give rise to problems with the sealing of the joints between the panels. Another important consideration is the need for good cover of the reinforcement.

Due to the development in transhipment the last decades (bigger vessels), the design depth of quay walls has increased dramatically, resulting in sheet pile walls with heavy profiles.

5.2.3 Relieving structures

Relieving structures are concrete structures places on top of the sheet pile wall just below the surface (see Figure 2-2). They were introduces to reduce the forces on the sheet piles, hence the reduction of sheet pile profiles. The use of a relieving platform introduces several benefits, particularly in circumstances where the ground conditions limit the efficacy of anchor piles in tension while capacity in compression is good. More particularly since the platform slab carries the entire load on top of the relieving floor and directly transfer theses forces into the deeper subsoil by the diaphragm wall and bearing piles, it substantially reduces the height of retained soil. It also provides vertical surcharge to the sheet piles to assist against pull-out forces and to improve passive resistance to the embedded section. Another important benefit is that the relieving platform reduces active earth pressure on the uppermost part of the sheet pile wall. The most important effects are the savings on cost of sheet piles through a reduction of moment and pile depth.

TUDelft
Delft University of Technology

Earthquake analysis of quay walls
- Seismic Analysis-

Gemeentewerken
Gemeente Rotterdam

5.3 Primary forces on a quay wall in general

Many forces act on a quay wall during its lifetime. The quay wall structure must be strong enough to resist these forces. Representative or characteristic loads must be determined. To determine the relevant combination of loads, it is also important to know which situation leads to extreme loads. An overview of specific loads acting on the quay wall is listed below:

- Static Earth pressure
- Static Water pressure
- Bolder force
- Fender force
- Crane loads
- Surcharge load
- Own weight of relieving structure

The two most dominant forces acting on the quay wall are the earth and water pressure forces. These two forces are always present during the lifetime of the structure. In contradiction to the earth and water pressure, the other forces are variable forces which are requirements made by the user (section 3.3) and will not be discussed further in this chapter.

5.3.1 Static earth pressure

Static earth pressure on retaining structures is strongly influenced by wall and soil movements. Active earth pressures develop as a retaining wall moves away from the soil behind it, including extensional lateral strain in the soil. When the wall movement is sufficient to mobilize the strength of the soil behind the wall, minimum active earth pressures act on the wall. Because very little wall movement is required to develop minimum active earth pressures, free-standing retaining walls are usually designed on the basis of minimum active earth pressures. Where lateral wall movements are restrained, such as in the cases of anchored walls, static earth pressures may be greater than minimum active. Passive earth pressures develop as a retaining wall moves toward the soil, thereby producing compressive lateral strain in the soil. When the strength of the soil is fully mobilized, maximum passive earth pressures act on the wall. Neutral earth pressure occur when the wall experience no lateral movement.

The three categories of earth pressure mentioned above are listed below:
- Neutral earth pressure: develops when the wall experiences no lateral movement. This typically occurs when the wall is restrained from movement (see Figure 5-3B).
- Active earth pressure: develops when the wall is free to move outward. The soil mass stretches sufficiently to mobilize its shear strength (see Figure 5-3A).
- Passive earth pressure: develops when the wall move into the soil. The soil mass is compressed sufficiently to mobilize its shear strength (see Figure 5-3C).

A) Active case   B) At rest case   C) Passive case
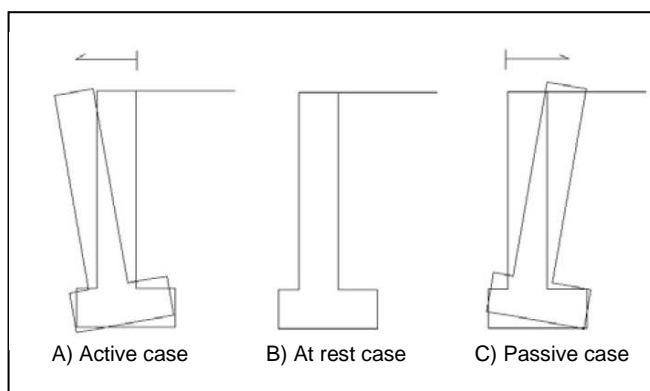
Figure 5-3 Wall movement
A) Active case: wall moves away
B) At rest case: No movement of wall
C) Passive case: Wall move into soil

Earth pressures reflect the state of stress in the soil mass. The concept of an earth pressure coefficient, k, is often used to describe this state of stress. The earth pressure coefficient is defined as the ratio of horizontal stresses (σ_h) to the vertical stresses (σ_v) at any depth below the soil surface:

$$k_0, k_a, k_p = \frac{\sigma_h}{\sigma_v}$$

Eq. 5-1

Earth pressures for any given soil-structure system may vary from an initial state of stress referred to as neutral (k_0) to minimum limit state referred to as active (k_a) or to a maximum limit state referred to as passive (k_p). The magnitude of the earth pressure exerted on the wall depends, among other effects, on the physical and strength properties of the soil, the interaction at the soil-structure interface, the ground-water conditions, and the deformations of the soil-structure system.

Neutral earth pressure refers to a state of stress where there is no lateral movement or strain in the soil mass. In this case, the lateral earth pressures are the pressures that existed in the ground prior to installation of a wall and are given as:

$$k_0 = 1 - \sin\varphi$$

Eq. 5-2

where
k_0:   neutral earth pressure coefficient
φ: the angle of internal friction of soil.

However, the stability of many retaining walls depends on the balance between active pressures acting predominantly on one side of the wall and passive pressures acting on the other. Even under static conditions, prediction of actual retaining walls forces and deformations is a complicated soil-structure interaction problem. A number of simplified approaches are available to evaluate static loads on retaining walls. The most commonly used are described in appendix B.

In the literature different notations is used for the definition of the problem geometry and the strength parameters of the backfill. In order to avoid confusion on the symbols, in this chapter are signed:

φ: angle of internal friction of soil
α_{pfl}:   angle of the planar failure surface respect to horizontal
α: slope inclination
β: inclination of back of wall to vertical
δ: angle of friction structure soil
k_v: seismic coefficient of vertical acceleration
k_h: seismic coefficient of horizontal acceleration
Ψ: inclination angle of the seismic coefficient k with the vertical
P: Earth pressure thrust
W: weight of sliding wedge
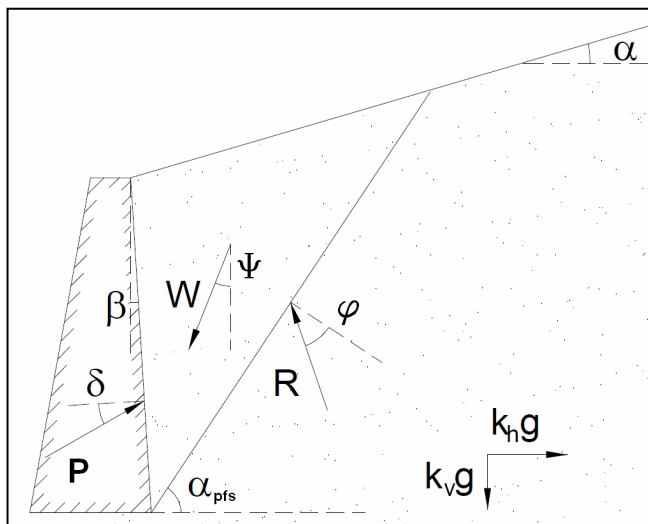
The assumed symbology is illustrated in Figure 5-4.

Figure 5-4: Utilized symbols for the geometry

TUDelft
Delft University of Technology

Earthquake analysis of quay walls
- Seismic Analysis-

Gemeentewerken
Gemeente Rotterdam

5.3.2 Static Water pressure

The total water pressures that act on retaining walls in the absence of seepage within the backfill can be divided in two components: hydrostatic pressure, which increases linearly with the depth and acts on the wall before, during and after the earthquake shaking, and hydrodynamic pressure (section 5.4.1), which results from the dynamic response of the water itself.

Distinguishes of two different types of water pressure must be made:

- Groundwater pressure (water in the backfill)
- Seawater pressure (water outboard of retaining wall)

The presence of water in the backfill behind a retaining wall influences the effective stresses and hence the lateral earth pressure that acts on the wall. Hydrostatic pressure due to the water must be added to the lateral earth pressure. Because the total lateral thrust on a wall retaining a saturated backfill is considerably greater than that on a wall retaining dry backfill, the provision of backfill drainage is an important part of retaining wall design.

Both water pressures are hydrostatic and can be determined using the following equation:

$$U_{stat} = \frac{1}{2}\gamma_w h^2$$

Eq. 5-3

where:
U_{stat} Hydraustatic force [kN]
γ_w Unit weight of water $[kN/m^2]$
h Water depth [m]

The resultant thrust of the hydrostatic water pressure acts at a height of h/3 from the base of the wall.

5.4 Seismic effects on quay wall

A lot of actions happen to the soil and quay wall structure when an earthquake strikes. When the magnitude of the earthquake is relative low, none of these actions will be noticeable. Once the magnitude is getting higher these actions become more noticeable and may cause damage to the quay wall structure. An earthquake has three possible effects on a soil-wall system. One is to increase the driving force (section 5.4.1). The second is to decrease the shearing resistance of the soil causing softening of the soil (section 5.4.1). The third is to cause the system to resonate in such a way that displacements becomes too large (section 5.4.2).

5.4.1 Seismic pressures on quay wall

Two primary forces acting on a quay wall during static conditions were mentioned section 5.3. These earth and water pressure forces also play a dominant role during a seismic event. However, a very few literature proposed the analysis of quay wall under the combined action of forces due to water and seismic earth pressure, as most of the literature deals with the individual forces acting on the waterfront retaining wall. Hence, till today, the complete solution for the combined effect of seismic active earth pressure and hydrodynamic pressure on the waterfront retaining wall with the consideration of wall inertia is scarce. Therefore in this thesis, forces acting on the quay wall structures are handled separately and were assumed not to influence each other.

Dynamic earth pressure
Shaking of the ground causes the soil particles to move. This movement depends on the direction of the incoming seismic waves as mentioned in chapter 4. The mobilization of active and passive ground will be influenced by these movements which results in a change the lateral earth pressure against the wall.

A common approach to the seismic design of retaining walls involves estimating the loads imposed on the wall during earthquake shaking and then ensuring that the wall can resist those loads. Because

TUDelft
Delft University of Technology

Earthquake analysis of quay walls
- Seismic Analysis-

Gemeentewerken
Gemeente Rotterdam

the actual loading on retaining walls during the earthquakes is extremely complicated, seismic earth pressures on retaining walls are usually estimated using simplified methods.

In the pseudo-static analysis of seismic lateral earth pressures, a constant horizontal and vertical seismic coefficient, k_h and k_v, respectively, is assumed for the entire soil mass involved. A seismic force, W, which is equal to the seismic coefficient times the weight of a soil mass, is assumed to act at the centre of gravity of the sliding soil mass. The seismic force is assumed to act in a direction at an angle Ψ from the vertical as shown in Figure 5-4.

Several researches in the recent past had given solutions for the computation of the seismic lateral earth pressure acting on a rigid retaining wall. The pioneering work by Okabe (1924) and Mononobe (1929), which is commonly known as Mononobe-Okabe method (referred as the M-O method during this Thesis), by considering the pseudo-static seismic accelerations, is still being used worldwide to compute the seismic lateral earth pressure. The M-O method is a direct extension of the static Coulomb theory to pseudo-static conditions. In a M-O analysis, pseudo-static accelerations are applied to a Coulomb active (or passive) wedge. The pseudo-static soil thrust is then obtained from the force equilibrium of the wedge. More details about the M-O method are presented in appendix C.

Dynamic water pressure
The presence of water plays a strong role in determining the loads on quay walls both during and after earthquakes. Water outboard of a retaining wall can exert dynamic pressures on the face of the wall. Water within a backfill can also affect the dynamic pressures that act on the back of the wall. Proper consideration of the effects of water is essential for the seismic design of retaining structures, particularly in waterfront areas.

Water outside of wall
Hydrodynamic water pressure results from the dynamic response of a body of water. The resulting relationship for hydrodynamic pressure on the face of the wall is a function of the horizontal seismic coefficient, k_h, the depth of water, h, the total depth of the pool of water, h_{total}, the fundamental period of the earthquake and the compressibility of the water. The hydrodynamic pressure is opposite in phase to the base acceleration and for positive base acceleration the hydrodynamic pressure is a tensile. For retaining walls, hydrodynamic pressures are usually estimated from Westergaard's solution for the case of a vertical, rigid wall retaining a semi-infinite reservoir of water that is excited by harmonic, horizontal motion of its rigid base. According to Westergaard's solution, the dynamic action of the water on the retaining structure can be visualized as that of a certain body of water moving together with the retaining structure while the remainder of the reservoir remains effectively stationary. The body of water moving with the retaining structure may be imagined as effectively having frozen into horizontal layers of ice, with the remainder of the reservoir being emptied. The layers of ice are considered to support one another by vertical forces only, with no shear force in between. The layers are attached firmly to the retaining structure so that the retaining wall will exert the horizontal forces necessary to move them back and forth as it oscillates. Therefore, the forces exerted on the up-stream face of the retaining structure can be represented as inertia forces similar to those due to the moving mass of the retaining structure itself. The shape of the body of water considered to be moving in concert with the retaining structure needs to be determined to evaluate the inertia forces which correspond to the pressure exerted by the water due to dynamic action. Westergaard proposed the following approximate solution for the hydrodynamic water pressure distribution: a parabolic dynamic pressure distribution, p_{wd}, described by the relation

$$p_{wd} = \frac{7}{8} k_h \gamma_w \sqrt{h h_{total}}$$

Eq. 5-4

The resultant hydrodynamic thrust computed by Westergaard, which acts at a height of 0,4h from the base of the wall, is given by:

$$U_{dyn} = \frac{7}{12} k_h \gamma_w h_{total}^2$$

Eq. 5-5

TUDelft
Delft University of Technology

Earthquake analysis of quay walls
- Seismic Analysis-

Gemeentewerken
Gemeente Rotterdam

where:

U_{dyn}	Resultant hydrodynamic thrust
p_{wd}	hydrodynamic pressure distribution
γ_w	Unit weight of water
k_h	Seismic coefficient of horizontal acceleration
h	Water depth
h_{total}	total depth of the pool of water

The total water pressure on the face of the retaining wall is the sum of the hydrostatic and hydrodynamic water pressures. Similarly, the total lateral thrust due to the water is equal to the sum of hydrostatic and hydrodynamic thrusts.

Water in backfill

The presence of water in the backfill behind a retaining wall can influence the seismic loads that act on the wall in two ways:

1. by developing hydrodynamic pressures within the backfill
2. by allowing excess pore water pressure generation due to cyclic straining of the backfill soils.

Hydrodynamic water pressures can also develop under free pore water conditions and must be added to the computed soil and hydrostatic pressures to obtain the total loading on the wall. Matsuo and Ohara (1965) had suggested the hydrodynamic pressure at the backfill side to be around 70% of that on the outboard of the wall.

One of the more significant factors leading to ground failure during earthquakes is the generation of excess pore pressures. Sands tend to compact during shaking. The water in the pores cannot escape quickly enough to accommodate instantaneously the compaction. Therefore, stresses are thrown on the water that increases the pore water pressure and reduce the effective stresses between the sand particles. Sand, a frictional material, depends on the effective stresses between the grains to mobilize shear strength and resistance to displacement. Therefore the increasing pore water pressure leads to strength loss (Figure 5-6). The resistance to shearing strain or deformation is also reduced by increasing pore water pressure. The shear modulus which controls the shearing strains is also a function of the mean normal effective stress and therefore as the seismic pore water pressures increase the shear modulus decreases. In the extreme case where nearly all shear strength and shear stiffness is lost, the sand behaves like a liquid, with disastrous consequences for structures (Figure 5-5). This liquid behaviour of soil particles is called liquefaction. Further details about the liquefaction phenomena can be found in Appendix D.

Normal porewater pressure
no earthquake

High poorwater pressure due
to earthquake
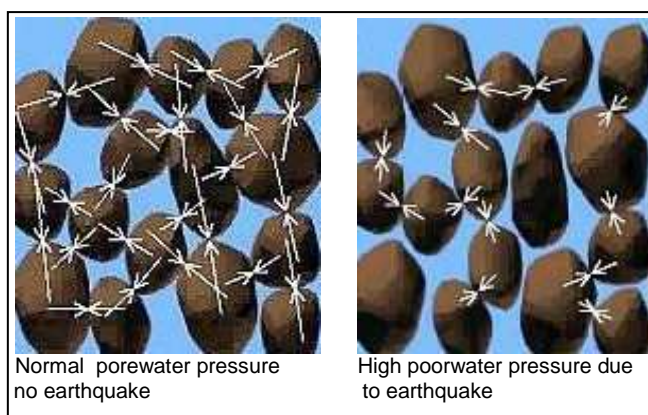
Figure 5-6 Behaviour of soil grains in a soil deposit during an earthquake. The length of the arrows represent the size of the contact forces between individual soil grains. The contact forces are large when the porewater pressure is low.

Figure 5-5 Damage Kobe Port due to liquefaction during the 1995 earthquake.

After complete loss of effective stress, sand had neither shear modulus nor shear strength, and consequently develops large deformation even under minor shear stress. Figure 5-7 shows a typical cyclic mobility stress path of undrained saturated dense sand. As cyclic loading progress, there is a

TUDelft
Delft University of Technology

Earthquake analysis of quay walls
- Seismic Analysis-

Gemeentewerken
Gemeente Rotterdam

progressive increase in excess pore water pressure, $\triangle u$, and corresponding reduction in mean effective stress, p'. The excess pore pressure ratio, r_u, increases to a maximum value of 100%, which corresponds to liquefaction. The main feature of the stress path is the distinctive butterfly profile arising from the alternate phases of dilation and densification. With each cycle of applied shear loading, q, the sand alternates between being incrementally dilative (p' increasing) and incrementally contractive (p' decreasing) in its response, with the transition from incrementally contractive to incrementally dilative response being phase transformation. The axial strains remain relatively small until r_u nears 100%, after which the strain grow rapidly with each additional cycle of loading. Note that the triggering of r_u=100% typically corresponds to shear strains of about 2 to 3%. The strain hardens at the end of each load cycle and develops enough shear strength to resist the peak applied shear load. The resulting inverted s-shaped stress-strain loops shown in Figure 5-7 are an example of what is termed cyclic mobility.
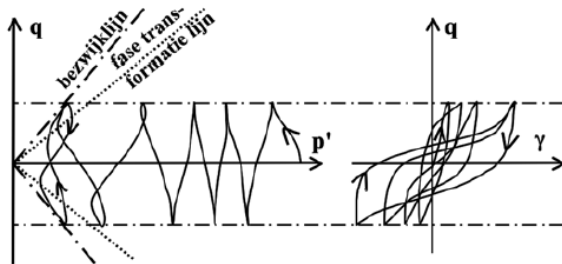
Figure 5-7 Effective stress path for undrained cyclic traxial test.
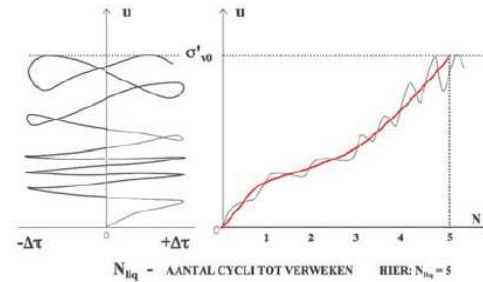
Figure 5-8 Development pore water pressure for undrained cyclic traxial test

Development of pore pressure, including its appearing, developing and disappearing is an important factor in determining the soil behaviour. Knowing is that development of excess pore water pressure depends on the number of cycles of loading (earthquake duration), shear stress (earthquake magnitude) and the soil type. Figure 5-8 shows a typical development of pore water pressure for undrained saturated dense sand. However, there is still very little research work on it till now and no specific field testing were performed needed for computing the excess pore pressure for the project location. Therefore, excess pore water generation is assumed during this analysis.

For restrained pore water conditions, the M-O method can be modified to account for the presence of excess pore water within the backfill (Matsuzawa et al., 1985). Representing the excess of pore water pressure in the backfill, Δu, by the pore pressure ratio, $r_u = \Delta u / \sigma'_v$, the active soil thrust acting on a yielding wall can be computed from equation (C-1) replacing γ_{eff} by $\gamma_{eff,1}$ and ψ by ψ_1:

$$\gamma_{eff,1} = (\gamma - \gamma_w)(1 - r_u)$$

Eq. 5-6

$$\psi_1 = \tan^{-1}\left[\frac{\gamma \cdot k_h}{\gamma_{eff,1}(1 - k_v)}\right]$$

Eq. 5-7

where
$\gamma_{eff,1}$ effective unit weight of soil with excess pore pressure
ψ_1 seismic inertia angle with excess pore pressure

An equivalent hydrostatic thrust based on a fluid of unit weight $\gamma_{eq} = \gamma_w + r_u(\gamma - \gamma_w)$ must be added to the soil thrust. Note that as r_u approaches 1 (as it could in liquefiable backfill), the wall thrust approaches that imposed by a fluid of equivalent unit weight $\gamma_{eq} = \gamma$.

5.4.2 Resonance of structure

Each structure has a fundamental frequency. Fundamental frequency is the frequency at which a system naturally vibrates once it has been set into motion. It depends on both the material properties (specifically stiffness or modulus of elasticity) and the geometry of the structure. If a structure is subjected to vibration at its fundamental frequency, the displacements of that structure will reach a

TUDelft
Delft University of Technology

Earthquake analysis of quay walls
- Seismic Analysis-

Gemeentewerken
Gemeente Rotterdam

maximum. Greater displacements results in greater stresses that are developed in the framing members and connections of the structure.

5.5 Failure mechanisms

Failure of a quay wall occurs when a quay wall can fulfill his main functions (section 5.2) due to large displacement or damage to the quay. Additional pressures and reduction in strength due to an earthquake, as mentioned in section 5.4 can cause a quay wall to fail functioning. This section will handle some possible failure mechanisms that may occur during earthquakes. Due to the diversity in quay wall structures and their differences in load transfer, distinction in failure has been made for the two types of quay walls which were investigated during this Thesis.

5.5.1 Failure Gravity wall

A gravity quay wall is made of a caisson or other rigid wall put on the seabed, and maintains its stability through friction at the bottom of the wall. Typical failure modes during earthquakes involve seaward displacement, settlement and tilt. For a quay wall constructed on a firm foundation, an increase in earth pressure from the backfill plus the effect of an inertia force on the body of the wall result in the seaward movement of the wall as shown in Figure 5-9(a). If the width to height ratio of the wall is small, tilt may also be involved. Case histories for gravity quay walls subjected to earthquake shaking often belong to this category. When the subsoil below the gravity wall is loose and excess pore water pressure increases in the subsoil, however, the movement of the wall is associated with significant deformation in the foundation soil, resulting in a large seaward movement involving tilt and settlement as shown in Figure 5-9(b). The latter mode of failure has received wide attention since the Kobe earthquake, Japan, in 1995.
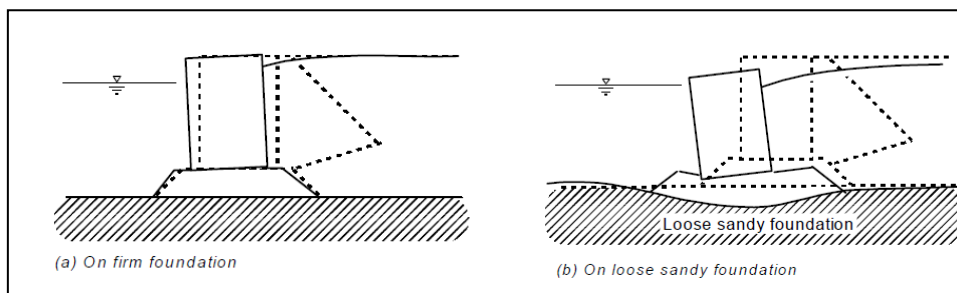
Figure 5-9 Deformation/failure mode of gravity walls **[5.3]**

5.5.2 Failure sheet pile wall with anchor

An anchored sheet pile wall is composed of a wall, anchors and tie-rods. Each structural component contributes to the stability of the whole structure. Excessive displacements of the anchor are undesirable. A small movement of the anchor, however, contributes to reducing the tension in the tie-rods and the bending moment in the wall. Well-balanced response of the wall and anchor is essential for ascertaining the reasonable performance of the anchored sheet pile wall during earthquakes.

Agbabian Associates (1980) summarize the performance of anchored sheet pile walls at 26 harbors during earthquakes in Japan, the United States, and South America. Their survey indicates that the catastrophic failures of sheet pile walls are due to the large scale liquefaction of the backfill and/or the foundation, including the foundation soil located in front of the sheet pile wall and below the dredge level. For those structures that underwent excessive movements but did not suffer a catastrophic failure, there was little or no evidence of damage due to the vibrations of structures themselves. The sources of movements for those walls whose backfill and foundation soils did not liquefy but did exhibit excessive wall movements during the earthquake are mentioned below.

A variety of geotechnical conditions can result in a variety of failure modes of an anchored sheet pile wall. In particular, three failure modes may be identified depending on the extent of loose, saturated sandy soils relative to the position and geometry of the wall. If the deformation of a loose deposit mainly affects the stability of anchors as shown in Figure 5-10(a), the anchors will move toward the

sea, resulting in the seaward movement of the wall. This mode of deformation/failure has been the most frequently observed at waterfronts. If the deformation of the loose deposit mainly affects the backfill of the wall as shown in Figure 5-10(b), the earth pressure increase will cause an excessively large bending moment in the wall, resulting in yielding of the wall. This mode of failure has also been observed during past earthquakes.

If the deformation of the loose sandy deposit mainly affects the stability of the embedment portion of the wall as shown in *Figure 5-10*(c), a gross instability of the wall at the embedment portion should exist. This mode of failure occurs only when the anchor is strong and firmly embedded, and both the wall and tie-rods are very strong.

The above mentioned failure modes are due to soil failure. Another important kind of failure is structural failure. If the bending moment acting on the sheet pile wall will become excessively large due to the high pressure acting behind the sheet pile wall, an opening or a crack in the wall may occur as shown in *Figure 5-10*(d). These high pressures against the sheet pile wall also makes the wall wants to displace toward sea. Anchors and tie-rods prevent this from happening. But when the pressure becomes too large and the force in the tie-rods exceeds the resistant strength, the tie-rods will break and the sheet pile will move towards sea as shown in *Figure 5-10*(d).
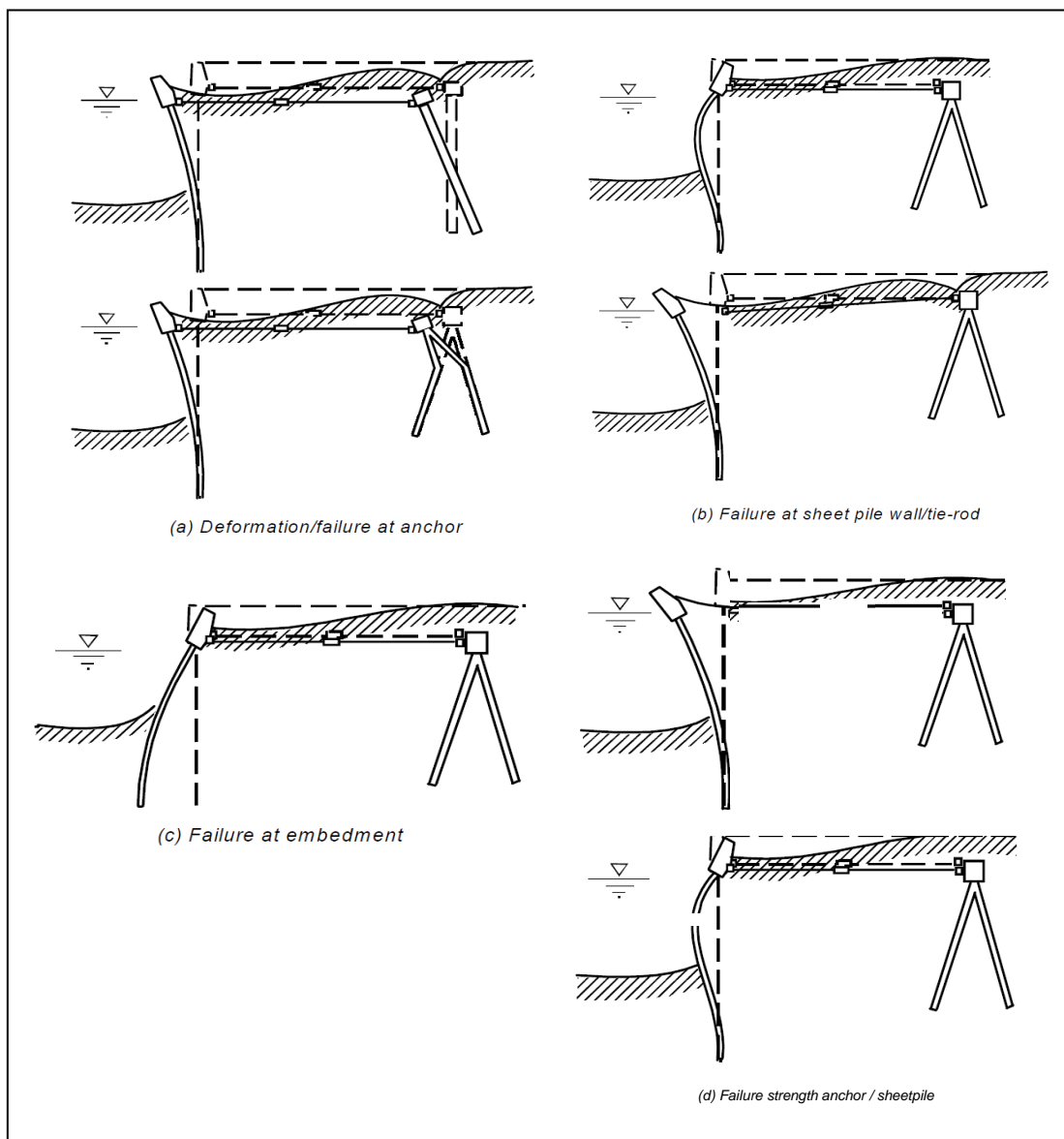

(a) Deformation/failure at anchor

(b) Failure at sheet pile wall/tie-rod

(c) Failure at embedment

(d) Failure strength anchor / sheetpile

Figure 5-10 Deformation/failure mode of anchored sheet pile walls [5.3]

TUDelft
Delft University of Technology

Earthquake analysis of quay walls
- Seismic Analysis-

Gemeentewerken
Gemeente Rotterdam

5.6 Risk assessment

The Port of Rotterdam is the biggest sea port in Europe which has a major contribution to the national and European economy. Failure of the Euromax quay wall will directly influence the functionality of the Port in which indirectly influences the national and European economy. Therefore a rough risk assessment is performed to determine the expected loss for the Port of Rotterdam soley due to the failure of the Euromax terminal caused by an earthquake with high magnitude. Notion must be made that during this risk assesment the influence due to loss of reputation of the port is not included neither does the effects on the national and European economy.

During the assessment it is assumed that a failure of the diaphragm quay wall will results in total closure of Euromax terminal. The duration of the closure depends on the duration of reparations that needs to be performed.

The risk assessment is a systematic and comprehensive methodology to evaluate risks associated with hazards like earthquakes. Here the risk is characterized by two quantities:

1. the magnitude of the possible adverse consequence
2. the probability of occurrence an event

The consequence for the performed risk assessment in this master thesis concerns the failure of the existing diaphragm quay wall due to an earthquake. The consequences due to the failure of the quay wall are expressed as damage in euros where the probability of occurrence is expressed as the probability that a quay wall will fail due to an earthquake. The total risk is the expected loss which can be expressed in the consequences multiplied by their probabilities.

Consequences
The consequences for the Port of Rotterdam caused by the closure of the Euromax terminal is distinguish into two types of losses:

- Economic loss: loss due to no income during the closure
- Removal and reparation cost: loss due to removal and reparation of the quay wall.

According to the annual report of the Port of Rotterdam [5.4] the total operating income for the year 2010 was around 551 million euros. In the ports statistic report of the Port of Rotterdam [5.5] it was found that 26,1% of the total Cargo throughput is transported by containers of which 60% of this is transported over sea. Based on the percentages mentioned earlier and assuming that the total income is evenly divided over different cargo throughputs it can be taken that the container terminals located at the Port of Rotterdam generates a proximate annual income of 86,3 million euros. Five different sea container terminals are established at the Port of Rotterdam which result in an annual income of 17,26 million euros per container terminal.
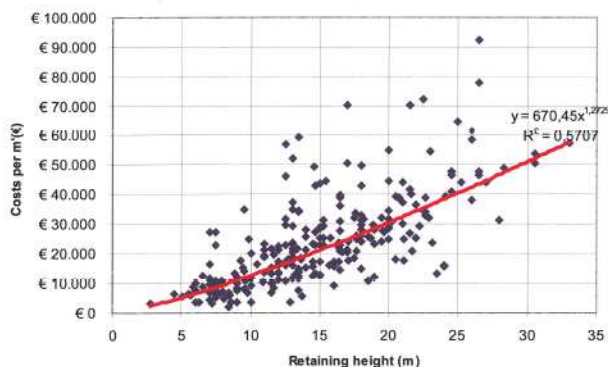
Figure 5-11 Cost of quay walls in euro (2008 values) around the world as a function the retaining height [5.6]

Critical failure mechanism for the diaphragm wall located at the Euromax terminal during an earthquake is the breakage of the diaphragm wall and is determined in chapter 8. The whole quay wall needs to be replaced when this type of failure occur. The duration of removing and replacing the existing quay wall is assumed to be 2,0 years. An estimation of construction cost is made based on

Earthquake analysis of quay walls
- Seismic Analysis-

Gemeentewerken
Gemeente Rotterdam

TUDelft
Delft University of Technology

the retaining height of the quay wall structure [5.6]. The construction cost per length quay wall is around 40000 euros for a quay wall with retaining height around 25 meters as shown in Figure 5-11. For a quay length of 1900 meters this becomes 76 million euros only for the construction of a new Euromax quay wall. When assuming that the cost needed for removing the broken caisson, reparations of the cranes and other materials is 30% of the construction cost of the quay wall, the total cost needed to make the quay wall function again becomes 98,8 million euros.

The total consequences can now be determined which is a loss 133,3 million euros.

Probabilities

For the normative load combination 2, failure of the diaphragm quay wall occurs when an earthquake with acceleration greater than 0,05g m/s^2 strikes the Euromax terminal (see chapter 8). The return period of an earthquake with acceleration of 0,05g m/s^2 is 2365 years (see section 6.3) which gives a probability of occurrence of $4,22 \cdot 10^{-4}$. Assuming that the probability of occurrence of the normative load combination is 0,2, The probability of the quay wall failure becomes $8,44 \cdot 10^{-5}$.

Risk

The risk is the expected annual loss and is determined by the consequences multiplied by their probabilities. Therefore the annual risk of the Port of Rotterdam soley due the losses of the Euromax terminal is:

$$Risk = 133,3 \cdot 10^6 * 8,44 \cdot 10^{-5} = 11250 \text{ euros}$$

The determined risk of 11250 euros is less than 0,1% compared to the annual income of 17,26 million euros generated by the Euromax terminal and therefore is worthy to be taken. Also the determined probability of failure of the quay wall is less than the allowable probabilities of failure for a quay wall with relieving platform of $3,369 \cdot 10^{-4}$ which is mentioned in the CUR 211 [5.1].

A lot of uncertainties and assumptions are made during this risk assessment and therefore the reliability of this assessment is not high. However, the purpose for this risk assessment is to get a rough insight about the risk caused by the failure of the Euromax terminal. Even when the annual risk of 11250 euros is multiplied by two, the annual risk is still very small compared to the annual income of the terminal. Therefore it can be said that there is no need for taking earthquakes into account in the general design of quay walls in the Netherlands.

5.7 References

[5.1]   CUR 211, Handbook quay walls, 2005
[5.2]   A. Verruijt, Soil mechanics, Delft university press, 1999
[5.3]   International navigation association, PIANC, MarCom-wg34, 2001
[5.4]   Port of Rotterdam, annual report 2011
[5.5]   Port of Rotterdam, Port statistics 2010
[5.6]   J.G. de Gijt, A history of quay walls – techniques, types, costs and future, 2010

TU Delft
Delft University of Technology

Earthquake analysis of quay walls
- Seismic Analysis-

Gemeentewerken
Gemeente Rotterdam

6. Seismic hazard analysis

6.1 Introduction

The main goal of the seismic hazard analysis is to define the earthquake motion and its magnitude. Based on a combination of different seismic parameters relations defined by different engineers over the past decades, a seismic hazard analysis has been computed for the Euromax terminal. These relations are all determined empirically and will be presented to you in this chapter.

6.2 Methodology of seismic hazard analysis

Majority of earthquakes in the Netherlands occurs in the south-eastern part of the country and is related to tectonic movements along the Roer Valley Graben (Figure 6-1). The major faults are the Feldbiss and the Peel Boundary Faults on either side of the Roer Valley Graben. Some other earthquakes have been observed in the North of the Netherlands since 1986. This kind of earthquake has been classified as induced seismicity due to the exploration of oil- and gas fields.

Engineer T.H. de Crook found different relations between earthquake parameters during his seismic hazard analysis for the Netherlands [6.1]. The relations derived by the Crook are in principle valid for the south-eastern part of the Netherlands, where most earthquakes has been observed. No specific research on earthquake parameters relations has been

Figure 6-1 Seismotectonic map of the Lower Rhine graben system in the border area of Belgium, Germany and the Netherlands [6.5].

performed near the Euromax terminal due to the few earthquake observations (Figure 6-3). By using the seismic zoning map created by de Crook with a given returnperiod of 475 years (Figure 6-2), a relation can be made between the earthquake parameters at the Euromax terminal and the south east of the Netherlands. Crook's zoning map shows that the horizontal peak ground acceleration at the south-eastern part of the Netherlands is 4,55 times higher than at the Euromax terminal. This Master thesis uses this ratio in determining the return period of different seismic magnitudes for the Euromax terminal.
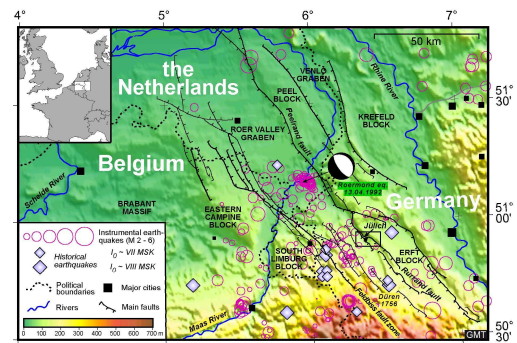

Figure 6-3 Historical earthquakes in the Netherlands between 1904-2004 [6.6]
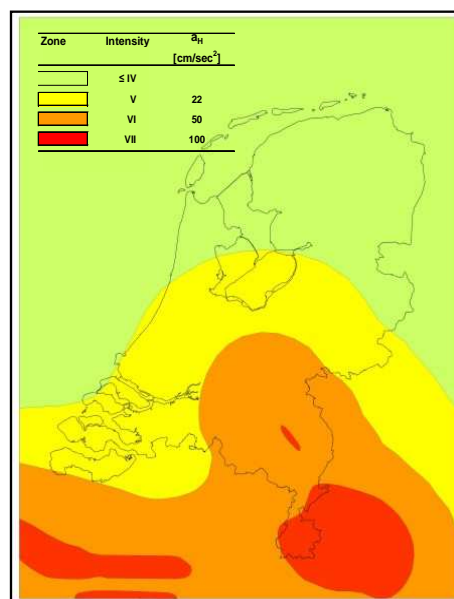
Figure 6-2 Seismic zoning map of the Netherlands [6.1]

Many engineers have done researches about the relation between earthquake parameters. Relations that are used during this thesis are listed below:

Relation between			By engineer(s)
Return period	-	Local magnitude	De Crook
Epicentral intensity	-	Local magnitude	De Crook
Horizontal peak acceleration	-	Modefied mercalli intensity	Murphy and O'brien
Moment magnitude	-	Local magnitude	Reamer and Hinzen

The frequency-magnitude relation for the Netherlands given by De Crook [6.1] was based on only 23 measurement points. While the intensity-magnitude relation for the Netherlands was determined from 42 observed tectonic earthquakes.

J.R. Murphy and L.J. O'Brien carried out an analysis of correlations between acceleration and intensity in June 1977 [6.2]. This relation was based on analysis using a variety of statistical models using 1500 strong-motion accelerograms achieved from all over the world. This relation was used in this report for determining the Peak ground accelerations for different magnitudes.

Reamer and Hinzen [6.3] determined the relation between M_L and M_W for the southern part of the Netherlands based on 20 seismic events. This relation is needed due to the fact that earthquake magnitudes in the Netherlands are determined in local magnitude (M_L), but in the seismic hazard analysis the moment magnitude (M_W) will be used.

Relations that were derived by the above mentioned engineers are shown below. Within the relations of de Crook, some coefficients are still not determined yet and are denoted with a $\pm$ sign followed with a standard deviation. The reason is that Crook's relation counts for the South east area of the Netherlands and within this area the relation are not the same.

$$^{10}\log(N) \pm 0.07 = (1.34 \pm 0.10) - (0.67 \pm 0.03)M_L \qquad \text{[de Crook]} \qquad \textbf{Eq. 6-1}$$

$$I_0 \pm 0.48 = (-1.05 \pm 0.28) + (1.47 \pm 0.08)M_L \qquad \text{[de Crook]} \qquad \textbf{Eq. 6-2}$$

$$^{10}\log a_H = 0.25 I_{MM} + 0.25 \qquad \text{[Murphy and O'brien]} \qquad \textbf{Eq. 6-3}$$

$$M_W = 0.843 M_L + 0.1954 \qquad \text{[Reamer and Hinzen]} \qquad \textbf{Eq. 6-4}$$

where
N   the annual number of events with magnitude equal to or larger than M_L [-]
1/N.   mean annual return period [-]
M_L local magnitude [-]
I_0 the maximum observed epicentral intensity of an earthquake [-]
a_H peak horizontal ground acceleration [cm/s^2]
I_{MM} Modified Mercalli intensity [-]

The seismic zoning map of de Crook (Figure 6-2) shows that, for the south-western part of the Netherlands, an earthquake with a return period of 475 years results in an intensity $I_0 = 7$ and a horizontal peak ground acceleration of $a_H = 100$ cm/s^2. Hence, equation 6-1 and 6-2 can be modified and rewritten as:

$$^{10}\log(N) = 1.32 - 0.69 M_L \qquad \textbf{Eq. 6-5}$$

$$I_0 = -1.3 + 1.43 M_L \qquad \textbf{Eq. 6-6}$$

Earthquake parameters for the South-eastern part of the Netherlands can now be determined. Knowing that the horizontal peak ground acceleration at the south-eastern part of the Netherlands is

TUDelft
Delft University of Technology

Earthquake analysis of quay walls
- Seismic Analysis-

Gemeentewerken
Gemeente Rotterdam

4,55 times higher than at the Euromax terminal, the earthquake parameters for the Euromax terminal also can be determined.

6.3 Results of seismic hazard analysis Euromax

Based on historical observations of tectonic earthquakes and seismic hazard analysis done by T.H. de Crooks [6.1], it can be concluded that there are nearly zero seismic activities at the project location, see Figure 6-3. Earthquakes that probably do occur will have low magnitude and are not likely to cause damage to the quay wall structures. By using the four relations mentioned in the previous section, seismic parameters with a longer return period can be determined for the Euromax terminal as shown in Table 6-1. Some relations between the parameters were plotted in Figure 6-4. Notion must be made that the determined earthquake parameters are due to natural earthquake.

During the analysis is assumed that the intensities I_0 and I_{MM} are equal. Which means that the maximum observed epicentral intensity of an earthquake is located at the Euromax terminal itself. This assumption is very conservative because seismic waves are progressively damped as they travel. Due to the lack of information about the surrounding soil profile, the propagation and epicenter of the earthquake have made it is very difficult to determine the relation between I_0 and I_{MM}.

PGA (a_H)	Return Period (R)	Magnitude		Intensity (I_{MM})
		M_L	M_W	
0.3 m/s^2	880 years	4.3	3.9	4.9
0.4 m/s^2	1540 years	4.7	4.2	5.4
0.5 m/s^2	2365 years	5	4.4	5.8
1.0 m/s^2	9015 years	5.8	5.1	7
1.5 m/s^2	19700 years	6.3	5.5	7.7
2 m/s^2	34350 years	6.6	5.8	8.2
2 .25 m/s^2	43100 years	6.8	5.9	8.4
2.5 m/s^2	52850 years	6.9	6.0	8.6
2.75 m/s^2	63500 years	7	6.1	8.8
3 m/s^2	75100 years	7.1	6.2	8.9
3.5 m/s^2	100100 years	7.3	6.4	9.2
4 m/s^2	130100 years	7.5	6.5	9.4
4.5 m/s^2	164500 years	7.6	6.6	9.6
5 m/s^2	201500 years	7.7	6.7	9.8

Table 6-1 Earthquake parameters determined for the Euromax terminal when assuming that the epicenter of the earthquake is located directly below the Euromax terminal.
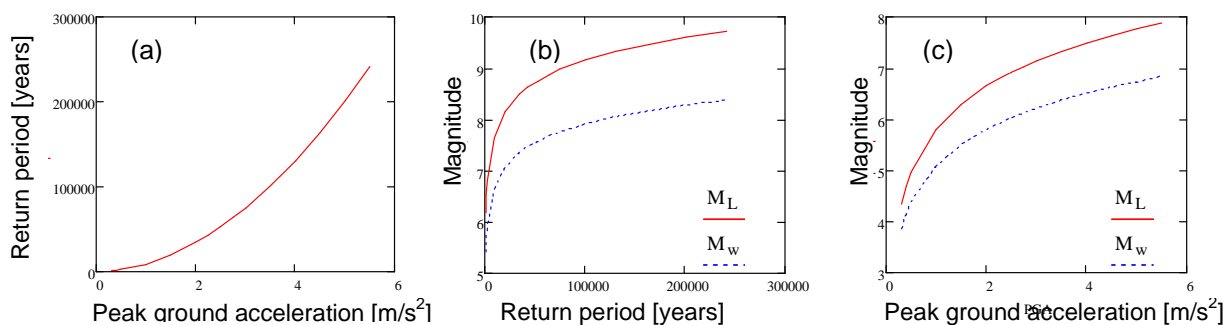
Figure 6-4 Relation between earthquake parameters

        a) Graph of Return period – Peak ground acceleration relation
        b) Graph of Return period – Magnitude relation
        c) graph of Peak ground acceleration – Magnitude relation

According to Eurocode 8 [6.4], a quay wall needs to withstand an earthquake with a return period of 475 years. This results in a horizontal peak ground acceleration of $0,022g$ m/s^2 at the Euromax terminal. This is relatively small compared to what could occur in Japan and will probably not cause any damage. Therefore higher return periods are taken in this thesis which results in a higher earthquake magnitude. This higher magnitude will give a better impression of the behaviour of the quay wall under seismic circumstances.

6.4 References

[6.1] Crook, de Th, A seismic zoning map coforming to Eurocode 8 and practical earthquake parameter relations for the Netherlands, Geologie en mijnbouw, No 75 , page 11-18, 1996
[6.2] Murphy J.R. and L.J. O'Brien, The correlation of peak ground acceleration amplitude with seismic intensity and other physical parameters, 1977
[6.3] Reamer S.K. and K.G. Hinzen, An earthquake catalog for the northern Rhine area, central Europe (1975-2002), seismological research letters 75, page 713-725, 2004
[6.4] Nen-en 1998, Eurocode 8, Design of structures for earthquake resistance, 2005
[6.5] www.aardbevingen.be, 08-2010
[6.6] www.knmi.nl, 08-2010

7. Liquefaction analysis Euromax

7.1 Introduction

Soil liquefaction is a major concern for structures constructed in sandy soils. It is known that earthquakes have the unfavorable effect of increasing active and decreasing passive lateral earth pressures as presented in section 5.4.1. An earthquake can also reduce the shear resistance of a soil during liquefaction. The reduction in the shear resistance of a soil during an earthquake is only effective when the magnitude of the earthquake exceeds a certain limit and the ground conditions are favorable for such a reduction. For this purpose a liquefaction analysis has been performed to determine the dynamic soil response during earthquake.

7.2 liquefaction methodology

It is widely accepted that only recent sediments or fills of saturated, cohesionless soils at shallow depths will liquefy during a large magnitude earthquake. The liquefaction susceptibility of a specific deposit is affected by geologic history, confining pressure, density, and characteristics of the soil grains. An approximate assessment of liquefaction potential can be made on the basis of ground water levels and depositional history.

More quantitative assessments of liquefaction susceptibility are possible with information from subsurface soil explorations. Two basic approaches can be used to predict the liquefaction potential of soil strata:

- Evaluations based on a comparison of the stresses induced by an earthquake and the stress conditions causing liquefaction in cyclic laboratory tests on soil samples.
- Empirical methods based on measurements of in situ soil strength and observations of field performance in previous earthquakes.

Unfortunately, liquefaction assessments based on laboratory tests are hindered by limitations in the ability of laboratory to reproduce field stress conditions in small soil samples. Even more problematic, disturbance of field samples is nearly impossible to avoid and very difficult to quantify in laboratory tests. As a result, early evaluations based on laboratory tests were often overly conservative in predicting liquefaction. Consequently, empirical correlations based directly on observations of field behavior are usually preferred for assessments of liquefaction potential in soil deposits. These methods are commonly based on field penetration tests that can be correlated to the cyclic shear resistance of the in situ soil. In situ penetration tests are also preferred because field measurements provide an economical indication of deposit variability. That is, several penetration tests will yield a better understanding of highly variable natural sediments than careful laboratory testing. For this reason, empirical methods based on in situ penetration tests are almost always favored for engineering assessments of liquefaction potential.

An empirical method developed by Professor H.B. Seed [7.1] to estimate the potential for cyclic liquefaction due to earthquake loading was used in this liquefaction analysis. This stress based approach requires an estimate of the cyclic stress ratio (CSR) profile caused by the design earthquake and the cyclic resistance ratio (CRR) of the soil. A simplified method to determine the CSR was also developed by Seed and Idriss [7.1] based on the peak ground surface acceleration (a_{max}). This simplified method can be summarized as follows:

$$CSR = 0.65 \left[\frac{a_{max}}{g} \right] \left(\frac{\sigma_{vo}}{\sigma'_{vo}} \right) r_d$$

Eq. 7-1

where

$r_d = 1.0 - 0.00765z$ if   z ≤ 9.15m

$r_d = 1.174 - 0.0267z$ if   z > 9.15m

T U Delft
Delft University of Technology

Earthquake analysis of quay walls
- Seismic Analysis-

Gemeentewerken
Gemeente Rotterdam

a_{max} = peak ground surface acceleration [m/s^2]

g = acceleration due to gravity (9.81 m/s^2)

σ_{vo} = vertical total stress [MPa]

σ'_{vo} = vertical effective stress [MPa]

z = numerical value of the depth of the layer

r_d = shear stress reduction factor

In the present study, two simplified cone penetration test (CPT) based methods where used to determine the CRR. The first method was proposed by Robertson & Wride [7.2] (further pronounced by R&W method) and the second by Juang et al. (further pronounced by Juang method) [7.3]. These methods follows the same format as in the simplified procedure originated by Seed and Idriss, in which a chart with a boundary curve that separates

Figure 7-1 Cyclic resistance ratio (CRR) from the CPT for clean sands. [Robertson and Wride. 1998]

liquefied cases from non-liquefied cases based on field experiences, is created and used to judge whether liquefaction will occur. The major difference between the two methods is that the boundary curve of R&W method were largely drawn through visual inspection of data plotted on a 2D graph (Figure 7-1) and the boundary curve of Juang method was based on artificial neural network analysis of field cases.

The methodology by Robertson and Wride and Juang et al. to estimate CRR7.5 (CRR with a moment magnitude of 7.5) from a cone penetration test is summarized in Figure 7-2 and Figure 7-3.

After determining CRR$_{7.5}$ and CSR, the factor of safety (FS) against liquefaction has been calculated using the following equations:

$$FS = \frac{CRR_{7.5}}{CSR} MSF$$
Eq. 7-2

$$MSF = \frac{174}{M^{2.56}}$$
Eq. 7-3

MSF is the magnitude scaling factor, which converts the CRR$_{7.5}$ to the equivalent CRR for the design earthquake Magnitude.

Many investigators have employed statistical and probabilistic methods for assessing liquefaction. But Juang et al. [7.4] developed a different approach to characterize the deterministic model, in which Bayes theorem was used to map the calculated safety index, such as reliability index (β) or factor of safety (FS), to the probability of liquefaction (P$_L$). Simplified procedures for soil liquefaction evaluation, based on the standard penetration test, cone penetration test, and shear wave velocity measurement were used as the basis for developing Bayesian mapping functions. To calibrate the two different deterministic methods used in this thesis, the general mapping function proposed by Juang et al. was used. This function maps the calculated FS to the probability of liquefaction (P$_L$) as shown in equation 7-4.

$$P_L = \frac{1}{1 + (FS/A)^B}$$
Eq. 7-4

where

$A = \begin{cases} 1 & for & Roberston \& Wride \\ 0.96 & for & Juang\,et\,al. \end{cases}$, $B = \begin{cases} 3.3 & for & Roberston \& Wride \\ 4.5 & for & Juang\,et\,al. \end{cases}$

Earthquake analysis of quay walls
- Seismic Analysis-

Gemeentewerken
Gemeente Rotterdam

TUDelft
Delft University of Technology

q_c : tip resistance, f_s : sleeve friction
σ_{vo} , σ_{vo}' : in-situ vertical total and effective stress
units: all in kPa

initial stress exponent : n = 1.0 and   calcualte Q, F, and I_c
if $I_c \leq 1.64$,   n = 0.5
if $1.64 < I_c < 3.30$,   n = (I_c −1.64)*0.3 + 0.5
if $I_c \geq 3.30$,   n = 1.0
iterate until the change in n, $\Delta n < 0.01$
if σ_{vo}' > 300 kPa, let n = 1.0 for all soils

$$C_n = \left(\frac{100}{\sigma_{vo}'} \right)^n$$

$$Q = \frac{(q_c - \sigma_{vo})}{100} \cdot C_n \quad , \quad F = \frac{f_s}{(q_c - \sigma_{vo})} \cdot 100$$

$$I_c = \sqrt{\left[(3.47 - \log Q)^2 + (1.22 + \log F)^2 \right]}$$

if $I_c \leq 1.64$, $K_c = 1.0$
if $1.64 < I_c < 2.60$, $K_c = -0.403 I_c^4 + 5.581 I_c^3 - 21.63 I_c^2 + 33.75 I_c - 17.88$
if $I_c \geq 2.60$,   evaluate using other criteria; likely non- liquefiable if F > 1%
BUT, if $1.64 < I_c < 2.36$ and F < 0.5%, set $K_c = 1.0$

$$(q_{c1N})_{cs} = K_c \cdot Q$$

$$CRR_{7.5} = 93 \cdot \left(\frac{(q_{c1N})_{cs}}{1000} \right)^3 + 0.08 \ , \ \text{if } 50 \leq (q_{c1N})_{cs} < 160$$

$$CRR_{7.5} = 0.833 \cdot \left(\frac{(q_{c1N})_{cs}}{1000} \right) + 0.05 \ , \ \text{if } (q_{c1N})_{cs} < 50$$

if $I_c \geq 2.60$,   evaluate using other criteria; likely non- liquefiable if F > 1%

Where

q_v =Tip resistance [kPa]

f_s = Sleeve friction [kPa]

σ_{VO} = In-situ vertical total stress grains [kPa]

σ_{VO}'   = In-situ vertical effective stress grains [kPa]

Q   = Normalized CPT penetration resistance

F   = Normalized friction ratio [%]

I_c = Soil behavior type index [Robertson,1990]

K_c = Correction factor that is a function of grain characteristics of the soil

$(q_{c1N})_{cs}$ = Clean sand normalized cone penetration resistance

$CRR_{7.5}$ = Cyclic resistance ratio for a 7.5 magnitude earthquake

Figure 7-2 Flow chart to evaluate cyclic resistance ratio (CRR) from CPT according to the R&W [Robertson and Wride, 1998]

q_c : tip resistance,
f_s : sleeve friction
σ_{vo}, σ_{vo}' :in-situ vertical total and effective stress
Units: all in kPa

$$q_{c1N} = q_c / (\sigma_{vo}')^{0.5}$$
Both q_c and σ_{vo}'
must be in the unit of atm.

$$F = f_s / (q_c - \sigma_{vo}) \times 100\%$$

$$I_c = \left[(3.47 - \log q_{c1N})^2 + (\log F + 1.22)^2 \right]^{1.5}$$

$$(q_{c1N})_{cs} = q_{c1N} \left(2.429 I_c^4 - 16.943 I_c^3 + 44.551 I_c^2 - 51.497 I_c + 22.802 \right)$$

$$C_\sigma = -0.016 (\sigma_{vo}'/100)^3 + 0.178 (\sigma_{vo}'/100)^2 - 0.063 (\sigma_{vo}'/100) + 0.903$$

$$CRR_{7.5} = C_\sigma \exp \left[-2.957 + 1.264 ((q_{c1N})_{cs}/100)^{1.25} \right]$$

Where

q_v =Tip resistance [kPa]

f_s = Sleeve friction [kPa]

σ_{VO} = In-situ vertical total stress grains [kPa]

σ_{VO}'   = In-situ vertical effective stress grains [kPa]

q_{c1N} = Normalized CPT penetration resistance

$(q_{c1N})_{cs}$ = clean sand normalized cone penetration resistance

F   = normalized friction ratio [%]

I_c = Soil behavior type index [Robertson,1990]

$CRR_{7.5}$ = Cyclic resistance ratio for a 7.5 magnitude earthquake
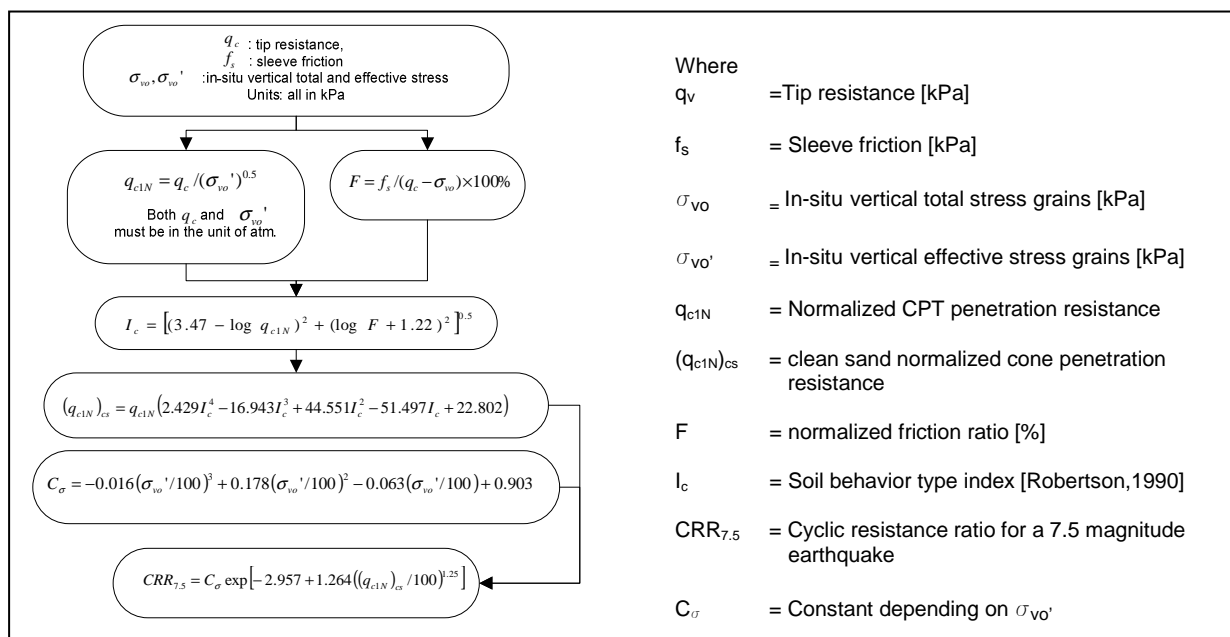
C_σ = Constant depending on σ_{VO}'

Figure 7-3 Flow chart to evaluate cyclic resistance ratio (CRR) from CPT according to the method of Juang et al. [Juang et al., 2003]

TUDelft
Delft University of Technology

Earthquake analysis of quay walls
- Seismic Analysis-

Gemeentewerken
Gemeente Rotterdam

During the analysis some assumptions were made and are listed below:

- Some soil layers have a soil behaviour type index (I_c) higher than 2.6 during analyzing using the Robertson and Wride method. This method is not applicable in these cases. Although these cases should be further evaluated by other methods such as the SPT-based method, their probabilities of liquefaction are assumed to be zero in the present study, as they are generally considered too clay-rich to liquefy in the Robertson and Wride method.
- Assumed during this analysis was that liquefaction will occur if the probability of liquefaction is equal or higher than 0,6.
- Influences of liquefiable layers to each other are not included in this analysis. Assumed was that a liquefiable layer will not trigger other layers to liquefy at an earlier stage. This assumption is not totally correct because a frictional material like sand will get influenced by their surrounding. This assumption was taken due to the state of the art of this phenomenon
.

7.3 Liquefaction results

The Euromax terminal has a total quay length of 1900 meters. Diversity in ground profile occurs beneath the terminal. Analyzing the soil beneath the total quay length per running meter is very time consuming. Therefore, 14 different ground profiles, which assumed to represent the whole quay length, have been used for this research in determining the liquefaction potential. The ground profile within each section can be assumed equal. These 14 ground profiles follows from the research did by BAM as mentioned in section 3.2.2 and will not be further questioned. More information about the location of these ground profiles can be found in appendix A.

A liquefaction potential analysis has been performed for the 14 ground profiles using the two methods mentioned in section 7.2. All the results obtained from these two CPT-based methods for these ground profiles are presented in appendix D.

The liquefaction predictions made with these two methods are compared in the analysis. Both the methods are showing the same liquefiable layers for the 14 different ground profiles. It must be noted that liquefaction only occurs at saturated soils without draining, therefore, no liquefaction will occur above the ground water table and places where drainage is adopted.

The result of the liquefaction analysis shows that ground profile at section 1 (location 0-100m) is the most sensitive to liquefaction compared to the others. Several layers of loose sand occur in this profile, see Figure 7-4. This result is in agreement with the theory of liquefaction, because liquefaction potential for these loose sand layers is very high.
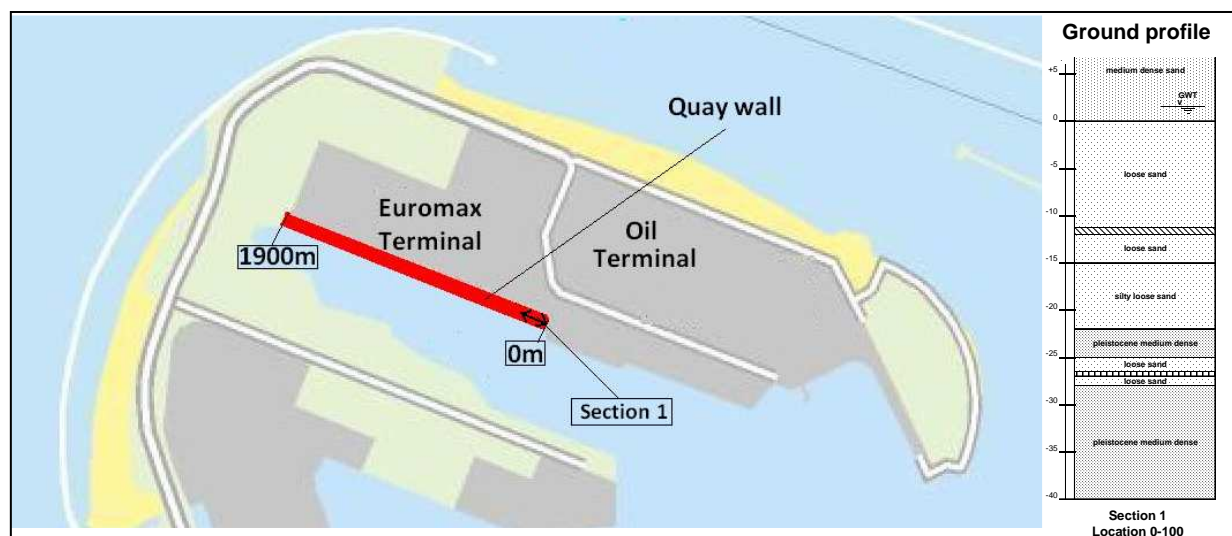

Figure 7-4 Liquefiable layers using the normative earthquake parameters according to the Robertson and Wride method, Return period: 7510 years, section 1 of the Euromax terminal.

Almost all the layers with loose sand are probably going to liquefy if an earthquake with horizontal peak ground acceleration of 0,3g occurs (Figure 7-5). Non-liquefy loose sand layers according to the Robertson and Wride method in between of two liquefiable layers are also assumed liquefiable due to the loss of the bearing capacity of the soil beneath, hence causes the non-liquefy soil to be unstable and tending to go to a liquefiable state. This result corresponds with the research conducted by Okamoto [7.5]. Okamoto indicated that when the average ground acceleration is larger that 0.3g, liquefaction occur and there is a considerable reduction in strength for most soils. However, he claimed that in many cases, the ground acceleration is less than 0.3g and the mechanical properties of most soils do not change significantly in these cases.

Soils made out of loam or clay are not liquefiable according to the analysis result. These layers are very thin and are located between liquefiable layers. Just like non-liquefy loose sand layers, these clayey and loam soil will probably loose their stability and tend to liquefy. The only layers which are not liquefiable are the layers made out of Pleistocene medium dense sand located between Nap -21m and Nap -25 and below NAP -28m.

For further calculation during this analysis, findings achieved from the Robertson and Wride method will be used. Liquefaction will occur if and only the earthquake magnitude is at least 0,3g. This corresponds with an earthquake return period of 75100 years based on the seismic hazard analysis done in Chapter 6.

7.4 References

[7.1]   Seed H.B. and Idriss I.M., Simplified procedure for evaluation soil liquefaction potential, J. Soil Mech. Found. Div., ASCE, 107, page 1249-1274,1971
[7.2]   Robertson P.K. and Wride C.E., Evaluating cyclic liquefaction potential using the cone penetration test, 1998
[7.3]   Juang C.H. and Yuan H. and Lee D.H. and Lin P.S., A simplified CPT-based method for evaluating liquefaction resistance of soil, Journal of geotechnical and geo-environmental engineering, vol 129, No. 1, page 66-80,2003
[7.4]   Juang C.H. and Jiang T., assessing probabilistic methods for liquefaction potential evaluation, ASCE geotechnical special publication no. 107, page 148-162, 2000
[7.5]   Okamoto S., Introduction earthquake engineering, University of Tokyo Press, page 62, 1973

Cyclic liquefaction		
From (m NAP)	till (m NAP)	Thickness layer
-1,13	-2,77	1,64 m
-3,23	-3,81	0,58 m
-4,15	-11,21	7,06 m
-11,55	-19,01	7,46 m
-19,37	-21,04	1,67 m
-24,91	-25,19	0,28 m
-25,48	-26,31	0,83 m
-26,88	-28,14	1,26 m

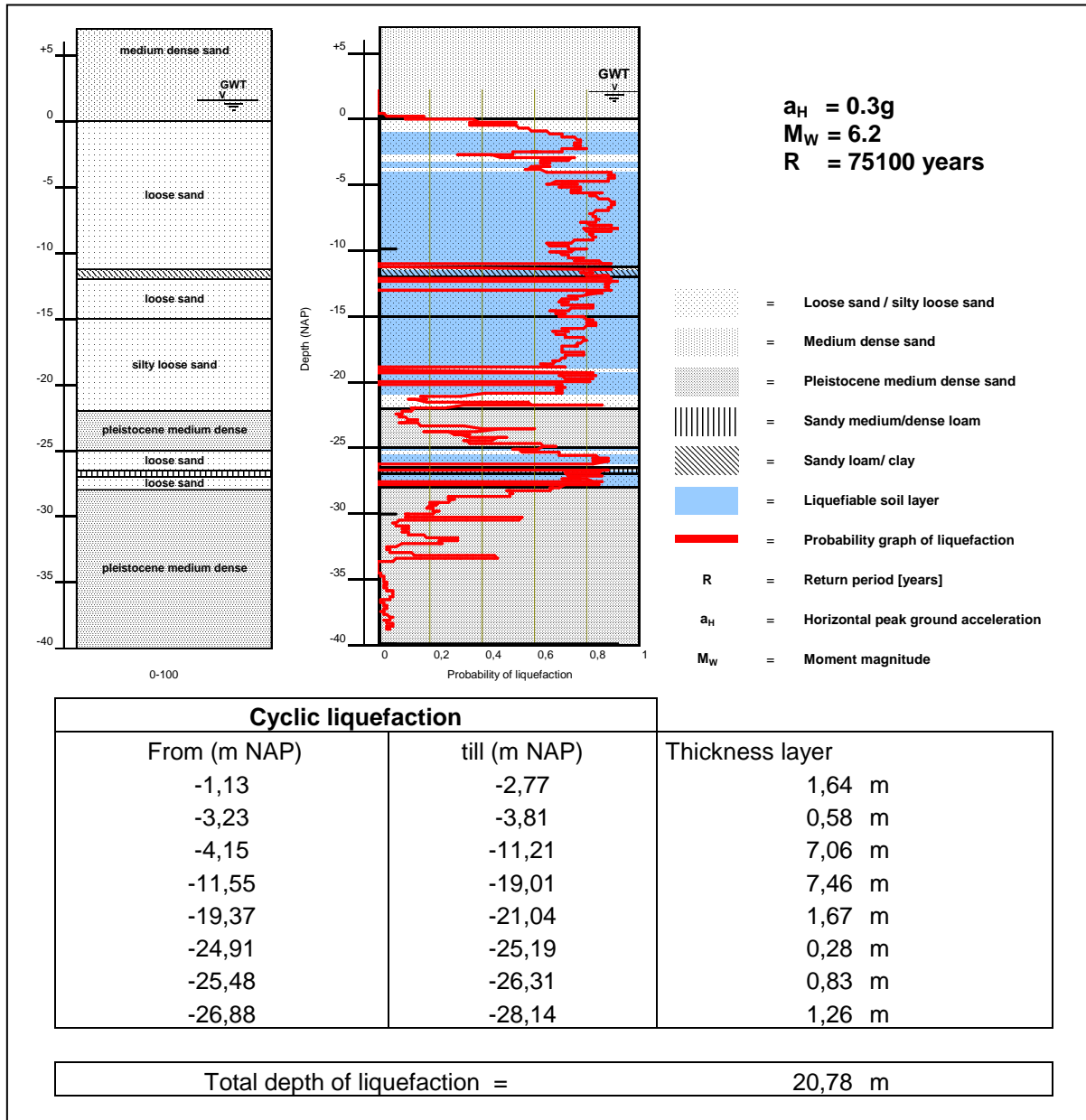| Total depth of liquefaction =	20,78 m

Figure 7-5 Liquefiable layers using the normative earthquake parameters according to the Robertson and Wride method, Return period: 7510 years, section 1 of the Euromax terminal.

Earthquake analysis of quay walls
- Seismic Analysis-

TUDelft
Delft University of Technology

Gemeentewerken
Gemeente Rotterdam

8. Seismic analysis of diaphragm quay wall

8.1 Introduction

The seismic response of quay wall structures is a complex soil-structure interaction problem. Wall movements and dynamic earth pressures depend on the response of the soil underneath the wall, the response of the backfill, the inertial and flexural responses of the wall itself, and the nature of the input motions.

A static analysis of the diaphragm quay wall was performed which in a later stadium can be compared with the seismic analysis. Seismic forces were not included during this static analysis. Thereafter, seismic behaviour of the quay wall was investigated by performing a dynamic analysis. This was done in two ways. To get a first impression of the stresses within the diaphragm quay wall due to seismic forces, a pseudo static analysis was performed based on hand calculations using the Westergaard and M-O method mentioned in section 5.4.1. Finally, a finite element method was used to give an even more accurate result in the behaviour of the diaphragm quay wall during earthquakes. To validate the finite element model, the two static analysis mentioned above will be compared. Also the results of the design calculation performed by DMC [8.3] will be compared.

8.2 Static analysis of diaphragm quay wall

8.2.1 Static analysis with the subgrade reaction method

For a first approximation an analysis is made using the subgrade reaction method. In order to perform this analysis, the program Msheet of Geodelft's M-series is used. Msheet is a program that models sheet pile walls as linear elastic beams based on Bernoulli's equation under the assumption that plane sections remain plane. This is valid for relatively small deformations. The soil is modeled as a foundation of uncoupled springs. Effects of cyclic loading, arc effects, second order effects of soil displacement, effects of displacement of the anchor wall on the quay wall and stress dependent stiffness moduli are not accounted for here. Hence, for determining the internal forces of the wall this is a reasonable approximation, but for deformation issues a more advanced program is indispensable. However the calculation with the subgrade reaction method is meant to illustrate the internal forces and the bending behaviour of the diaphragm wall.

The geometry of the Msheet model is based on design drawings of the Euromax quay wall Figure 2-2 and the soundings at quay wall section 1 Figure 7-4 which is the most sensitive section to liquefaction. Pile and wall stresses due to the forces acting on the relieving structure are determined in Appendix F. Hence, spring support was placed at NAP-1,5m to simulate the anchor force of the MV-pile and a moment load was placed at NAP-1,5m due to the eccentricity between the relieving floor and diaphragm wall. By doing so, the forces coming from the relieving floor are added to the diaphragm wall whereby the relieving floor and it loads can be left out in the geometry. Schematisation of the Msheet geometry is illustrated in Figure 8-1. The corresponding material properties and soil parameters of this geometry can be found in Appendix G.
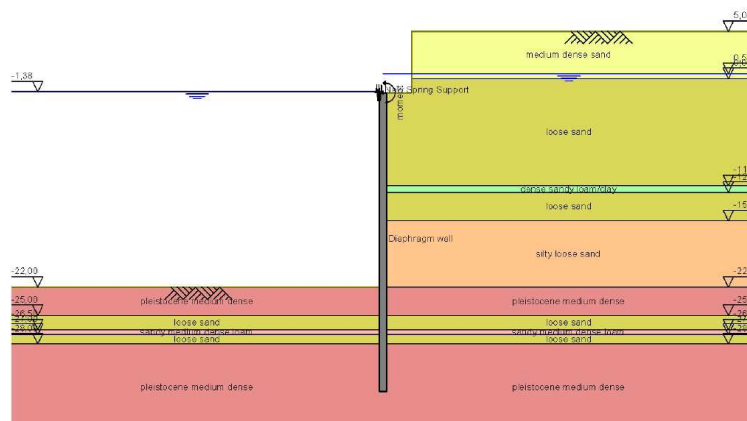

Figure 8-1 schematized geometry in Msheet

To find the normative stresses in the

TUDelft
Delft University of Technology

Earthquake analysis of quay walls
- Seismic Analysis-

Gemeentewerken
Gemeente Rotterdam

diaphragm wall, the combination of the maximum occurring bending moments and normal force must be found. Furthermore, the maximum bending stresses and compressive stresses shall be calculated. Therefore, three load combinations have been studied. First combination includes only the permanent loads acting on the quay wall structure. For the second and third combination, variable loads were included depending on the occurrence and the direction of the load application. Notion must be made that not al the variable loads could be present at the same moment. Fender (pushing) and bolder (pulling) forces will not act at the same time. Through this, bolder force was included in load combination 2 and fender force for combination 3. As for the crane force, cranes in operation was chosen due to the fact that this results in much more vertical loading force compared to cranes during storms.

> Load combination 1: Permanent loads only
> Load combination 2: Permanent loads + surcharge load + crane load + bolder force
> Load combination 3: Permanent loads + surcharge load + crane load + Fender force

Load factors will be set as 1 because the real acting forces on the structure is needed for this analysis. The probability that extreme variable loads in a combination occur simultaneously is translated into a reduction factor called combination factor. The combination factors for permanent and variable loads are set to 1 and 0.7 respectively according to CUR 211 [8.6]. This will give a more realistic representation of the situation. The three load combinations including load and combination factors are listed in Table 8-1. The most normative load combination will be used during the dynamic calculation.

Load combination 1	Combi factor	Load factor
Own weight relieving platform	1	1
Crane load in operation		
Crane load during storm		
Bolder force		
Fender force		
Groundwater +0,52 NAP	1	1
Groun pressure +0,52 NAP	1	1
Seawater -1,38 NAP	1	1
Surcharge load above platform		
Surcharge load behind platform		
Surcharge load behind landside crane		

Load combination 2	Combi factor	Load factor
Own weight relieving platform	1	1
Crane load in operation	0,7	1
Crane load during storm		
Bolder force	0,7	1
Fender force		
Groundwater +0,52 NAP	1	1
Groun pressure +0,52 NAP	1	1
Seawater -1,38 NAP	1	1
Surcharge load above platform	0,7	1
Surcharge load behind platform	0,7	1
Surcharge load behind landside crane	0,7	1

Load combination 3	Combi factor	Load factor
Own weight relieving platform	1	1
Crane load in operation	0,7	1
Crane load during storm		
Bolder force		
Fender force	0,7	1
Groundwater +0,52 NAP	1	1
Groun pressure +0,52 NAP	1	1
Seawater -1,38 NAP	1	1
Surcharge load above platform	0,7	1
Surcharge load behind platform	0,7	1
Surcharge load behind landside crane	0,7	1

Table 8-1 Load combinations

Results

Static analyses with the subgrade reaction method are performed for the three load combinations mentioned in the upper section. Soil profile most sensitive to liquefaction is used during this analysis, which has been determined in section 7.3. Forces acting on the relieving floor were determined for each load combination and are shown in Appendix F. Pile and wall stresses due to forces acting on the relieving floor were determined for each load case separately by modeling the superstructure as statically determined. By combining these stresses of different load cases, total wall and pile stresses can be determined caused by the forces acting on the relieving structure. These stresses were used as input for the Msheet calculation. The Msheet model with the corresponding input parameters can be found in Appendix G. Results of the Msheet calculation is shown in Table 8-2. Extended calculations are also presented in Appendix G.

Msheet Stresses	Max. Bending moment diaphragm wall kNm/m	Normal force Diaphragm wall kN/m	Normal force MV-Pile kN/m	Normal force Vibro pile (in total) kN/m
Load combination 1	3232	-1305	331	-1166
Load combination 2	3998	**-3124**	**719**	-1486
Load combination 3	**4084**	-2576	86	**-1593**

Table 8-2 Wall and pile stresses for different load combinations according to Msheet

Disadvantages of Msheet are that no arching and second order effects are included during the calculation. Arching effects will cause a decrease in bending moment of the diaphragm wall and an increase of tension force of the MV-pile. On contrary, the second order effects will increase the bending moment of the diaphragm wall. Determination of these increase and decreases are based on CUR-166 [8.4] and can be found in Appendix G. The result of Msheet including arching and second

TUDelft
Delft University of Technology

Earthquake analysis of quay walls
- Seismic Analysis-

Gemeentewerken
Gemeente Rotterdam

order effects are shown in Table 8-3 where the normative stresses are marked bolt. Axial forces of the diaphragm wall and vibro piles are assumed not to change due to the arching and second order effects. This assumption is permitted because this is a first approximation.

Msheet Stresses	Max. Bending moment diaphragm wall kNm/m	Normal force Diaphragm wall kN/m	Normal force MV-Pile kN/m	Normal force Vibro pile (in total) kN/m
Load combination 1	2814	-1305	368	-1166
Load combination 2	**3785**	**-3124**	**769**	-1486
Load combination 3	3760	-2576	134	**-1593**

Table 8-3 Wall and pile stresses for different load combinations according to Msheet with arching and second order effects included

The result of Msheet shows that load combination 2 is normative for the bending moment and axial stress for the diaphragm wall and the MV-pile, were load combination 3 is normative for axial stresses of the vibro piles. The presence of bolder force has a major influence on the axial stress of the MV-pile. This force tends to pull the quay wall towards sea, which results in an increase of force of the tension piles. The calculated results after including arching and second order effects corresponds with the Msheet result performed by DMC [8.3].

8.2.2 Static analysis with the finite element method

Now that a first order magnitude of static stresses have been indicated by the subgrade reaction method, a more detailed static analysis can be performed by using a finite element program. For this static analysis, the program Plaxis 2D V9 is chosen. The wide range of applications, user friendly interface and experience among specialists from Delft University of Technology and IGWR are the main reasons for this decision. Plaxis 2D is a two dimensional finite element program to analyze the stability and deformation of geotechnical problems by making use of constitutive material models that simulate the real behaviour of the soil into a 2D geometry. The program transforms the real continuous situation into a discrete system of triangular elements. For each element, a system of differential equations is solved. Every element is coupled by means of nodes with a number of degrees-of-freedom per node. By assembling the system of elements of the mesh, the real behaviour of the entire problem area can be determined. Stresses and deformations of the ground are included in the calculation of Plaxis where for Msheet the deformations are only restricted to the diaphragm wall.

The geometry of the Plaxis model is based on design drawing of the Euromax quay wall Figure 2-2 and the soundings at quay wall section 1 Figure 7-4 which is the most sensitive section to liquefaction. On the contrarily to Msheet, all the elements of the quay wall are modeled in Plaxis which results in the following Plaxis geometry shown in Figure 8-2. The Boundary conditions, choice of material model, material properties and soil parameters of the Plaxis model can be found in Appendix H.
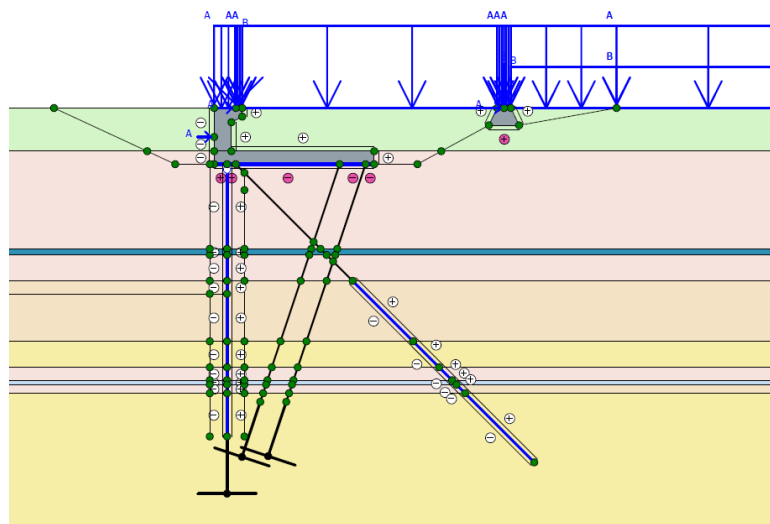

Figure 8-2 Schematization of the Plaxis geometry

TUDelft
Delft University of Technology

Earthquake analysis of quay walls
- Seismic Analysis-

Gemeentewerken
Gemeente Rotterdam

Results

The three load combination shown in Table 8-1 are implemented in the static analysis using Plaxis. The output of the Plaxis calculations and the method in which the model is created is clarified in Appendix H. The order in which the considerations about the model are described is the same order in which the model is given in Plaxis. Just like the subgrade reaction method, the soil profile most sensitive to liquefaction is analyzed. An improvement of Plaxis compared to the Msheet is that arching effects are included during the calculation. For this analysis no second order effects are included because no large deformations will occur which will result in small second order stresses. These second order stresses are just a very small fraction of the total stresses and therefore can be neglected. Results of the Plaxis calculation are shown in Table 8-4 and Table 8-5.

PLAXIS Stresses	Max. M diaphragm wall kNm/m	N diaphragm wall kN/m	Max. N MV pile kN/m	Max. N Vibro pile 1 kN/m	Max. N Vibro pile 2 kN/m
Load combination 1	2500	-1792	836	-822	-247
Load combination 2	**3130**	**-3527**	**851**	-1601	-545
Load combination 3	3020	-3039	428	**-1670**	**-611**

Table 8-4 Wall and pile stresses for different load combinations according to Plaxis

PLAXIS Displacements	Displacement seaside crane rail		Displacement landside crane rail	
	Horizontal	Vertical	Horizontal	Vertical
Load combination 1	-0,039 m	-0,005 m	-0,045 m	-0,048 m
Load combination 2	**-0,047 m**	**-0,008 m**	**-0,060 m**	**-0,285 m**
Load combination 3	-0,003 m	0,005 m	-0,031 m	-0,254 m

Table 8-5 Displacements of crane rails according to Plaxis

In accordance to the results achieved from the Msheet calculation, load combination 2 is also normative according to Plaxis calculations. Stresses and displacements are the highest for load combination 2. No large displacements were found near the seaside crane foundation. These small deformations are allowable according to the design requirements shown in chapter 3. In contradiction with the seaside crane foundation, the displacement of the landside crane foundation is too high. These large displacements are the results of heavy crane and surcharge load above the landside crane foundation.

8.2.3 Validation of Plaxis model

The results of the two different approaches are compared and shown in Table 8-6 and Table 8-7. Own weight of the diaphragm wall was added to the Msheet results in order to make a good comparison of the axial stresses of the diaphragm wall. For determining the own weight, the weight of the diaphragm wall under water was used which is $15kN/m^3$. The stresses of the diaphragm wall are quite similar for both methods. On the contrary, variations of pile forces are quite large. The reason for this is that the vibro piles are modeled as one pile during the Msheet calculation and two piles for the Plaxis calculation. Hence, different axial pile forces acts on both the vibro piles that result in a different horizontal and vertical force equilibrium, which have resulted in lower pile forces for the Msheet calculation.

	Diaphragm wall						
	Depth max. M_{Msheet} [m]	M_{Msheet} [kNm/m]	N_{Msheet} [kN/m]	N_{Msheet} (incl. own weight) [kN/m]	M_{PLAXIS} [kNm/m]	N_{PLAXIS} [kN/m]	$\dfrac{M_{PLAXIS}}{M_{Msheet}}$
Load combination 1	NAP-12,75	2814	-1305	-1507	2500	-1792	0,89
Load combination 2	NAP-14,25	**3785**	**-3124**	**-3354**	**3130**	**-3527**	0,93
Load combination 3	NAP-13,5	3760	-2576	-2792	3020	-3039	0,80

Table 8-6 Comparison of Msheet and PLAXIS results for the diaphragm wall

TUDelft
Delft University of Technology

Earthquake analysis of quay walls
- Seismic Analysis-

Gemeentewerken
Gemeente Rotterdam

	MV pile		Vibro piles	
	Max. N_{Msheet} [kN/m]	Max. N_{Plaxis} [kN/m]	Max. N_{Msheet} [kN/m]	Max. N_{Plaxis} [kN/m]
Load combination 1	368	836	-1166	-1069
Load combination 2	**769**	**851**	-1486	**-2146**
Load combination 3	134	428	**-1593**	-2281

Table 8-7 Comparison of Msheet and PLAXIS results for the MV and vibro piles

The Plaxis results are quite similar like the result of the design documents [8.3]. The differences of the results are smaller than 25%, which is a good result for a geo-engineering problem. In addition, onsite observations showed that there are indeed large settlements near the landside crane foundation, which indicated the Plaxis model corresponds with the real situation.

8.3 Dynamic analysis

8.3.1 Pseudo static analysis diaphragm wall by hand

To get a better impression how the different seismic forces will influence the behavior of the quay wall structures a simplified handmade calculations were made using a pseudo static analysis. The backfill soil is assumed to be a homogeneous loose sand layer with γ_{dry}=17 kN/m^3, γ_{wet}=19 kN/m^3 and φ=30°. The soil in front of the wall is assumed to be a homogeneous layer made out of Pleistocene medium dense sand with γ_{dry}= 18kN/m^3, γ_{wet}=20 kN/m^3 and φ=35° as illustrated in Figure 8-3.
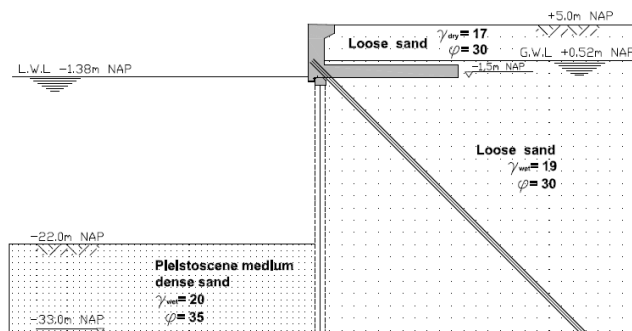

Figure 8-3 Simplified soil model

Three cases were analyzed depending upon the magnitude of excess pore water pressures generated during the earthquake. They range from the case for no excess pore water pressures (case 1) to the extreme case corresponding to the complete liquefaction (case 3) and the intermediate case of residual excess pore water pressures within the backfill of the quay wall (case 2). Peak ground acceleration caused by the earthquake is assumed equal for all three cases, which is 0,5 m/s^2. Earth and water pressures acting on the quay wall for the three different cases can be found in Figure 8-4. Only load combinations 2 is used during this analysis. According to the static analysis, this is the normative load combination, which will result in the highest stresses within the wall and piles of the quay wall structure. For the first approximation the forces acting on the relieving structure are assumed not to influence the diaphragm wall and the MV-pile.

Case 1: no excess pore water pressure
Case 2: excess pore water pressure is 50 percent of the initial vertical effective stress
Case 3: Complete liquefaction of backfill

In Figure 8-4 $U_{stat,back}$ corresponds to the steady state pore water pressure force along the back of the sheet pile wall, $U_{stat,sea,front}$ the hydrostatic water pressure force exerted by the free standing water along the front of the pool, $U_{stat,ground,front}$ is the steady state pore water pressure force along the front toe of the wall. $U_{dyn,sea,front}$ corresponds to the hydrodynamic water pressure force along the front of the wall due to earthquake shaking of the free standing water, $U_{dyn,ground,front}$ and $U_{dyn,ground,back}$ the hydrodynamic water pressure force of the pore water along the front and along the back of the sheet pile wall respectively. $U_{dyn,epwp,front}$ and $U_{dyn,epwp,back}$ corresponds to the excess pore water pressure force acting along the front of the wall and along the back of the wall (case 2). In case of liquefied

TUDelft
Delft University of Technology

Earthquake analysis of quay walls
- Seismic Analysis-

Gemeentewerken
Gemeente Rotterdam

backfill, $LF_{hydrostatic}$ and $LF_{hydrodynamic}$ are equal to the equivalent heavy fluid hydrostatic pressure of the liquefied backfill and the hydrodynamic due to the acceleration of the liquefied backfill (case 3).
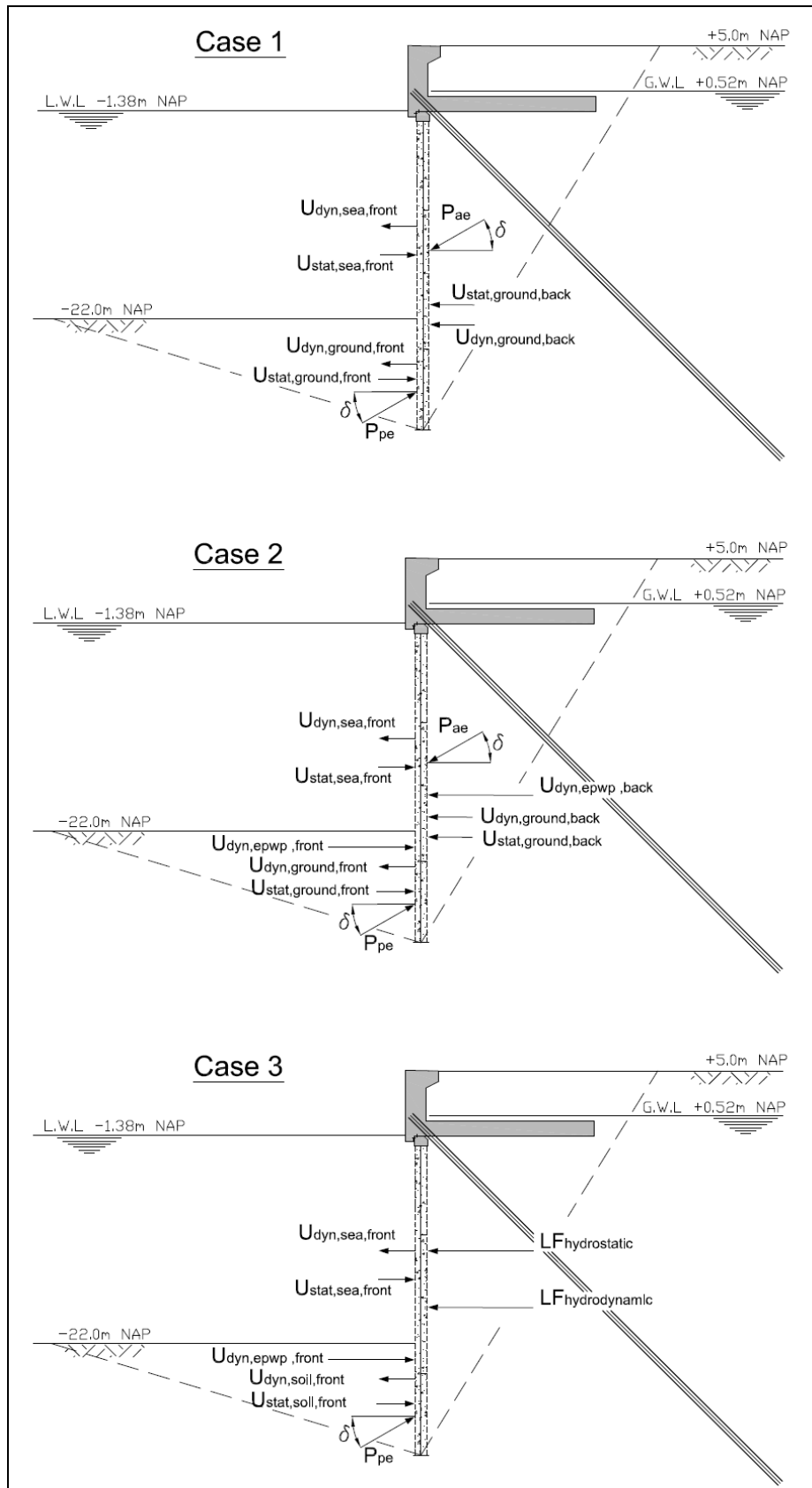

Figure 8-4 Forces acting on diaphragm wall or the three different cases

TUDelft
Delft University of Technology

Earthquake analysis of quay walls
- Seismic Analysis-

Gemeentewerken
Gemeente Rotterdam

For the purpose of the pseudo static analysis, the seismic action is represented by a set of horizontal and vertical static forces equal to the product of the gravity forces and a seismic coefficient. The vertical seismic action is considered as action upward or downward to produce the most unfavorable effect. Due to the absence of seismic studies near the project location, the horizontal and vertical seismic coefficients (k_h and k_v) affecting all the masses shall be taken according to the Eurocode 8 [8.9]. No national annex for this Eurocode is available for the Netherlands because of the few earthquakes that occur and the low seismicity of the earthquakes. Therefore, a response spectrum with a soil factor of 1.35 was adopted as recommended by the Eurocode 8. By knowing the horizontal peak ground acceleration, soil factor, the seismic coefficient k_h and k_v can be determined as shown below:

$$k_h = \frac{a_{pga}}{g} \frac{S}{r}$$ **Eq. 8-1**

$$k_v = 0.33 k_v$$ **Eq. 8-2**

Where
k_h, k_v = horizontal and vertical seismic coefficient [-]
g = gravitational acceleration [m/s^2]
S = soil factor (=1.35)
a_{pga} = horizontal peak ground acceleration [m/s^2]
r = factor depending on the type of retaining structure. In presence of saturated cohesionless soils susceptible to the development of high pore pressure, the r factor should be taken as 1 according to Eurocode 8 [-]

Seismic coefficients have been determined for different horizontal peak ground accelerations as shown in Table 8-8.

a_{pga} [m/s^2]	k_h	k_v
0.5	**0.067**	**0.022**
1	0.14	0.05
1.5	0.20	0.07
2	0.27	0.09
2.5	0.35	0.12
3	0.41	0.14
3.5	0.48	0.16

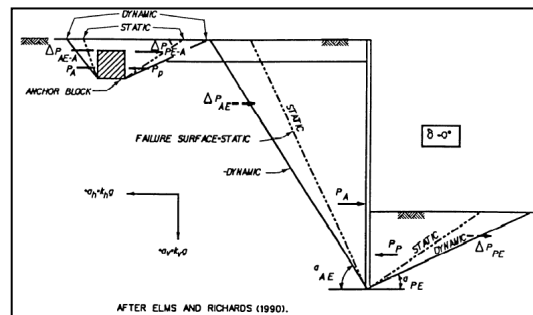*Table 8-8 Seismic coefficients for different peak ground accelerations*

Figure 8-5 normative Earthquake acceleration direction

Method used

Earthquake may cause different unpleasant effect to a quay wall structure. This includes development of additional dynamic earth and water force. The dynamic earth and water forces each can be separated into a fluctuating component and a non-fluctuating component, as shown in Figure 8-6. Fluctuating component are caused by the change of direction/movement of the earthquake. The non-fluctuating component of the dynamic resultant force consists of the non-fluctuating component of the dynamic earth force and the non-fluctuating component of the dynamic water force. The latter two forces are caused by the generation of excess pore water pressure in the soil.
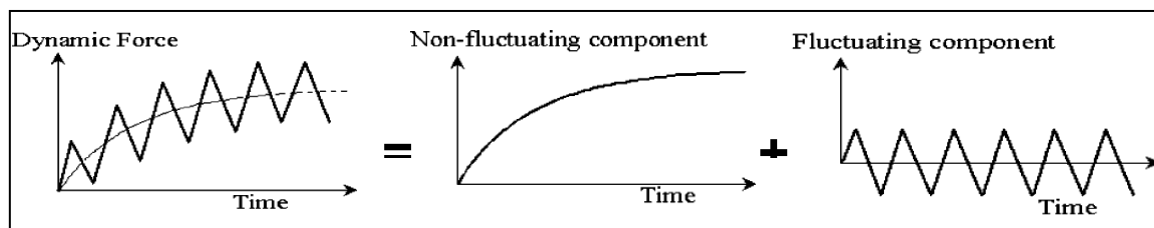

Figure 8-6 Division of fluctuating and non-fluctuating components

Earthquake analysis of quay walls
- Seismic Analysis-

Gemeentewerken
Gemeente Rotterdam

TUDelft
Delft University of Technology

The resultant thrust from the interaction among these force components during an earthquake develops at the contact surface between the backfill soil and the wall. The magnitude of each force component is computed as follows. Depending on the presence of excess pore water pressure the fluctuating dynamic earth pressure force (P_{ae}, P_{pe}) is determined using the M-O method (no excess pore water pressure) or the modified M-O method (with excess pore water pressure) mentioned in appendix C and section 5.4.1. The Westergaard solution was used in determining the fluctuating dynamic water pressure (section 5.4.1). An overview of methods that were used during this analysis is listed in Table 8-9.

Forces	method
Static earth pressure	Coulomb
Static water pressure	Hydrostatic pressure
Dynamic earth pressure (no excess pore pressure)	Mononobe & Okabe
Dynamic earth pressure (with Excess pore pressure)	Modified Mononobe & Okabe
Dynamic water pressure	Westergaard
Excess pore water pressure	Assumed
Surcharge load and crane load	Ohde

Table 8-9Overview of method that were used during the analysis

Seismic direction
Ground moves in different directions during an earthquake, vertically and horizontally. Each direction combination produces different forces acting on the sheet pile. The most unfavorable direction combination is used during this analysis. This is when the horizontal acceleration (a_h) is directed towards the backfill and the vertical acceleration (a_v) is directed downward (see Figure 8-5), causing the incremental dynamic earth pressure forces ($\Delta P_{AE/PE}$) acting away from the backfill. This has the normative effect of increasing the driving force behind the sheet pile and decreasing the stabilizing force in front of the sheet pile. The inertial forces due to the acceleration of the soil mass have the effect of decreasing the slope of the active and passive soil wedge failure surfaces, as shown in Figure 8-5. The slope angles α_{AE} and α_{PE} for the slip planes decrease (the slip planes become flatter) as the acceleration levels increase in value.

Calculations for the three different cases can be found in appendix I. The results of these calculations are shown below.

Case 1: Diaphragm wall with relieving platform - no excess pore water
In this case, no excess pore water pressure and an earthquake acceleration of 0,5m/s^2 is assumed. Dynamic earth pressures are calculated using the M-O method were the dynamic water pressures is determined using the Westergaard method. The impact surcharge and crane load on the wall can be estimated using the method created by Ohde [8.4]. By determining the static and dynamic forces acting on the diaphragm wall caused by the earthquake using the above mentioned method, the minimum required penetration depth of the diaphragm wall, the maximum bending moment of the diaphragm wall and axial pile force of the MV pile can be calculated using the horizontal and moment equilibrium as shown in appendix I.

The calculated required penetration depth of the wall is 7,21m resulting in a total wall height of 27,71m. This height is smaller than the existing wall height, which means the wall is stable and will not slip away from below for case 1. Hence, the ground near the toe of the wall will not be fully mobilized resulting in less passive earth pressure and more active earth pressure against the wall.

Once the required depth of wall penetration is determined the horizontal component of the anchor force per running meter width of the wall is computed using the equations for horizontal force equilibrium, resulting in anchor force of 1221kN/m. The centre to centre distance of the MV-piles are 5,6m resulting in a force of 6838kN for each pile. This pile force does not exceed the tensile capacity of the MV-pile of 11050kN which is determined by IGWR [8.5].

The maximum bending moment within the diaphragm wall is determined by calculating the internal bending moment at the elevation at which the shear is equal to zero. The maximum bending moment is 6409 kNm/m and is located an elevation of NAP-14,8m. The maximum bending moment exceeds the moment capacity of the diaphragm wall of 3744kNm/m which is calculated in Appendix L2

assuming an axial force of -4050 kN/m within the wall. The diaphragm wall will break resulting in failure of the quay wall.

Case 2: Diaphragm wall with relieving platform - with excess pore water pressure
Just like case 1, an earthquake acceleration of 0,5 m/s^2 is used. The only difference is that excess pore water pressure is generated that is 50% of the initial vertical effective stress. This results in different earth pressures, which can be determined using the modified M-O method. By determining the static and dynamic forces acting on the diaphragm wall caused by the earthquake the minimum required penetration depth of the diaphragm wall is using the horizontal and moment equilibrium as shown in appendix I.

The calculated required penetration depth of 17,6m exceeds the existing penetration depth of 11m. The diaphragm wall will slip away from below and become unstable resulting in a failure of the quay wall structure.

Case 3: Diaphragm wall with relieving platform - completely liquefied
This case assumes a fully liquefied backfill. In front of the quay wall, generation of excess pore pressure is assumed just like case 2. Liquefied soil behaves like a heavy fluid with equivalent unit weight of saturated sand. The impact of this heavy fluid on the wall is determined using the Westergaard's method. No cranes or surcharge load is present due to the liquefied backfill. Objects on the surface behind the quay wall will sink into the heavy fluid or just float on top of it and will not cause any additional force to the wall. MV pile cannot find any resistance of the backfill soil due to the frictionless shear properties of water and will get pulled out of the heavy fluid causing the wall to move forward into the sea. To see the influence of the liquefied backfill on the diaphragm wall the MV pile is assumed to get enough resisting force of the liquefied backfill resulting in no forward movement of the quay wall.

By determining the static and dynamic forces acting on the diaphragm wall caused by the earthquake the minimum required penetration depth of the diaphragm wall is determined by using the horizontal and moment equilibrium as shown in appendix I. The calculated required penetration depth of 19,6m exceeds the existing penetration depth of 11m. The diaphragm wall will slip away from below and become unstable resulting in a failure of the quay wall structure.

8.3.2 Dynamic analysis with subgrade reaction method

In order to perform this analysis, the program Msheet of Geodelft's M-series is used. Msheet is not programmed to calculated sheet piles under seismic conditions. Therefore it does not have a module that implements earthquakes. Hence, seismic loadings are implemented manually. By using the K_a, K_0, K_p model in Msheet, earth pressure coefficient can be changed manually. For that reason is the K_a, K_0, K_p model preferred over the C, phi, delta model and is used for this seismic analysis to replace the Static earth pressure coefficients (k_a, k_p) by the seismic earth pressure coefficient (k_{ae}, k_{pe}) determined using the (modified) M-O method. The seismic earth pressure coefficient determined using the M-O method is based on fully mobilized ground. According to Msheet result, ground is not everywhere fully mobilized resulting in a higher k_{ae} and lower k_{pe} compared to the M-O method.

The K_a, K_0, K_p model coincides with a couple of restrictions. The surface needs to be flat and horizontal and no surcharge loading is allowed besides uniform surcharge loading. Hence, forces acting on the wall due to of surcharge load, own weight behind the relieving structure and the landside crane load are implemented in Msheet as horizontal point loads directly acting on the wall. This is also done for the dynamic water pressures which are determined using the Westergaard's method. The implemented point loads and its locations are shown in Figure 8-7.

Msheet calculations for case 1 are given in Appendix J. The maximum bending moment of the diaphragm wall including arching and second order effect is 7794 kNm/m and is located at an elevation of NAP-16.43m. This elevation level is lower compared to the elevation level determined using the pseudo static calculation by hand of NAP-14,8m. The reasons are the different resulting point loads implemented in the Msheet calculation representing the variable loads. The maximum bending moment is located at a depth where the shear is equal to zero, which is influenced by the elevation level of these point loads. Since most of these point loads are located below the depth were zero shear occurs, this will results in lower elevation level of the maximum bending moment. Hence,

lower elevation level causes an increase of maximum bending moment of the wall. This maximum bending moment exceeds the moment capacity of the diaphragm wall of 3744kNm/m which is calculated in Appendix L2 assuming an axial force of -4050 kN/m within the wall. The diaphragm wall will break resulting in failure of the quay wall.
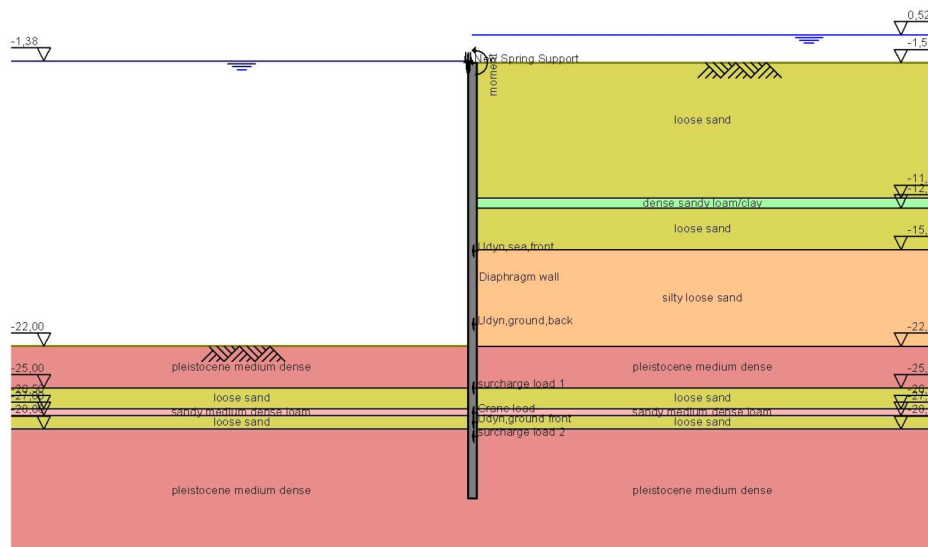

Figure 8-7 Geometry of Msheet dynamic model and the implemented point loads for case 1

For case 2 and case 3, Msheet gives no output that means that the sheet pile becomes unstable for both cases which corresponds to failure of the quay wall.

8.3.3 Dynamic analysis with Finite element program

The program Plaxis 2D V9 is chosen for this dynamic analysis just like the static analysis. In addition to the static analysis, the dynamic analysis module is used. The Plaxis dynamic module is an add-on module to the Plaxis 2D V9 version. This module can be used to analyze vibrations in the soil and their influence on nearby structures. In modeling the dynamic response of a soil structure, the inertia of the subsoil and the time dependence of the load are considered. Also, damping due to material and geometry is taken into account. Initially the HSsmall material model can be utilized for the simulation of the dynamic effects. This material model describes the behaviour of soil in the Plaxis model (see Appendix H.1.3).

A limitation of the HSsmall material model, like every other model in Plaxis, is that gradual softening of the soil during cyclic loading is not incorporated. In fact, softening due to soil dilatancy and debonding effects are not taken into account. Moreover, the HSsmall model does not incorporate the accumulation of irreversible volumetric straining nor liquefaction behaviour with cyclic loading. Even though vibrations often have 3D-characteristics, in Plaxis 2D, the dynamic model is limited to plane strain.

The procedure to perform a dynamic analysis with Plaxis is somehow similar to that for a static analysis. The same Plaxis model like the static Plaxis calculation is used during this dynamic calculation. Now a dynamic loading phase is included in which an earthquake is adopted. Other than the earthquake load the quay wall is subjected to load combination 2 which is the most normative load combination during the static analysis determined in section 8.2. The earthquake is modeled by imposing a prescribed acceleration at the bottom boundary resulting to shear waves that propagate upwards (see Figure 8-8). Besides harmonic loading there is also the possibility to real data from digitized load signal. Variations of different real accelerograms of earthquakes are used for this analysis. These accelerograms varies in magnitude caused by different earthquakes and are recorded at different stations over the United States by the United States Geological Survey. One of these acceleregrams is shown in Figure 8-9.
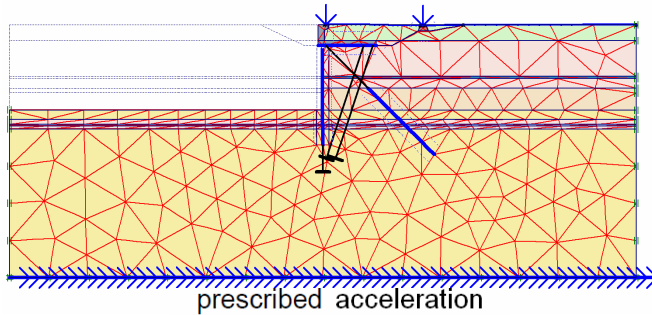
TUDelft
Delft University of Technology

Earthquake analysis of quay walls
- Seismic Analysis-

Gemeentewerken
Gemeente Rotterdam

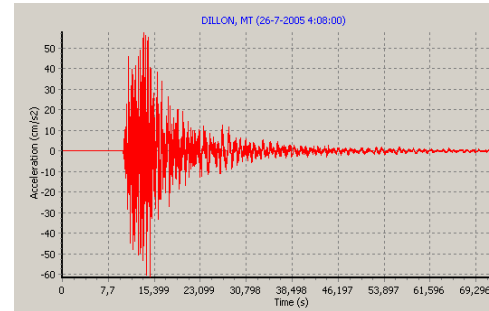Figure 8-8 Geometry of Plaxis dynamic model with prescribed acceleration

Figure 8-9 Real earthquake accelerogram used in Plaxis calculations a=0,06g

Excess pore pressure generation due to cyclic loading is not included in Plaxis. By reducing the internal friction angle φ excess pore water and even liquefaction are simulated in Plaxis. Reduction of φ results in increase and decrease of active and passive earth pressure coefficient respectively. Increase of active pressure behind the wall by reducing φ simulates the pressure increase due excess pore water generation and the heavy water during liquefaction. Another important notice is that by reducing φ shear friction between grains is also decreasing and having a more liquid like behaviour that simulated the shear strain loss during excess pore water generation and/or liquefaction.

Loose sand and silty loose sand are the only two soil types which is assumed to generate excess pore pressure. The other soil types are too compacted or too clayey for excess pore pressure to generate. Another assumption is made for the amount of excess pore water generation. The development from no excess pore pressure to full liquefaction is assumed linear. No decrease in φ means no excess pore water pressure is generated. On the other hand when φ reach zero, it is assumed that the soil is fully liquefied. From early calculations it is known that soil will liquefy at an earthquake acceleration of 0,3g. This results in the following expressions as shown in Table 8-10.

Percentage of excess pore pressure	φ after reduction	Earthquake acceleration [m/s^2]
0 %	30	0,00g
3,3%	29	0,01g
6,7%	28	0,02g
10%	27	0,03g
13,3%	26	0,04g
16,7%	25	0,05g
20%	24	0,06g
23,3%	23	0,07g
26,7%	22	0,08g
30%	21	0,09g
33,3%	20	0,1g

Table 8-10 Assumed excess pore pressure generation and the corresponding phi reduction

Two separate calculations are performed in determining the stresses within the quay wall. For the first calculation no excess pore pressure generation for all earthquakes is presumed. The second calculation includes excess pore pressure generation like shown in Table 8-10. By doing so, the influence of excess pore water pressure can be indicated.

Failure of quay wall structure can be analyzed by knowing the stresses within the quay wall induced by the earthquake. Three possible mechanisms that could cause the quay wall structure to fail are analyzed with Plaxis. These three mechanisms are:

1. Diaphragm wall failure: maximum bending capacity of wall is reached (see *Figure 5-10*d)
2. MV-pile failure: maximum tension force reached (see *Figure 5-10*a)
3. Displacement failure: maximum allowable displacements deviations between seaside and land side crane rail reached

TUDelft
Delft University of Technology

Earthquake analysis of quay walls
- Seismic Analysis-

Gemeentewerken
Gemeente Rotterdam

Diaphragm wall failure

The maximum bending moment capacity of the diaphragm wall must be larger than the bending moment caused by the earthquake to prevent failure of the diaphragm wall. The concrete diaphragm wall consists of different reinforcement bars spread all over the diaphragm wall. More reinforcements are placed at location were the bending moment is supposed to be large. However, the maximum moment capacity also depends on the axial force acting on the diaphragm wall which depends on the seismic force. In combination with the axial force determined with Plaxis the maximum moment capacity is determined. Results of the Plaxis calculation are shown in Appendix K and the moment capacity is determined in Appendix L.

A summary of results are shown in Table 8-11 and Table 8-12 and Figure 8-10. For the case were no excess pore generation is presence the diaphragm wall fails at an earthquake acceleration between a=0,07g and a=0,08g. With excess pore generation this is between a=0,05g and a=0,06g.

Without excess pore pressure	max. axial force diaphragm wall [kN/m]	max. moment diaphragm wall [kNm/m]	max. moment capacity diaphragm wall [kNm/m]
Satic (a=0,00g)	-4050	3130	3784
Earthquake 1 (a=0,01g)	-4100	3250	3744
Earthquake 2 (a=0,02g)	-4100	3290	3744
Earthquake 3 (a=0,03g)	-4110	3270	3736
Earthquake 4 (a=0,04g)	-4130	3410	3721
Earthquake 5 (a=0,05g)	-4080	3210	3760
Earthquake 6 (a=0,06g)	-4140	3500	3713
Earthquake 7 (a=0,07g)	**-4150**	**3480**	**3705**
Earthquake 8 (a=0,08g)	**-4330**	**3920**	**3562**
Earthquake 9 (a=0,09g)	-4330	4010	3562
Earthquake 10 (a=0,1g)	-4400	4380	3506

Table 8-11 Results of Plaxis calculation without excess pore pressure generation: Diaphragm wall

With excess pore pressure	max. axial force diaphragm wall [kN/m]	max. moment diaphragm wall [kNm/m]	max. moment capacity diaphragm wall [kNm/m]
0% (a=0,00g)	-4050	3130	3784
3,3% (a=0,01g)	-4100	3180	3744
6,7% (a=0,02g)	-4110	3340	3736
10% (a=0,03g)	-4100	3340	3744
13,3% (a=0,04g)	-4120	3490	3728
16,7% (a=0,05g)	**-4150**	**3470**	**3705**
20% (a=0,06g)	**-4240**	**4040**	**3634**
23,3% (a=0,07g)	-4300	4320	3586
26,7% (a=0,08g)	-4610	5160	3338
30% (a=0,09g)	-4560	5630	3378
33,3% (a=0,1g)	-4690	6450	3273

Table 8-12 Results of Plaxis calculation with excess pore pressure generation: Diaphragm wall
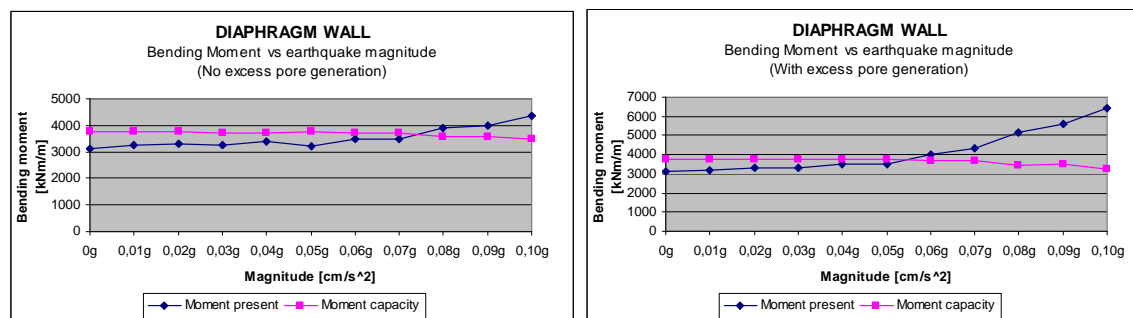

Figure 8-10 Bending moment diaphragm wall versus earthquake magnitude with and without excess pore generation

TUDelft
Delft University of Technology

Earthquake analysis of quay walls
- Seismic Analysis-

Gemeentewerken
Gemeente Rotterdam

MV-pile failure

The MV-pile prevents the quay wall leaning forwards into the sea. The tensile capacity of a MV-pile derives from the friction along the pile and is highly dependent on the quality of the execution of the work. Therefore, tests were performed to determine the tensile capacity during the construction of the quay wall. Tensile capacities of the MV-piles are 11050kN according to the design calculation performed by IGWR [8.5]. When the maximum tensile force reaches the tensile capacity, the quay wall will lean towards the sea resulting in large deformation and a possible loss of usage of the quay wall.

Tensile force determined with the Plaxis calculations are compared with the tensile capacity of the MV-pile to see whether the quay wall can resist the earthquake loading and are listen in Table 8-13 and shown in Figure 8-11.

No excess pore pressure	max. tensile force MV-pile per running meter wall [kN/m]	max. MV-pile force [kN]	max. tensile capacity MV-pile [kN]
Satic (a=0,00g)	851	4766	11050
Earthquake 1 (a=0,01g)	906	5074	11050
Earthquake 2 (a=0,02g)	913	5113	11050
Earthquake 3 (a=0,03g)	919	5146	11050
Earthquake 4 (a=0,04g)	963	5393	11050
Earthquake 5 (a=0,05g)	896	5018	11050
Earthquake 6 (a=0,06g)	1002	5611	11050
Earthquake 7 (a=0,07g)	996	5578	11050
Earthquake 8 (a=0,08g)	1190	6664	11050
Earthquake 9 (a=0,09g)	1220	6832	11050
Earthquake 10 (a=0,1g)	1390	7784	11050

Table 8-13 Results of Plaxis calculation without excess pore pressure generation: MV-pile

The resistance to shearing strain of the soil is reduced by increasing pore water pressure as mentioned in section 5.4.1. Friction between pile and soil which is needed to provide the necessarily resistance against seaward movement of the quay wall becomes less when excess pore water pressure is increasing. This will directly influence the tensile capacity of the MV-pile. The decrease of tensile capacity of the MV-pile due to increase of excess pore pressure is assumed to be linear. Tensile force determined with the Plaxis calculations with excess pore pressure generation are compared with the reduced tensile capacity of the MV-pile are listen in Table 8-14 and shown in Figure 8-11.

With excess pore pressure	max. tensile force MV-pile per running meter wall [kN/m]	max. MV-pile force [kN]	max. tensile capacity MV-pile [kN]
0% (a=0,00g)	851	4766	11050
3,3% (a=0,01g)	1150	6440	10682
6,7% (a=0,02g)	1190	6664	10313
10% (a=0,03g)	1210	6776	9945
13,3% (a=0,04g)	1260	7056	9577
16,7% (a=0,05g)	1270	7112	9208
20% (a=0,06g)	**1500**	**8400**	**8840**
23,3% (a=0,07g)	**1580**	**8848**	**8472**
26,7% (a=0,08g)	1870	10472	8103
30% (a=0,09g)	2010	11256	7735
33,3% (a=0,1g)	2220	12432	7367

Table 8-14 Results of Plaxis calculation with excess pore pressure generation: MV-pile

TUDelft
Delft University of Technology

Earthquake analysis of quay walls
- Seismic Analysis-
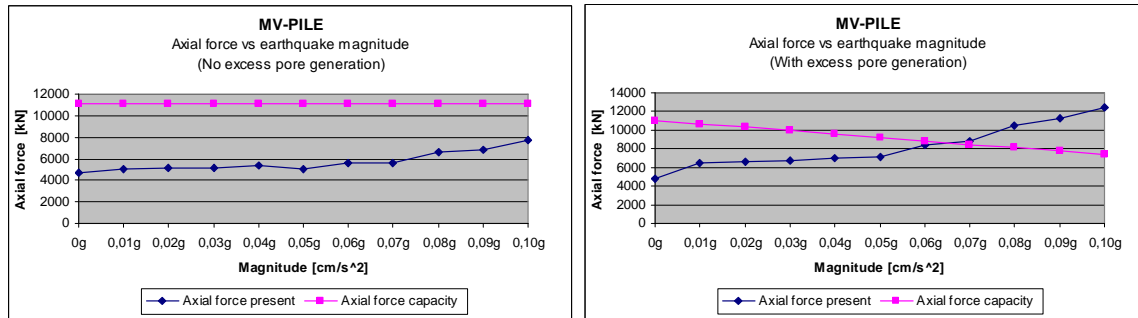
Gemeentewerken
Gemeente Rotterdam

Figure 8-11 Axial force MV-pile versus earthquake magnitude with and without excess pore generation

For the case were no excess pore generation is presence the MV-pile will not fail for the analyzed earthquake acceleration. With excess pore generation failure occur between earthquake acceleration of a=0,06g and a=0,07g.

Displacement failure
Maximum allowable displacement deviations between seaside and landside crane railing normal to quay wall is 80 mm for both horizontally and vertically direction (section3.3.6). The displacements listed in Table 8-15 are found during the static analysis of the diaphragm wall with Plaxis shown in section 8.2.2. Here, the vertical displacement of the landside crane foundation exceeds the maximum allowable displacement which corresponds to the onsite observations. Displacement failure of the quay wall occurs before an earthquake strikes the port. Assuming that this vertical displacement of the landside crane rail will be repaired this large displacement can be neglected and is assumed zero before the earthquake.

Static Analysis Plaxis Displacement	Hor. displacement After last phase	Vert. displacement After last phase
Seaside crane rail	-47 mm	-8 mm
Landside crane rail	-60 mm	-285 mm

Table 8-15 Displacement of crane rail during the static analysis

| Earthquake | No excess pore water | | With excess pore water | |
	Vert. displ. deviation crane railing [mm]	Hor. displ. deviation crane railing [mm]	Vert. displ. deviation crane railing [mm]	Hor displ. deviation crane railing [mm]
Satic (a=0,00g)	8	13	-	-
Earthquake 1 (a=0,01g)	6	12	12	12
Earthquake 2 (a=0,02g)	11	13	7	10
Earthquake 3 (a=0,03g)	10	12	7	10
Earthquake 4 (a=0,04g)	8	10	27	7
Earthquake 5 (a=0,05g)	2	12	1	9
Earthquake 6 (a=0,06g)	43	10	41	17
Earthquake 7 (a=0,07g)	**57**	**4**	**66**	**26**
Earthquake 8 (a=0,08g)	**106**	**10**	**115**	**25**
Earthquake 9 (a=0,09g)	120	2	148	34
Earthquake 10 (a=0,1g)	170	4	229	47

Table 8-16 Displacements of the crane foundations according to the Plaxis for the diaphragm wall

The horizontal movements of the seaside crane railing appeared to be in phase with the movements of the landside crane railing. The direction of these movements depends on the earthquake direction. Moreover, the horizontal displacement of the diaphragm wall becomes larger by in increasing earthquake magnitudes resulting in more vertical displacement of the landside crane foundation. The reason is that soil behind the wall is able to mobilize due to the available space that is created caused by the seaward movement of the wall. No large vertical displacement of the quay wall structure will

TUDelft
Delft University of Technology

Earthquake analysis of quay walls
- Seismic Analysis-

Gemeentewerken
Gemeente Rotterdam

occur due to the large bearing capacity of the Pleistocene sand beneath the quay wall structure. Therefore it can be concluded that the vertical displacement deviation between the seaside and landside crane rail is normative causing displacement failure of the diaphragm wall. It appeares that displacement failure occurs at a horizontal peak acceleration between a_H = 0,07g - 0,08g m/s^2 which corresponds with a local magnitude $M_L \approx 5,5$ and a return period of approximate 5000 years.

Earthquake acceleration between a=0,07g and a=0,08g will cause displacement failure of the quay wall according to the Plaxis calculation. Vertical displacement of the landside crane rail is normative. The seaside and landside crane foundation moves simultaneously to the left or right depending on the earthquake direction. Therefore the horizontal displacement deviation will not be large and is not normative. As the quay wall is subjected to higher earthquake acceleration, it slowly starts to move seaward. Hence soil behind the quay wall will mobilize and becomes less compacted resulting in larger vertical displacements of the landside crane. This mechanism will even increase more when excess pore pressure generation is assumed.

8.3.4 Resonance

Resonance is the tendency of a system to oscillate with larger amplitude at some frequencies than at others. These are known as the fundamental frequencies of the system. At these frequencies, even small periodic driving forces can produce large amplitude oscillations, because the system stores vibrational energy.

Earthquakes excitations are not harmonic by nature but random. This means that pure resonance is not possible, but that within certain frequency ranges an amplification by a factor 3 of 4 may be observed. This range runs roughly from 2 to 10 Hz. When the fundamental frequency of the quay wall system is near this frequency, large deformations and stresses can be expected. However, no extreme resonate rise is observed during the dynamic Plaxis calculation which indicates that the fundamental frequency of the quay wall system is not located near the seismic frequency range where extreme resonance rise will occur. To check if this observation is correct, the fundamental frequency of the diaphragm wall is determined and compared with the results achieved from Plaxis.

The fundamental frequency of a system can be explained by the following example. This example is taken from (Spijkers, 2008). When a mass-spring system (as shown in Figure 8-12a) is loaded with a harmonic load, the response of an undamped system will be harmonic (Figure 8-12b). When the frequency of the load is equal to the fundamental frequency of the system, resonance will occur and the amplitude of the response will be infinite (for an undamped system). In reality, always some (small) damping takes place and the amplitude of the response is finite (Figure 8-12c).
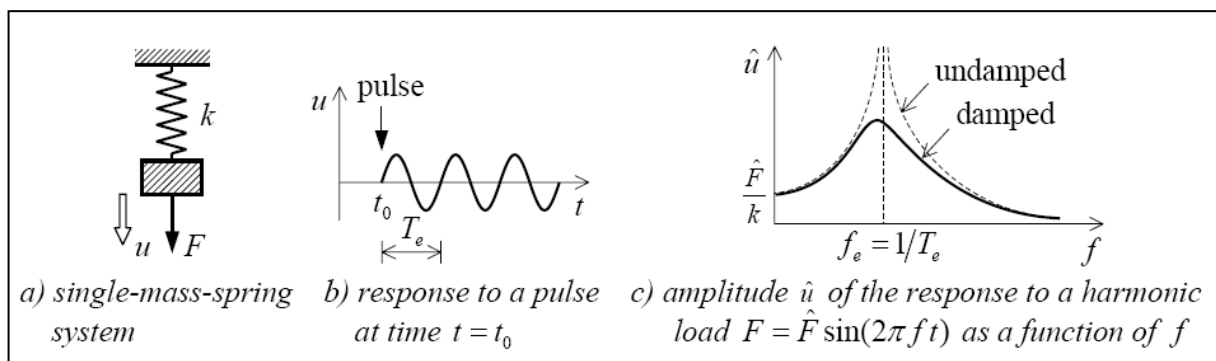

Figure 8-12 single mass-spring system loaded with a harmonic load

For a single degree of freedom oscillator, the natural frequency depends on two system properties: mass and stiffness. The natural frequency can be found by simply using the following equation:

$$f_n = \frac{1}{2\pi}\sqrt{\frac{k}{m}}$$

Eq. 8-3

TUDelft
Delft University of Technology

Earthquake analysis of quay walls
- Seismic Analysis-

Gemeentewerken
Gemeente Rotterdam

Where:

f_n = natural frequency [Hz]

k = stiffness of the spring [N/m]

m = mass of system [kg]

The stiffness of a beam can be calculated using the 'vergeet-mij-nietjes' (Figure 8-13):

$$w_2 = \frac{Fl^3}{3EI}$$

Eq. 8-4

Where:

w_2 = displacement [m]

ϑ_2 = angle of displacement [°]

F = force acting on wall [kN]

M = Moment acting on wall [kNm]

l = height of wall [m]

EI = Flexural rigidity wall [kNm^2]

Hence the stiffness of the wall can be calculated as follows:

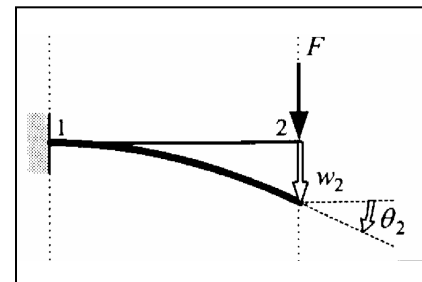$$k = \frac{F}{w_2} = \frac{3EI}{l^3}$$

Eq. 8-5

Figure 8-13 vergeet-mij nietjes

A simplified spring model is created to determine the horizontal fundamental frequency of the diaphragm quay wall system as shown in Figure 8-14. The own weight of the relieving structure and the surcharge load on top of the structure are being represented by the mass, m. The own weight of the wall and piles are not included during this calculation neither do the weight of the soil and water near the diaphragm wall above dredge level. By doing so, the upper limit of the fundamental frequency is determined (increase of m results in decrease of f_n). The vibro piles are placed vertically while the MV-pile still is inclined under an angle of 1:1. The MV-pile is schematized as a hinged bar and is assumed to deform only in axial direction and not due to bending. The diaphragm wall and vibro piles are assumed to be fixed on the ground and freely supported on the relieving structure. The horizontal deformation occurs only due to bending of the wall/pile.
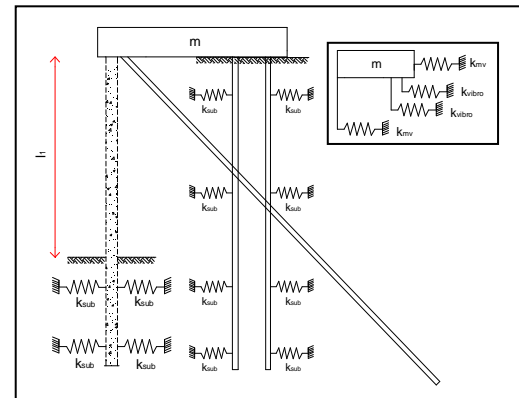

Figure 8-14 simplified spring model of diaphragm quay wall

The horizontal stiffness of the whole system (diaphragm quay wall) depends on the horizontal stiffness of the diaphragm wall, vibro piles and the MV-pile denoted as k_{dw}, k_{vibro} and k_{mv} respectively (see Figure 8-14). The horizontal fundamental frequency can now be written as:

$$f_n = \frac{1}{2\pi}\sqrt{\frac{(k_{dw} + 2k_{vibro} + k_{mv})}{m}} = \frac{1}{2\pi}\sqrt{\frac{(k_{dw} + 2k_{vibro} + k_{mv})g}{W_g}}$$

Eq. 8-6

The diaphragm wall is partly penetrated into the soil which has its own stiffness, k_{sub}. To determine the horizontal stiffness of the diaphragm wall, k_{dw}, equation 8-5 is adjusted to implement the stiffness of the ground by making use of the equivalent fixity method [8.7]. The equivalent fixity length of the wall

Earthquake analysis of quay walls
- Seismic Analysis-

Gemeentewerken
Gemeente Rotterdam

TUDelft
Delft University of Technology

from the ground surface is given by $1/\beta$. Hence the equivalent horizontal stiffness of the diaphragm wall can be determined with:

$$k_{dw} = \frac{3EI}{\left(l_1 + \frac{1}{\beta_{dw}}\right)^3} \qquad \beta_{dw} = \sqrt[4]{\frac{k_{sub}B_{dw}}{4EI_{dw}}} \qquad \textbf{Eq. 8-7}$$

Where:
k_{sub} = coefficient of subgrade reaction [MPa/m]
B_{dw} = Width of diaphragm wall [m]
EI_{dw} = Flexural rigidity of diaphragm wall [kNm^2]
l_1 = length of wall above ground [m]
W_g = surcharge and dead weight of relieving structure [kN/m]
g = acceleration of gravity (9,8 m/s^2)
$\frac{1}{\beta}$ = Length of equivalent fixity wall below ground [m]

The horizontal stiffness of the vibro piles are determined the same way as for the diaphragm wall. Here, the only difference is that the vibro piles are totally penetrated into the ground which results in $l_1=0$.

For determining the horizontal stiffness of the MV-pile a horizontal force F was places on the MV-pile which results in an axial force within the MV-pile of $\sqrt{2}F$ as shown in Figure 8-15. Hence, the MV-pile will extend due to this axial force by

$$\Delta l = \frac{\sqrt{2}Fl}{EA} . \qquad \textbf{Eq. 8-8}$$

When we ignore the shortening of the wall in relation to the extension of the MV-pile, the horizontal displacement at the top is equal to

$$u = \frac{2Fl}{EA} . \qquad \textbf{Eq. 8-9}$$

Hence, the horizontal stiffness of the MV-pile can be schematized as a spring with a stiffness of

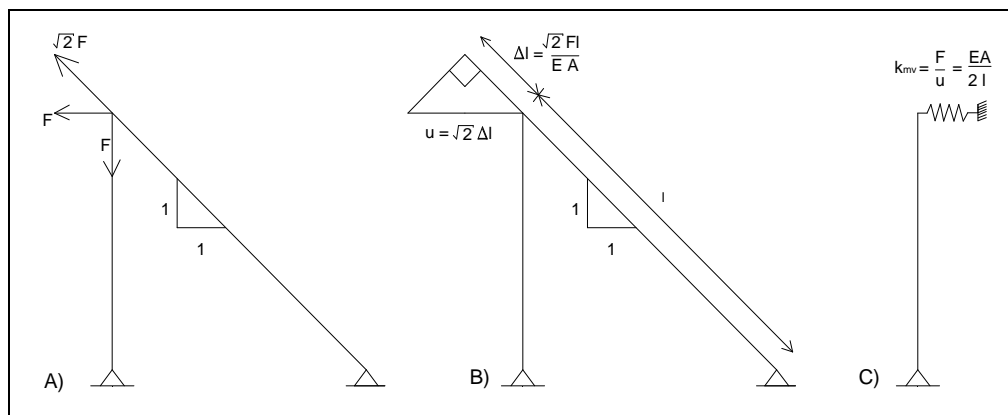$$k_{mv} = \frac{F}{u} = \frac{EA}{2l} . \qquad \textbf{Eq. 8-10}$$

Figure 8-15 illustration in determining the horizontal stiffness of the MV-pile

The horizontal stiffness of the whole system is determined using the equations mentioned above. The material and geotechnical parameters are listed in Table 8-17. The coefficient of subgrade reaction for Pleistocene sand is based on data achieved from experience for the Netherlands as mentioned in the CURR 166 [8.4].

Parameter	Symbol	
Coefficient of subgrade reaction (pleistoscene sand)	k_{sub}	30000 kN/m^3 [8.4]
Flexural rigidity of diaphragm wall	EI_{dw}	$1,87*10^6$ kNm^2/m (App. H.1.5)
Flexural rigidity of vibro pile	EI_{vp}	$1,64*10^5$ kNm^2 (App. H.1.5)
Axial rigidity of MV-pile	EA_{mv}	$5,67*10^6$ kN (App. H.1.5)
Surcharge and dead weight of relieving structure	W_g	4026 kN/m (Table F-2)
length of wall above ground	l_1	20,5 m
Diameter vibro pile	D_{vp}	0,56 m
Thickness of diaphragm wall	B_{dw}	1,2 m

Table 8-17 Material and geotechnical parameters

The horizontal fundamental frequency of each quay wall element is calculated. Notion must be made that the stiffness is determined per meter quay length and therefore the stiffness of the MV-pile vibro pile are divided by its centre to centre distance.

K_{dw} =387 kN/m k_{vp}=11246 kN/m k_{mv}=10376 kN/m

$$ f_n = \frac{1}{2\pi}\sqrt{\frac{(k_{dw}+k_{vp}+k_{mv})g}{W_g}} = \frac{1}{2\pi}\sqrt{\frac{(387+2\cdot11246+10376)\cdot9,8}{4026}} = 1,4Hz $$

The fundamental frequency of the quay wall structure according to the calculations is 1,4 hertz. The fundamental frequency of 1,4 Hz is just outside the ranges of extreme resonance rise (between 2 and 10 hertz) which corresponds to an amplification factor between 3 and 4. But still an amplification between 1,5 and 2,5 may be expected. Hence, no extreme resonance will occur for the diaphragm quay wall. This corresponds with the results found in Plaxis.

8.3.5 Conclusions

During the static analysis several load combinations are analyzed using two different methods, subgrade reaction method (Msheet) and finite element method (Plaxis). According to both methods, based on the pile and wall stresses and displacement of the quay wall structure, load combination 2 is normative. Stresses within the diaphragm wall elements are of the same order of magnitude for both methods and results of the Plaxis calculation are quite similar to the results from the design documents which validate the Plaxis model. Also the calculated big deformation under the landside foundation calculated with Plaxis corresponds with the real deformation observed onsite.

The effect of the additional dynamic loading could not really been performed with a pseudo static approach. The M-O method which determines the seismic soil pressure assumes that the soil is fully mobilized which in reality will not happen. This will results in an underestimation of the active earth pressure and an overestimation of the passive earth pressure. Also the Msheet program was not designed to calculate dynamic problems like earthquake which has resulted in an inaccurate prediction. It can be concluded that the M-O method and the Msheet program is not suited in determining the seismic behaviour of a diaphragm wall. However, the pseudo static calculations shows that occurrence of excess pore water generation during earthquakes increases the total horizontal thrust acting behind the wall. Hence, the penetration depth of the diaphragm wall becomes insufficient and eventually will slip away and become unstable.

With the finite element program called Plaxis, a more realistic seismic behaviour of the diaphragm quay wall could be obtained because this program has a dynamic module which incorporates earthquakes. However, limitation of the Plaxis program is that gradual softening of the soil during

TUDelft
Delft University of Technology

Earthquake analysis of quay walls
- Seismic Analysis-

Gemeentewerken
Gemeente Rotterdam

cyclic loading and excess pore generation behaviour due to cyclic loading is not incorporated. By reducing the angle of internal friction φ, excess pore water and soil softening has manually been simulated in Plaxis. Notion must be made that this is only an approximation assumption to incorporate excess pore water generation and soil softening in Plaxis which is not validated. Stresses within the quay wall elements and deformation of the crane foundations are determined using Plaxis for different earthquake accelerations and checked whether or not they fulfill the strength and displacement requirements that needed to make the quay wall functional (see Table 8-18).

Failure type	Critical earthquake acceleration	
Failure diaphragm wall	No excess pore pressure generation	a = 0,07g – 0,08g
	With excess pore pressure generation	**a = 0,05g – 0,06g**
Failure MV-pile	No excess pore pressure generation	a > 0,1g
	With excess pore pressure generation	a = 0,06g – 0,07g
Displacement failure crane foundation	With and without excess pore pressure generation.	a = 0,07g – 0,08g

Table 8-18 Critical earthquake accelerations for diaphragm quay wall determined using Plaxis

No extreme resonance rise occur and therefore the normative failure of the diaphragm quay wall is caused by insufficient strength of the diaphragm wall to resist stresses within the wall. This will occur between earthquake acceleration a = 0,05g – 0,06g as shown in Table 8-18.

8.4 References

[8.1]   Delta marine consultants, kadeconstructie Euromax – ontwerp, report O-R-013 rev B, 06-2005
[8.2]   NEN 6720, Voorschriften beton constructieve eisen en rekenmethoden (VBC), 1995
[8.3]   Delta marine consultants, Berekening kadeconstructie aanbieding 2, 022518-rap-u-0008 rev B 03-2005
[8.4]   CUR 166, Damwandconstructies, 4^e druk, 2005
[8.5]   IGWR, MV palen kademuur Euromax – interpretatie geschiktheidproeven, 04-2006
[8.6]   CUR 211, Handbook quay wall, 2005
[8.7]   Pianc, Seismic design guidelines of port structures
[8.8]   http://earthquake.usgs.gov
[8.9]   Eurocede 8

TUDelft
Delft University of Technology

Earthquake analysis of quay walls
- Seismic Analysis-

Gemeentewerken
Gemeente Rotterdam

9. Seismic analysis of gravity quay wall

9.1 Introduction

Gravity retaining walls are the oldest and simplest type of retaining walls. Due to the relative large bending stiffness the deformations are small compared to sheet pile walls. Their movement occurs essentially by rigid body translation and or by rotation. Under static condition (no earthquake) the retaining wall is subjected to the following forces:

- body forces related to mass of the wall
- by soil and water pressure
- by external forces such as fender force, bolder force, crane load, surcharge load and others

A properly designed gravity wall will achieve equilibrium of those forces including shear stresses that approach the shear strength of soil. During earthquake, however the inertial forces and changes in the soil strength may violate the equilibrium and cause permanent deformation of the wall. Failure whether by sliding, tilting, bending or some other mechanism occurs when these permanent deformations becomes excessive.

Analysis of a gravity wall under seismic conditions is performed too see the difference in behaviour between a gravity wall and diaphragm wall located at the Euromax container terminal. To make a comparison in behaviour between the two different types of quay walls an early disapproved concept gravity quay wall [10.1] is used during this seismic analysis. By doing so, it can be assumed that the function, starting points, boundary conditions and environmental conditions will not differ to much in relation to each other. More information about the gravity wall can be found in section 9.2.

A static analysis of the gravity quay wall is performed to see if the chosen dimensions of the gravity wall are capable to withstand the static forces acting on the wall. Thereafter, seismic behaviour of the quay wall is investigated by performing a dynamic analysis. This is done in two ways. To get a first impression of the stresses within the gravity wall due to seismic forces, a pseudo static analysis was performed based on hand calculations using the Westergaard and Mononobe-Okabe method mentioned in section 5.4.1. Finally, a finite element method was used to give an even more accurate result in the behaviour of the gravity quay wall during earthquakes. A Comparison is done between static analysis and the seismic analysis to derive insight in the difference.
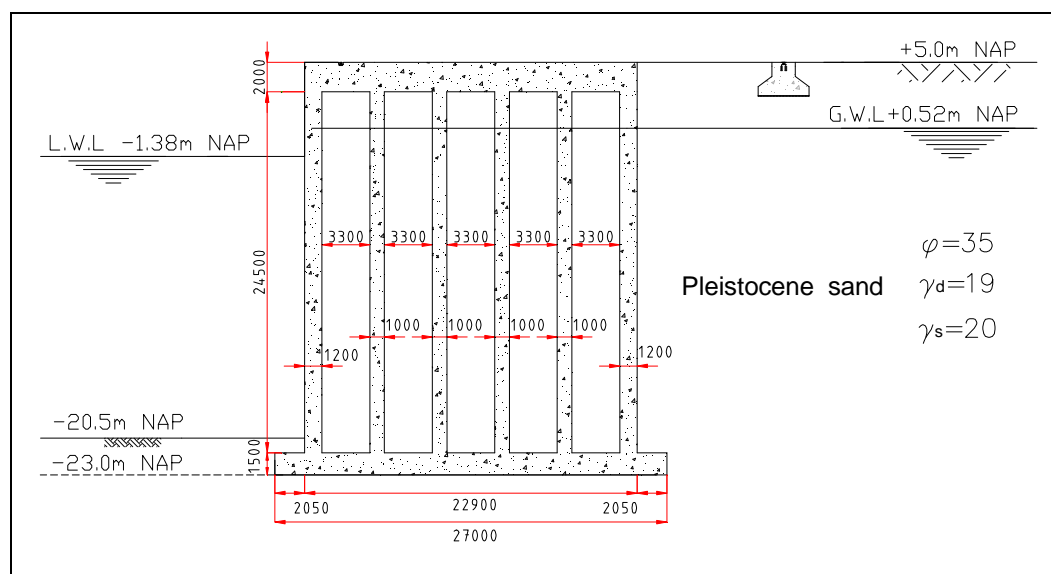

Figure 9-1 Caisson type gravity quay wall

TUDelft
Delft University of Technology

Earthquake analysis of quay walls
- Seismic Analysis-

Gemeentewerken
Gemeente Rotterdam

9.2 Caisson gravity wall

The caisson is consists of a concrete box-shaped construction with five compartments. The compartments have a length of 22,0m. By placing several caissons in a row next to each other a retaining gravity wall is created. The floor and the roof of the caisson have a thickness of 1,5m and 2,0m respectively. The front wall on the seaside shares the same thickness with the back wall on the landside of 1,2m. The thickness of the side walls are 1,0m. Five compartments with a width of 3,3m are formed by casting four walls inside concrete box shaped construction, each with a wall thickness of 1,0m. A global estimation of reinforcement within these walls is determined in section 9.3.2. Footing of the caisson is extended on both seaside and landside with 2,05m resulting in a total width of 27,0m. A crane foundation is placed behind the quay wall to spread the crane load evenly into the ground. The above mentioned caisson is shown in Figure 9-1.

9.3 Static analysis of gravity quay wall

Earth retaining structures shall be designed to fulfill their function without suffering significant structural damage. Permanent displacement, in the form of combined sliding and tilting, the latter due to irreversible deformation of the foundation soil, may be acceptable if it is shown that they are compatible with functional and/or aesthetic requirements.

An static analysis is performed to check if the estimated dimensions of the quay wall mentioned in section 9.2 fulfill the strength and stability requirements of a caisson according the Eurocode 7 [10.2]. The aim of design based on Eurocode is to prevent ultimate limit states, which lead to a state where a construction would collapse or can not be used any more. In former design codes, one global safety factors is often used. In the Eurocode, partial safety factors are applied to separate loads and resistances. Loads are multiplied with a safety factor $\gamma \geq 1$, resistances are divided by a safety factor $\gamma \geq 1$. Stabilizing actions (favorable loads) are multiplied by a safety factor $\gamma \leq 1$. Safety factors for the Netherlands are listed in Table 9-1 and are used during the static analysis.

Loads		Symbol	Safety factor
Permanent action	Unfavourable	$\gamma_{G,dst}$	1,35
	Favourable	$\gamma_{G,stb}$	0,9
Variable action	Unfavourable	$\gamma_{Q,dst}$	1,5
	Favourable	-	-
Accidental action	Unfavourable	$\gamma_{A,dst}$	1,0
	Favourable	-	-
Resistances			
Coefficient of shearing resistance (tanφ')		$\gamma_{\varphi'}$	1,25
Effective cohesion (c')		$\gamma_{c'}$	1,45
Undrained shear strength (c_u)		γ_{cu}	1,75
Unconfined compressive strength (q_u)		γ_{qu}	1,75
Weight density (γ)		γ_{γ}	1,0

Table 9-1 Safety factors with Reliability Class 2 according to Eurocode 7 [10.2]

Tilting or sliding of the caisson is prevented by sufficient self-weight and shear resistance between soil and bottom of caisson. Surcharge load above the caisson quay wall is neglected due to the fact that this load will increase the self-weight and shear resistance which will increase the stability of the caisson. Horizontal component of the crane load acts towards the sea resulting in an unfavorable situation for the stability of the caisson. On the other hand, the vertical component acts downward resulting in a favorable situation of the stability. Therefore, two load combinations have been investigated to find the normative stresses in the walls and the normative displacement of the caisson quay wall. These load combinations can be found in Table 9-2. It is necessary to take into account that the probability of a simultaneous combination of loads must be smaller than the probability that one of the loads occurs. In addition to the permanent loads, Eurocodes take into account the

occurrence of one leading variable load combined with other variable loads. Depending on the character of the loads, the variable loads in the load combination are reduced by means of reduction factor Ψ called the combination factor and are listed in Table 9-2.

Load combination 4	Comb. factor
Own weight relieving platform	1
Crane load in operation	0,7
Bolder force	1
Groundwater +0,52 NAP	1
Ground pressure +0,52 NAP	1
Seawater -1,38 NAP	1
Surcharge load behind platform	0,7
Surcharge load behind landside crane	0,7

Load combination 5	Comb. factor
Own weight relieving platform	1
Bolder force	1
Groundwater +0,52 NAP	1
Ground pressure +0,52 NAP	1
Seawater -1,38 NAP	1
Surcharge load behind platform	0,7
Surcharge load behind landside crane	0,7

Table 9-2 Load combination and combination factors used during the caisson analysis

9.3.1 Stability check

Gravity wall usually fail by rigid body mechanism such as sliding, overturning or by not sufficient bearing capacity of the soil. The three failure mechanisms are checked during this static caisson analysis for both load combinations 4 and 5 which is listed in Table 9-2. The static forces acting on the caisson as listed in section 9.1 are determined in Appendix M and the resultant thrusts are shown in Figure 9-2.
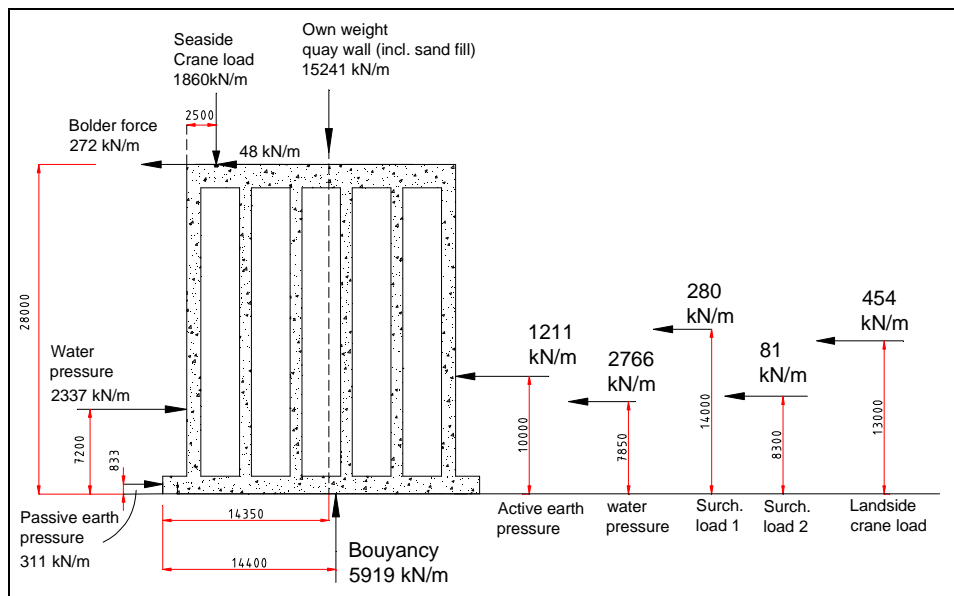

Figure 9-2 Resultant thrusts acting on the caisson quay wall during static conditions

Sliding failure occurs when horizontal force equilibrium is not maintained. The friction force between the caisson floor and soil must withstand the resultant horizontal forces acting on the caisson otherwise the caisson will start to move. Overturning failure occurs when moment equilibrium is not satisfied. Calculations are performed to see whether or not the chosen caisson and its dimensions are capable to resist sliding and overturning by determining the factors of safety against sliding and overturning. The bearing capacity of the soil is checked to find out if the soil can support the caisson structure and the landside crane foundation. Calculations can be found in Appendix M.

To produce an active soil state, a sufficient amount of wall movement is necessary to occur which is made possible by sliding or rotating. Static stability analysis results of the caisson shows that the chosen dimensions of the quay wall is sufficient to prevent excessive sliding and overturning for both load combinations 4 and 5. The factor of safety related to sliding is 1,25 for both load combinations.

TUDelft
Delft University of Technology

Earthquake analysis of quay walls
- Seismic Analysis-

Gemeentewerken
Gemeente Rotterdam

Factor of safety against overturning is 1,74 and 1,76 for load combination 4 and 5 respectively. This indicates that no specific load combination is normative when looking at the stability aspect.

Settlement due to insufficient bearing capacity could lead to large deformations and rotation of the caisson quay wall. The bearing capacity is proven to be sufficient during the calculations performed in Appendix M for both the soil beneath the caisson structure and landside crane foundation.

9.3.2 Strength check

The walls of the caisson are checked if they can resist the stresses occurring during the static conditions. The concrete caisson consists of six concrete walls (Figure 9-3) which need reinforcement to resist the bending moment stresses due to static loading. Stresses within each wall are determined using the finite element program Plaxis which can be found in Appendix N. Stresses within the walls according to Plaxis for load combination 4 and 5 are shown in Table 9-3. Strength check of the reinforced concrete floor and roof are not included during this analysis because the stresses occurring in the walls are the highest and therefore is the most normative construction element.
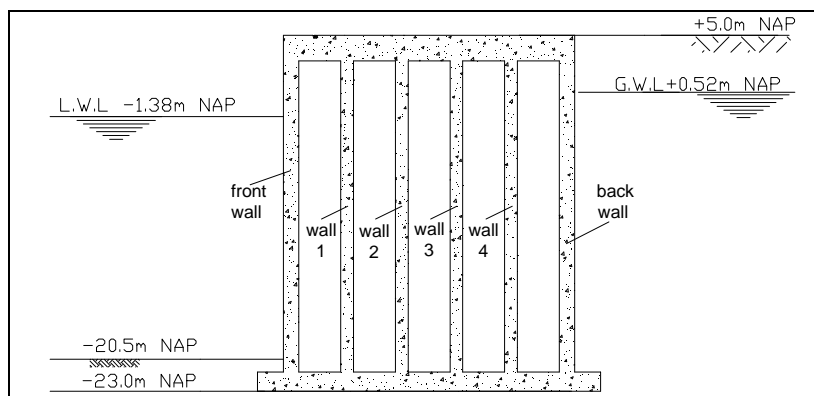
Figure 9-3 Notation of caisson walls

Plaxis Stresses Load Combi. 4	M_{max} kNm/m	Max. axial force kN/m	Plaxis Stresses Load Combi. 5	M_{max} kNm/m	Max. axial force kN/m
Front wall	-3490	-1920	Front wall	-3420	-1140
Wall 1	-2480	-1680	Wall 1	-2560	-1210
Wall 2	-2910	-1270	Wall 2	-2610	-1050
Wall 3	-3260	-1080	Wall 3	-2540	-983
Wall 4	-3140	-860	Wall 4	-2200	-836
Back wall	-3150	-819	Back wall	-1910	-929

Table 9-3 Maximum bending moment and maximum axial forces of caisson walls

The maximum bending moment capacity of the caisson walls must be larger than the maximum bending moment caused by static loads to prevent failure of the walls. Hence, a global amount of reinforcement is determined which is needed to resist this maximum bending moment. The limit state design of reinforced concrete flexural members is based on the principles of strain compatibility and force equilibrium. The balanced flexural strength of a member is reached when the strain in the extreme compression fiber reaches the ultimate strain of concrete at the time the tension reinforcement reaches yield strain. It is essential to design a reinforced concrete member with sufficient ductility to avoid brittle failure in flexure. Therefore, maximum and minimum reinforcement ratio are introduces in national standards of ω_{min}=0,18% and ω_{max}=1,93% for Concrete class C28/35 and steel class FeB500 [10.3]. Calculations are made to determine the amount of reinforcement in the walls and can be found in Appendix M.

After including safety and combination factors it was found that 12 reinforcement bars with diameter of 40mm is sufficient enough to resist the maximum bending moment during static conditions. Design stresses and moment capacities of the caisson walls using the 12 reinforcement bars are listed in Table 9-4. The differences in bending moment capacity between the two load combinations are due the differences in axial forces within the pile which is needed to determine the bending capacity. The

TUDelft
Delft University of Technology

Earthquake analysis of quay walls
- Seismic Analysis-

Gemeentewerken
Gemeente Rotterdam

normative load combination for strength failure is load combination 4 and will be used during the dynamic analysis of the caisson quay wall.

Plaxis Stresses Load Combi. 4	N_d kN/m	M_d kNm/m	M_{cap} kNm/m	Plaxis Stresses Load Combi. 5	N_d kN/m	M_d kNm/m	M_{cap} kNm/m
Front wall	-2496	-4537	-4982	Front wall	-1482	-4446	-5503
Wall 1	-2184	-3224	-4011	Wall 1	-1573	-3328	-4175
Wall 2	-1651	-3783	-4155	Wall 2	-1365	-3393	-4227
Wall 3	-1404	-4238	-4240	Wall 3	-1278	-3302	-4248
Wall 4	-1118	-4082	-4285	Wall 4	-1087	-2860	-4293
Back wall	-1065	-4095	-5503	Back wall	-1208	-2483	-5455

Table 9-4 Design moments M_d, design axial forces N_d and moment capacity M_{cap} of caisson wall

The amount of 12 reinforcement bars with diameter of 40mm is used at places where the bending moments are near the maximum bending moment. Sections where the occurring bending moments are less, less reinforcement can be used. Determination of this lower amount of reinforcement is not included in this analysis because the stresses are not normative within these sections. Configurations of the 12 reinforcement bars for the front and back wall are shown in Figure 9-4. For wall 1,2,3 and 4 the exact same amount reinforcement is placed at the same locations. The only difference is the thickness of the wall which is 1000mm.
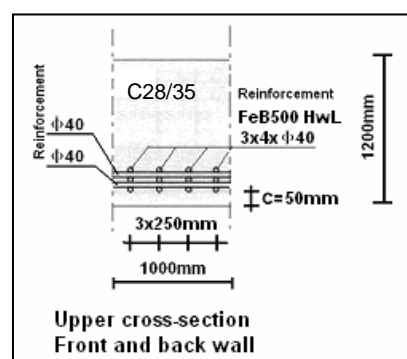

Figure 9-4 Configuration reinforcement bars of the caisson walls at normative sections

9.3.3 Displacements

Displacements of the caisson during static conditions are determined with the finite element program called Plaxis and can be found in Appendix N. The maximum displacements of the crane foundations are listed in Table 9-5. It shows that the displacements occurring at load combination 4 are larger compared to load combination 5. The normative displacement direction for the seaside crane foundation is horizontally towards the sea while for the landside crane foundation it is downward directed. The downward displacement of the landside crane foundation is not due to insufficient bearing capacity, which has been calculated in Appendix M3, but due to the seaward movement of the caisson. This seaward movement creates room for the backfill to mobilize causing the landside crane foundation to settle.

Load combination 4 Max. Displacement	Hor. displacement After last phase	Vert. displacement After last phase
Seaside crane rail	-0,064 m	-0,022 m
Landside crane rail	-0,042 m	-0,086 m

Load combination 5 Max. Displacement	Hor. displacement After last phase	Vert. displacement After last phase
Seaside crane rail	-0,027 m	-0,005 m
Landside crane rail	-0,017 m	-0,026 m

Table 9-5 Maximum displacements of seaside and landside crane foundation of caisson quay wall

Maximum allowable displacement deviation between seaside and landside crane railing normal to quay wall for is 80 mm for both in horizontal and vertical direction (see section 3.3.6). This critical displacement will not be reach during static conditions.

T U Delft
Delft University of Technology

Earthquake analysis of quay walls
- Seismic Analysis-

Gemeentewerken
Gemeente Rotterdam

9.4 Dynamic analysis of gravity quay wall

9.4.1 Pseudo static analysis by hand

Just like the pseudo static analysis of the diaphragm quay wall the same three cases are analyzed depending upon the magnitude of excess pore water pressures generated during the earthquake. They range from the case for no excess pore water pressures (case 1) to the extreme case corresponding to the complete liquefaction (case 3) and the intermediate case of residual excess pore water pressures within the backfill of the quay wall (case 2). Horizontal peak ground acceleration caused by the earthquake is assumed equal for all three cases, which is 0,5 m/s^2. In reality no excess pore generation and therefore no liquefaction will occur behind the caisson quay wall because the backfill (Pleistocene sand) is assumed to be compacted well enough to prevent this from happening. However, excess pore water pressure is included in this pseudo static analysis to inquire the effects on the caisson quay wall.

Case 1: no excess pore water pressure
Case 2: excess pore water pressure is 50 percent of the initial vertical effective stress
Case 3: Complete liquefaction of backfill

Earth and water pressures acting on the quay wall for the three different cases can be found in Figure 9-5. Only load combinations 4 is used during this analysis. According to the static analysis, this is the normative load combination, which will result in the highest stresses within the walls of the caisson quay wall structure. For the purpose of the pseudo static analysis, the seismic action is represented by a set of horizontal and vertical static forces equal to the product of the gravity forces and a seismic coefficient. The vertical seismic action is considered as action upward or downward to produce the most unfavorable effect. Due to the absence of seismic studies near the project location, the horizontal and vertical seismic coefficients (k_h and k_v) affecting all the masses shall be taken according to the Eurocode 8 [10.4] and listed in Table 8-8.

In Figure 9-5 $U_{stat,back}$ corresponds to the steady state pore water pressure force along the back of the caisson quay wall, $U_{stat,front}$ the hydrostatic water pressure force exerted by the water along the front of the pool. $U_{dyn,front}$ corresponds to the hydrodynamic water pressure force along the front of the wall due to earthquake shaking of the water, $U_{dyn,ground,back}$ the hydrodynamic water pressure force of the pore water along the back of the caisson wall. $U_{dyn,epwp,front}$ and $U_{dyn,epwp,back}$ corresponds to the excess pore water pressure force acting along the front of the wall and along the back of the wall (case 2). In case of liquefied backfill, $LF_{hydrostatic}$ and $LF_{hydrodynamic}$ are equal to the equivalent heavy fluid hydrostatic pressure of the liquefied backfill and the hydrodynamic due to the acceleration of the liquefied backfill (case 3).
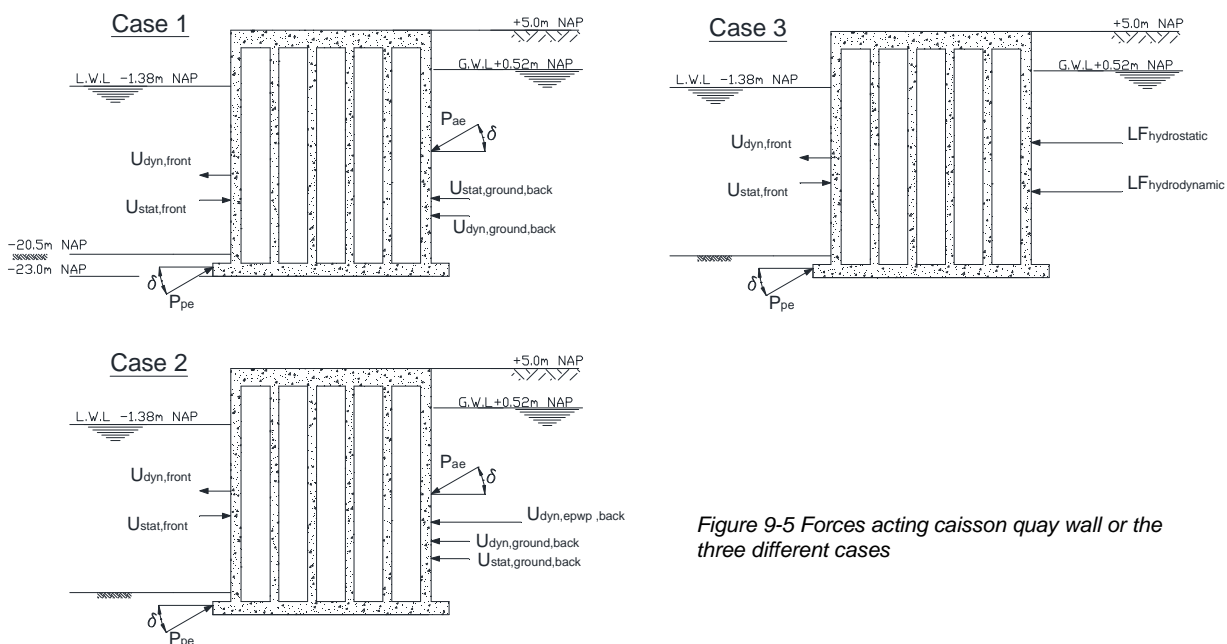

Figure 9-5 Forces acting caisson quay wall or the three different cases

TUDelft
Delft University of Technology

Earthquake analysis of quay walls
- Seismic Analysis-

Gemeentewerken
Gemeente Rotterdam

Method used

The resultant thrust from the interaction among force components during an earthquake develops at the contact surface between the backfill soil and the wall. It should be noted that the forces that arise due to the inertia of the wall must be considered in the seismic analysis of the caisson quay wall. The magnitude of each force component is computed as follows: the inertia force of the caisson ($F_{inertia}$) is calculated by multiplying the mass of the wall by the wall acceleration. Depending on the presence of excess pore water pressure the dynamic earth pressure force (P_{ae}, P_{pe}) is determined using the M-O method or the modified M-O method mentioned in appendix C and section 5.4.1 respectively. This method is based on plasticity theory and is essentially an extension of the Coulomb sliding wedge theory in which the transient terms of the weight of the wedge multiplied by a seismic coefficient. The Westergaard solution was used in determining the dynamic water pressure (section 5.4.1). An overview of methods that were used during this analysis is listed in Table 9-6.

Forces	method
Static earth pressure	Coulomb
Static water pressure	Hydrostatic pressure
Dynamic earth pressure (no excess pore pressure)	Mononobe & Okabe
Dynamic earth pressure (with Excess pore pressure)	Modified Mononobe & Okabe
Dynamic water pressure	Westergaard
Excess pore water pressure	Assumed
Surcharge load and crane load	Ohde

Table 9-6 Overview of method that were used during the analysis

Seismic direction

Soil moves in different directions during an earthquake, vertically and horizontally. Each direction combination produces different forces acting on the sheet pile. The most unfavorable direction combination is used during this analysis. This is when the horizontal acceleration (a_h) is directed towards the backfill causing the incremental dynamic earth pressure forces ($\Delta P_{AE/PE}$) acting away from the backfill. Vertical acceleration (a_v) is directed downward (see Figure 8-5) causing a reduction of the own weight which results in less friction between sand and caisson floor. This has the normative effect of increasing the driving force behind the caisson and decreasing the stabilizing force.

Stability of caisson quay wall under seismic action

There are three different modes of instabilities, namely sliding, overturning and bearing capacity failure. Sliding occurs due to inadequate sliding resistance. When seismic loading is exerted on a retaining wall, moment and bearing pressure will increase. When the overturning moment exceeds the restoring moment, the caisson will rotate and overturning instability occurs. When the overturning moment becomes close to the restoring moment, very high and concentrated bearing pressure will be generated near the wall heel. Therefore, unless the founding material is very strong the wall will tend to rotate about the heel due to inadequate bearing capacity. The founding material of the caisson quay wall consists of dense sand which the bearing capacity is proven to be sufficient enough (Appendix M) to prevent rotation due to bearing instability and bearing capacity failure.

The procedure for computing the dynamic factors of safety against sliding and overturning is same as that for static calculation, except that the inertia of the gravity wall itself must also be included when earthquake loading is considered. No safety factors are used because real occurring forces are needed to see whether or not the caisson is stable or not during an earthquake. Combination factors listed in Table 9-2 are used. Calculations for the three different cases can be found in Appendix O. The results of these calculations are summarized below.

Case 1: Caisson quay wall - no excess pore water

In this case, no excess pore water pressure is assumed. An horizontal earthquake acceleration of 0,5m/s^2 is used which results in a horizontal and vertical seismic coefficient of k_h=0,67 and k_v=0,23 respectively. Dynamic earth pressures are calculated using the M-O method were the dynamic water pressures is calculated using the Westergaard method. The impact of surcharge and crane load on the wall can be estimate using the method created by Ohde [10.5]. By determining the static and dynamic force components acting on the caisson quay wall caused by the earthquake using the above mentioned method (Appendix O.1.1), the stability of the caisson is checked for both sliding and

TUDelft
Delft University of Technology

Earthquake analysis of quay walls
- Seismic Analysis-

Gemeentewerken
Gemeente Rotterdam

overturning by making use of force and moment equilibrium (Appendix O.1.2). The friction resistance force must withstand the horizontal forces acting on the caisson otherwise the caisson will start to slide, while when the overturning moment exceeds the restoring moment, the caisson will rotate and overturning instability occurs. The factor of safety against sliding and overturning for case 1 is 1,31 and 2,71 respectively, which indicates that the caisson will not slide and not overturn and therefore is stable.

Case 2: Caisson quay wall - with excess pore water pressure
Just like case 1, an horizontal earthquake acceleration of 0,5 m/s^2 is used. The only difference is that excess pore water pressure is generated behind the caisson that is 50% of the initial vertical effective stress. This results in a change of earth pressure coefficient which results in different forces acting against the caisson quay wall. Earth pressure coefficient and earth pressures are determined using the modified M-O method. The impact of crane and surcharge load can be determined using the method of Ohde using the newly determined earth pressure coefficient. Calculation in determining the resultant thrusts acting against the caisson quay wall for case 2 can be found in Appendix O.2.1. Stability check for case 2 is performed and can be found in Appendix O.2.2. The factor of safety against sliding and overturning for case 2 is 0,96 and 2,19 respectively. Caisson will move in seaward direction by sliding causing an unstable situation.

Case 3: Caisson quay wall - completely liquefied
This case assumes a fully liquefied backfill. Liquefied soil behaves like a heavy fluid with equivalent unit weight of saturated sand. The impact of this heavy fluid on the wall is determined using the Westergaard's method. No cranes or surcharge load is present due to the liquefied backfill. Objects on the surface behind the quay wall will sink into the heavy fluid or just float on top of it and will not cause any additional force to the wall. The factor of safety against sliding for case 3 is 0,78 whilst against overturning it is 2,28. Just like case 2 the caisson quay wall slides towards the sea.

From the above results it follows that overturning will not occur for all three cases. Sliding is the normative stability failure mechanism. For a horizontal earthquake acceleration of 0,5 m/s^2 the caisson quay wall will approximately start to slide just before the 50% excess pore pressure generation is reached. The factor of safety decreases by increasing excess pore water generation which results in an unfavorable stability situation. This is due to the increase of resultant horizontal thrusts behind the caisson by increase of excess pore water pressure.

9.4.2 Dynamic analysis with Finite element program

The program Plaxis 2D V9 is chosen for this dynamic analysis just like the static analysis. In addition to the static analysis, the dynamic analysis module is used. The Plaxis dynamic module is an add-on module to the Plaxis 2D V9 version. This module can be used to analyse vibrations in the soil and their influence on nearby structures. In modeling the dynamic response of a soil structure, the inertia of the subsoil and the time dependence of the load are considered. Also, damping due to material and geometry is taken into account. The boundary conditions, choice of material model, material properties and soil parameters are the same as the static calculations of the caisson and can be found in Appendix N.
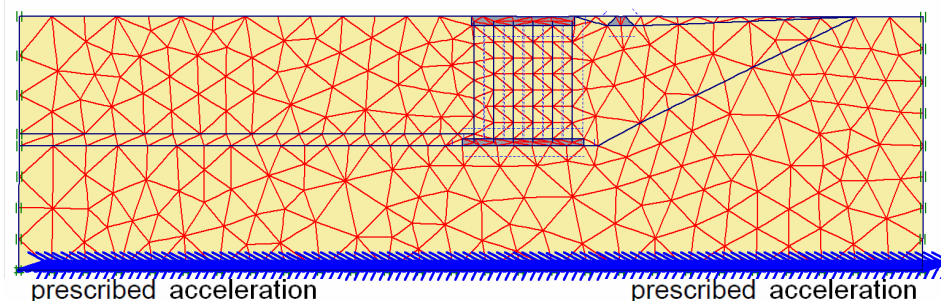

Figure 9-6 Geometry of Plaxis dynamic model with prescribed acceleration

The limitations of the HSsmall material model and procedure to perform a dynamic analysis with Plaxis are mentioned in section 8.3.3. Differences in this Plaxis model compared to the static model and the dynamic model of the diaphragm wall is that vertical earthquake acceleration is implemented as shown

![TU Delft logo] TUDelft
Delft University of Technology

Earthquake analysis of quay walls
- Seismic Analysis-

Gemeentewerken
Gemeente Rotterdam

in Figure 9-6. The reason is that the large self-weight of the caisson structure which generate resistance against sliding and tilting changes during upward and downward motions caused by the earthquake. Hence, this vertical motion will influence the stability of the structure. The vertical acceleration is kept 1/3 of the horizontal acceleration which is a reasonable assumption according to Eurocode 8 [10.4].

Excess pore pressure generation due to cyclic loading is not included in Plaxis. This is not needed during the dynamic calculation of the caisson structure because excess pore pressure is not able to develop in very dense soil which is assumed to be the case in this Plaxis model. Therefore, no excess pore water generation is assumed during this dynamic analysis using Plaxis.

Three failure mechanisms are analyzed based on the results achieved from the dynamic Plaxis calculations: Stability of the caisson, displacement crane foundation and strength of the caisson. The dynamic input and output result of this Plaxis calculation can be found in Appendix P.

Stability failure

The increase of inertia forces, horizontal thrust behind the quay wall and changes in shearing resistance between wall and soil caused by the earthquake can result in sliding and overturning. For this reason stability of the caisson quay wall is checked on sliding and overturning. Mechanism triggering these stability failures is mentioned in section 9.3.1. Displacements of the caisson are analyzed for earthquake accelerations varying from 0g to 0,09g m/s^2. The results of vertical and horizontal displacements of the front wall of the caisson (Figure 9-7) calculated with Plaxis are shown in *Figure 9-8*. Notion must be made that the two peak deviations shown *Figure 9-8*a and b are due to the longer duration of the peak acceleration which is implemented in the Plaxis model for that particular earthquake acceleration.
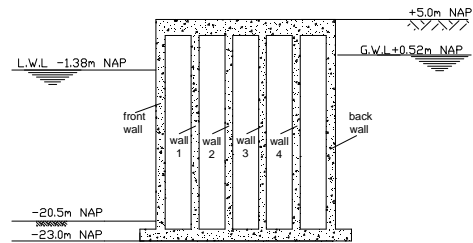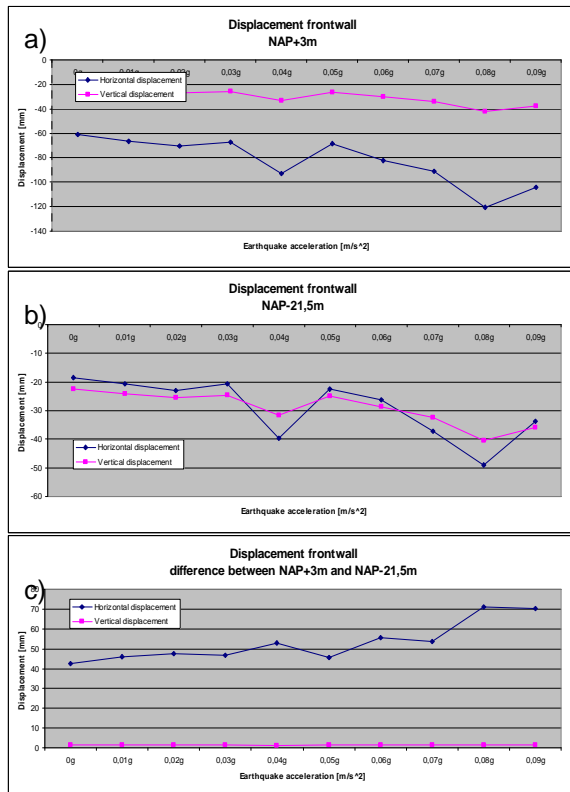

Figure 9-7 Caisson wall indication

Figure 9-8 Displacement front wall of caisson
  a) displacement at level NAP+3m
  b) displacement at level NAP-20,5m
  c) displacement difference

The results shows that an increase of earthquake acceleration (and therefore increase of earthquake magnitude) results into an increase of vertical (downward) and horizontal (seaward) displacement of the caisson. The horizontal displacements are higher at the top compared to the bottom of the caisson which will only increase when the earthquake acceleration becomes higher. This indicates the higher the earthquake acceleration the more the wall will bend/rotate towards the sea. The horizontal and vertical displacement due to this bending/rotation at the top of the caisson is around 70mm and 1mm respectively for an earthquake acceleration of 0,09g (see *Figure 9-8*c). This bending/rotation will not cause instability of the caisson and is therefore allowable.

The horizontal displacements at the bottom of the caisson front wall indicate that the caisson will slide towards the sea. However, the increase of sliding is just around the 25mm for an earthquake acceleration of 0,09g. This is not a large displacement for a caisson type retaining structure and is allowable.

From the result shown above, the caisson is stable for the analyzed earthquake acceleration (till 0,09g).

Displacement failure

TUDelft
Delft University of Technology

Earthquake analysis of quay walls
- Seismic Analysis-

Gemeentewerken
Gemeente Rotterdam

Crane tracks must satisfy strict tolerances which are set by the crane supplier and are given in section 3.3.6. Maximum allowable displacement deviations between seaside and landside crane railing normal to quay wall for a future contract depth of NAP -22m is 80 mm for both horizontally and vertically. The displacement of the crane railing during earthquakes are determined with Plaxis and given in Appendix P. The results of the Plaxis calculation are summarized in Figure 9-9. The graph indicates the horizontal (blue line) and vertical (pink line) displacement deviation of the seaside and landside crane railing. A polynomial trend line was applied to interpolate the results achieved from Plaxis. This was done because earthquakes which are applied in Plaxis are coming from different sources. These earthquakes have different frequency and durations and will have different impacts on the caisson quay wall.

The increase of displacement deviation in vertical direction is higher compared to displacement deviation in horizontal direction with increasing earthquake acceleration. This is mainly due to the settlement of the landside crane foundation and seaward movement of the caisson. Space will be available to mobilize the sand behind the caisson when the caisson moves horizontally toward the sea. This will result in settlement behind the caisson quay wall in which the crane foundation is located on. The vertical displacement deviation will reach the allowable displacements at an earthquake horizontal peak acceleration between $a_H=0,05g$ and $a_H=0,06g$ whilst the horizontal displacement of the crane foundations for the analyzed earthquake accelerations satisfied the tolerances.
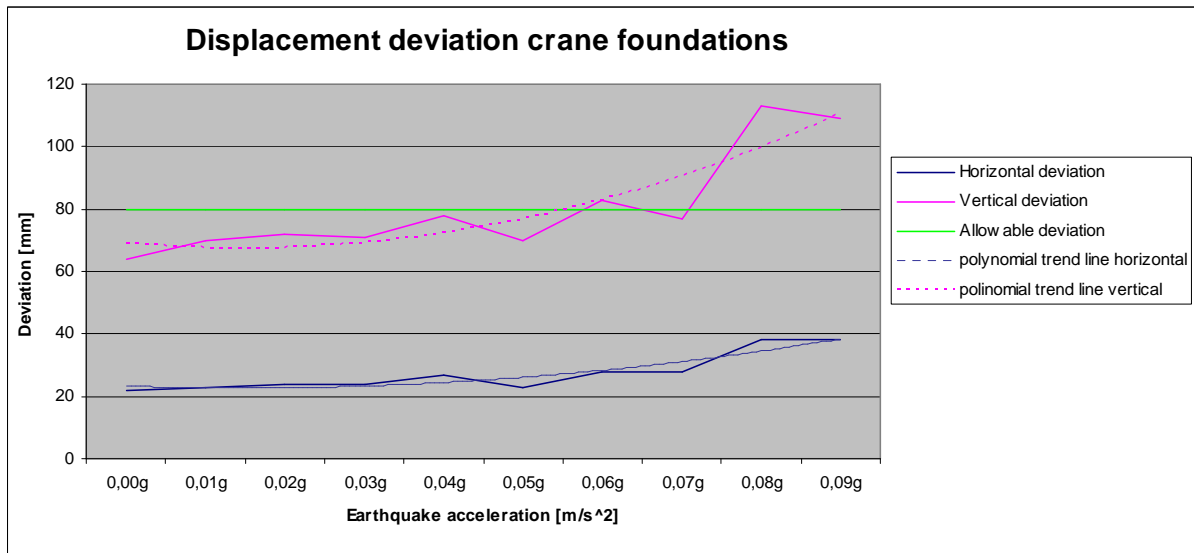

Figure 9-9 Horizontal and vertical displacement deviation of crane foundations during earthquakes, caisson quay wall

Caisson wall failure

The maximum bending moment capacity of the caisson walls must be larger than the bending moment caused by the earthquake to prevent failure of the walls. The bending capacity depends on the amount of reinforcement bars and axial stresses within the wall. Reinforcement bars are placed all over the wall. The amount of reinforcement depends on the occurring stresses within the wall with varies along the wall. However, in this Thesis the amount of reinforcement bars is only determined for the most normative cross-section of each wall and can be found in section 9.3.2. Therefore, the strength analysis of the walls are only limited to the normative cross-sections of the caisson walls.

The maximum bending moment within the walls are determined with Plaxis and the bending moment capacities of each wall have been determined based on the principles of strain compatibility and force equilibriumand. Calculation result of Plaxis and calculations in determining the bending moment capacities can be found in Appendix P.

Critical walls of the caisson are the front wall and wall number 3 (see Figure 9-7 for wall indication). This is due to the fact that the bending moment in these two walls are the largest. A summary of results for the two critical walls are shown in Table 8-11Table 9-7 for increasing earthquake accelerations till a=0,09g.

TUDelft
Delft University of Technology

Earthquake analysis of quay walls
- Seismic Analysis-

Gemeentewerken
Gemeente Rotterdam

Moment Capacity: Front Wall				Moment Capacity: Wall 3			
Earthquake acceleration [m/s²]	Max. axial force [kN/m]	M_{max} [kNm/m]	M_{cap} [kNm/m]	Earthquake acceleration [m/s²]	Max. axial force [kN/m]	M_{max} [kNm/m]	M_{cap} [kNm/m]
0,01g	-1900	-3420	-5211	0,01g	-975	-3040	-4318
0,02g	-1890	-3450	-5215	0,02g	-977	-3090	-4318
0,03g	-1900	-3440	-5211	0,03g	-975	-3060	-4318
0,04g	-1910	-3540	-5208	0,04g	-941	-3350	-4326
0,05g	-1880	-3430	-5219	0,05g	-980	-3010	-4317
0,06g	-1900	-3580	-5211	0,06g	-947	-3450	-4324
0,07g	-1890	-3610	-5215	0,07g	-944	-3310	-4325
0,08g	-1880	-3810	-5219	0,08g	-891	-4000	-4337
0,09g	-1870	-3840	-5222	0,09g	-920	-3900	-4330

Table
9-7 Moment capacity front wall and wall 3 of the caisson quay wall

All the walls of the caisson quay wall are able to resist the bending moment stresses during earthquakes. Therefore, failure of the caisson walls will not occur for earthquakes till a=0,09g.

9.4.3 Resonance

Just like the diaphragm wall, no extreme resonate rise is observed during the dynamic Plaxis calculation of the caisson quay wall. The fundamental frequency of the caisson structure is determined to confirm the Plaxis results.

A simplified spring model is used in determining the horizontal fundamental frequency of the caisson as shown in Figure 9-10. The caisson is places on top of the soil sitting on an elastic foundation. The influence of the weight of the soil and water behind in and front of the caisson is included in this calculation. By doing so, the upper limit of the fundamental frequency is determined (increase of m results in decrease of f_n).

In determining the fundamental frequency of the caisson quay wall a pseudo-elastic approach was used. In this approach, the fundamental frequencies of the horizontal mode for a block sitting on an elastic foundation is given by

$$f_{caisson} = \frac{1}{2\pi}\sqrt{\frac{k_{caisson}}{m}}$$

Eq. 9-1

Where

$f_{caisson}$ = horizontal fundamental frequency of caisson

$k_{caisson}$ = horizontal stiffness of the caisson foundation [kN/m]
m = Own weight of caisson over whole quay length [kg]

An estimate of $k_{caisson}$ has been provided by Zeng [10.6]

Figure 9-10 Schematized caisson on elastic foundation

$$k_{caisson} = \frac{GB}{2\cdot(1-\nu)}\left[6,8\left(\frac{L}{B}\right)^{0,65}+0,24\right] = 4,0\cdot10^7 \text{ kN/m}$$

Eq. 9-2

Where
B = width of caisson foundation = 27 m
L = quay length caisson =1900 m
ν = poisson ratio soil = 0,3
E = youngs modulus for linear elastic material = E_{50} = 50000 kPa

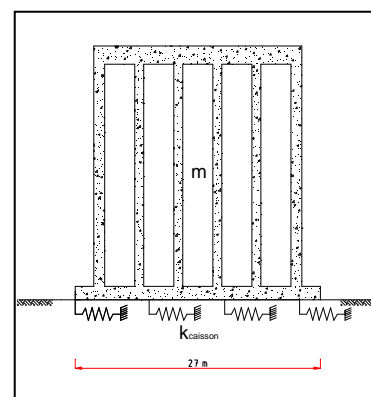G = shear modulus of soil = $\dfrac{E}{2\cdot(1+\nu)}$ = 19231 kPa

The own weigh of the caisson is already determined in Appendix M2 which is 951kg per running meter quay length. For the total quay length of 1900m, the weight becomes m = $1,8 \cdot 10^6$ kg. By applying m and $k_{caisson}$ into equation 9-1 the horizontal fundamental frequency of the caisson is determined, which is $f_{caisson} = 0,75$ hertz. The fundamental frequency of 0,75 hertz is just outside the range of extreme resonance which is between 2 to 10 hertz. However, an amplification between 1,0 and 2,0 still may be expected. The base is sufficiently rigid and no extreme resonant rise between the base and the caisson will occur.

9.4.4 Conclusions

Stability calculation was performed to determine the right dimension of the caisson quay wall. During this calculation two load combinations where used and the factor of safety concerning sliding and overturning where determined. The bearing capacity of the densified backfill soil is large enough to prevent settlements of the caisson and landside crane foundation. It was found that no specific load combination was normative concerning stability. However, according to static calculation using Plaxis, load combination 4 is normative concerning stresses within the caisson walls. Based on these stresses, reinforcement of the concrete walls has been determined.

A first impression of seismic behaviour of the caisson quay wall obtained making use of a pseudo static approach. Seismic earth pressure which is determined using the M-O method is much more suited for gravity type quay walls compared to sheet pile quay walls because sliding of a gravity quay wall will result in fully mobilization of the total ground behind the wall. The pseudo static calculations show that occurrence of excess pore water generation during earthquakes increases the total horizontal thrust acting behind the caisson. This will results in sliding of the caisson. Because sliding is the normative stability failure mechanism overturning will not occur.

Another dynamic analysis was performed using the finite element program called Plaxis. Excess pore pressure is not included during this dynamic calculation because excess pore pressure is not able to develop in very dense soil which is assumed to be the case in this Plaxis model. Instead of the excess pore water pressure a vertical acceleration component was added in this Plaxis model which is recommended by the Eurocode 8.

Three failure mechanisms are analyzed based on the results achieved from the dynamic Plaxis calculations: Stability of the caisson, displacement crane foundation and strength of the caisson walls. The results can be found in Table 9-8. Notion must be made that behaviour of the caisson subjected to earthquake accelerations higher than 0,09g where not analyzed and therefore unknown.

Failure mechanism	Critical earthquake acceleration
Stability of caisson	Caisson is stable for earthquakes acceleration between 0,00g till 0,09g
Displacement failure Crane railing	**The tolerated vertical displacement deviation of 80mm will be reached for an earthquake with horizontal peak acceleration between a_H=0,05g and a_H=0,06g**
Strength failure Caisson walls	Caisson walls are strong enough to resist the seismic forces caused by earthquakes with earthquake acceleration between 0,00g till 0,09g

Table 9-8 Critical earthquake accelerations for diaphragm quay wall determined using Plaxis

No extreme resonate rise occur and therefore the normative failure of the caisson quay wall is caused by displacement failure of the crane railing. This will occur around earthquake acceleration a=0,04g as shown in Table 9-8.

9.4.5 References

[10.1] IGWR, Studie ontwerpvarianten containerkade Euromax, 04-2002

[10.2] Eurocode 7

[10.3] NEN 672,Voorschriften beton – Constructieve eisen en rekenmethode (VBC 1995),09-1995

[10.4] Eurocode 8

[10.5] CUR 166, Damwandconstructies, 4^e druk, 2005

[10.6] Zeng X., Seismic response of gravity walls – Centrifuge modelling, Journal geotechnical engineering – ASCE, p406-427, 1998

TUDelft
Delft University of Technology

Earthquake analysis of quay walls
- Seismic Analysis-

Gemeentewerken
Gemeente Rotterdam

10. Conclusions & Recommendations

10.1 Introduction

Before the conclusions are discussed, the research questions made out of the presumed objective of this report will be answered and stated again.

In the past, earthquakes have caused several severe damages to port structures all over the world (Kobe port, 1995). For this reason, the Port of Rotterdam wants more insight in the consequences of earthquakes for the hydraulic structures in the port of Rotterdam. At now there are limited seismic researches and measurements available in the Netherlands in comparison with other countries. The researches and measurements that are available are particularly for the northern and south-eastern part of the Netherlands. At the Maasvlakte and therefore at the location of this master thesis there is no specific data available. By answering the main question the port authorities will achieve more insight in the state of the art and the results might support to map out the consequences of an earthquake to the Port of Rotterdam. The main question of this thesis was:

> *How do different types of quay wall structures at the Euromax terminal (maasvlakte) behave during high magnitude earthquakes?*

The sub-questions are formulated below:
a) What is the probability of occurrence of an earthquake at the Maasvlakte?
b) What are the effects of an earthquake to a quay wall in general?
c) Which earthquake magnitude will cause the current Euromax quay wall (diaphragm wall) to fail and what is the failure mechanism?
d) How will a gravity quay wall behave at the Euromax terminal to earthquakes?

The main objective of this master thesis is to gain insight in the behaviour and failure mechanisms of different types of quay wall structures near the Euromax Terminal during earthquakes.

Based on results of the above mentioned studies, a conclusion can be made which type of quay wall at the Euromax terminal is the least sensitive to earthquakes. An answer can be found whether it makes sense to include earthquake analysis into the designing of port structures for the Port of Rotterdam.

10.2 General conclusion

The seismic analysis to compare the seismic behaviour of different types of quay wall structures is elaborated by answering the sub-questions above separately.

> *a) What is the probability of occurrence of an earthquake at the Maasvlakte?*

Due to the limited amount of available research data (earthquake measurements), it is relative difficult to determine the probability of occurrence of an earthquake at the Maasvlakte. By making use of a seismic hazard analysis the peak ground acceleration, magnitude and return period have been determined for natural earthquakes. During this seismic hazard analysis the empirical methods of de Crook, Murphy and Reamer are used. A higher return period results in a lower probability of occurrence of the corresponding peak ground acceleration or magnitude. It was found that by increase of the peak ground acceleration the return period will increase exponential. The peak ground acceleration at the south-eastern part of the Netherlands, which is located at a seismic region, is a factor 4,55 higher than at the Euromax terminal and therefore the earthquakes have a much lower return period and a higher probability of occurrence. According to Dutch standards, a quay wall needs to withstand an earthquake with a return period of 475 years. This results in a peak ground acceleration of 0,022g m/s^2 at the Euromax terminal. The relations between the return period, the peak ground acceleration and the magnitude are shown in Figure 6-4 which assumes that the earthquake epicenter is located directly below the Euromax terminal.

Based on historical observations of tectonic earthquakes and the performed seismic hazard analysis, it can be concluded that there are nearly no seismic activities at the project location. Earthquakes that

TUDelft
Delft University of Technology

Earthquake analysis of quay walls
- Seismic Analysis-

Gemeentewerken
Gemeente Rotterdam

probably do occur will have low magnitude and are not likely to cause damage to the quay wall structures. A relative rough risk analysis is mad. The results of this analysis are not so accurate/reliable but it show that there is no need for taking earth quakes into account in the general design of quay wall in the Netherlands.

b) *What are the effects of an earthquake to a quay wall in general?*

To determine the effects of an earthquake on different types of quay walls, insight in the response of the soil due to an earthquake is needed. A tectonic earthquake occurs due to the movement of tectonic plates against each other causing seismic waves to travel. These waves are the energy that travels through the earth and is recorded on seismographs. There are several different kinds of seismic waves, and they all move in different ways. The two main types of waves are body waves and surface waves. Body waves can travel through the earth's inner layers, but surface waves can only move along the surface of the planet like ripples on water. Earthquakes radiate seismic energy as both body and surface waves. The soil, which is a load on one hand and on the other hand contributes to the stability of a quay wall, will be influenced by these seismic waves.

It appeared that one of the significant factors leading to ground failure during earthquakes is the generation of excess pore pressures which is the increase of pressures of groundwater held within a soil. The resistance to shearing strain or deformation is reduced by the increase of pore water pressure resulting in softening of the soil. In extreme cases where nearly all shear strength and shear stiffness is lost, the sand behaves like a liquid. This phenomenon is called liquefaction. An analysis regarding to liquefaction has been performed. It was found that liquefaction plays a crucial role near the Euromax quay wall. Especially the eastern side of the terminal (section 1) has a high susceptibility to liquefaction because the soil strata on this location consist of several loose sand layers. Triggering of liquefaction at this section occurs for an earthquake with a moment magnitude of $M_W = 6,2$. This corresponds with a horizontal peak ground acceleration of $a_H = 3$ m/s^2 and a return period of 751000 years when assuming the epicenter of the earthquake is located directly below the Euromax terminal.

Besides excess pore water generation, dynamic earth and water pressure are being developed during earthquakes which increases the horizontal thrust acting on the quay wall structure. Moreover, resonance might occur during an earthquake. When the quay wall structure is subjected to vibrations of its fundamental frequency, the displacements of that structure will be amplified by a factor between 3 and 4. Larger displacements results in larger stresses that are developed in the framing members and connections of the quay wall structure. It can be concluded that earthquakes cause an increase in horizontal force, cause a softening of the soil and might trigger the quay wall to resonate. These events are able to lead to large displacements, instability or insufficient strength of the quay wall structure.

The main failure mechanisms of different types of quay wall are determined and have been investigated. It appeared that typical failure mechanisms of a gravity quay wall caused by an earthquake are seaward displacement, settlement and tilting of the structure. While for the sheet pile wall this can be divided in displacement failure at anchor, displacement failure at sheet pile wall, failure at embedment and failure strength anchor/sheet pile.

c) *Which earthquake magnitude will cause the current Euromax quay wall (diaphragm wall) to fail and what is the failure mechanism?*

The quay wall structure located at the Euromax terminal is a diaphragm quay wall. This quay wall consists of a concrete front wall (retaining wall), MV-piles (tensions piles) and vibro piles (bearing piles). To relieve the front wall from horizontal forces, a relieving floor was constructed which directly transfers the load on top of the floor into the deeper soil layers by the bearing elements. For this type of quay wall the following failure mechanism have been analyzed:

1 *Failure of the diaphragm wall*: bending moment capacity derived from the dimensions of the diaphragm wall is insufficient to resist the maximum occurring bending moment. This will result in breaking of the front wall causing loss of retaining function.
2 *Failure of the MV-piles*: tensile capacity due to friction between pile and soil are insufficient causing the quay wall lean forward into the sea.
3 *Displacement failure*: the maximum allowable horizontal/vertical displacement deviation of the crane railing is exceeded causing the cranes not function properly.

TUDelft
Delft University of Technology

Earthquake analysis of quay walls
- Seismic Analysis-

Gemeentewerken
Gemeente Rotterdam

Static and dynamic analyses have been performed for the existing Euromax quay wall to determine the critical failure mechanism and the corresponding earthquake magnitude. In order to analyze the seismic behaviour of the diaphragm quay wall, a pseudo static approach and a finite element method (Plaxis) have been used. During the pseudo static approach, dynamic earth and water pressures have been determined using the Mononobe-Okabe method and the Westergaard's solution respectively. These two methods have become one of the most widely used procedures in the design of quay walls in seismic region by practical engineers. It was found that the effect of the seismic loading on a diaphragm wall could not really been performed with a pseudo static approach due to the fact that the seismic earth pressure could not be determined accurately. Another attempt was made using the subgrade reaction method called Msheet. Msheet which is a frequent used program in the Netherlands to design quay walls also appeared to be not suitable to model the seismic behaviour of a quay wall because it was not programmed to perform dynamic calculations. However, it was used to validate the more advanced finite element model.

With the finite element program called Plaxis, a more realistic and reliable seismic behaviour of the diaphragm quay wall is obtained. However, a limitation of the Plaxis program is that gradual softening of the soil during cyclic loading and excess pore generation behaviour due to cyclic loading is not incorporated. By reducing the angle of internal friction φ, excess pore water and soil softening has manually been simulated in Plaxis. Different real earthquake accelerograms measured in the USA are used as input in the Plaxis calculation. Therefore, the conclusions that are made with Plaxis are only valid for the in Plaxis introduced type of earthquake acceleration. Stresses and displacements of the diaphragm quay wall obtained from the Plaxis calculation have been checked whether or not they fulfill the strength and displacement requirements that are needed to make the quay wall functional. It appeared that the failure of the diaphragm wall is the critical failure mechanism. Failure occurs when an earthquake with horizontal peak acceleration between $a_H = 0{,}05g - 0{,}06g$ m/s^2 hit the diaphragm wall. According to the seismic hazard analysis performed for the Euromax terminal this earthquake acceleration corresponds with a local magnitude $M_L \approx 5{,}1$ with a return period of approximate 2500 years when assuming the epicenter of the earthquake is located directly below the Euromax terminal.

d) *How will a gravity quay wall behave at the Euromax terminal to earthquakes?*

During the case study of the project Euromax performed in 2002 by Rotterdam Public Works the option of constructing a caisson was also investigated. This early disapproved concept has been used in this thesis to gain insight of the seismic behaviour of gravity wall located at the Euromax terminal. The dimensions of the caisson quay wall were determined with static calculations according to the Dutch design codes. For the gravity type of quay wall the following failure mechanisms have been analyzed:

1. *Stability failure:* extensive sliding or overturning of the caisson quay wall causing the quay wall not operational.
2. *Displacement failure*: the maximum allowable horizontal/vertical displacement deviation of the crane railing is exceeded causing the cranes not function properly.
3. *Caisson wall failure*: bending moment capacity derived from the dimensions of the caisson wall is insufficient to resist the maximum occurring bending moment. This will result in breaking of the front wall causing loss of retaining function.

An impression of seismic behaviour of the caisson quay wall is obtained by a pseudo static approach. Seismic earth pressure which is determined using the Mononobe-Okabe method is much more suited for gravity type quay walls compared to sheet pile quay walls because sliding of a gravity quay wall will result in full mobilization of the total soil behind the wall which also is assumed in the Mononobe-Okabe method. Hence, the earth pressures are determined more accurately compared to the sheet pile quay wall. It was founded in the pseudo static analysis that the occurrence of excess pore water generation during earthquakes increases the total horizontal thrust acting behind the caisson. This will results in sliding of the caisson. Because sliding is the normative stability failure mechanism overturning will not occur.

Another dynamic analysis has been performed for the caisson quay wall using the finite element program Plaxis. Backfilled soil during the construction of the caisson quay wall is assumed to be compacted well enough that excess pore water pressure generation will not occur. Therefore, excess pore water pressure is not included during this dynamic calculation. Instead of the excess pore water

Earthquake analysis of quay walls
- Seismic Analysis-

Gemeentewerken
Gemeente Rotterdam

TUDelft
Delft University of Technology

pressure a vertical acceleration component was added in this Plaxis model which is recommended by the Eurocode 8. It appeared that the displacement failure of the crane foundations is the critical failure mechanism. Failure occurs when an earthquake with horizontal peak acceleration between a_H = 0,05g - 0,06g m/s^2 hit the caisson quay wall. According to the seismic hazard analysis performed for the Euromax terminal this earthquake acceleration corresponds with a local magnitude $M_L \approx 5,1$ with a return period of approximate 2500 years when assuming the epicenter of the earthquake is located directly below the Euromax terminal.

10.3 Main conclusion

Finally the main question in this master thesis can be answered.

How do different types of quay wall structures at the Euromax terminal (maasvlakte) behave during high magnitude earthquakes?

It appeared that the caisson and diaphragm quay wall have different failure mechanisms during a seismic event. Failure of the diaphragm wall due to insufficient bending capacity has appeared to be the most critical failure mechanism of the diaphragm quay wall. The most critical failure mechanism of the caisson quay wall is the vertical displacement failure of the landside crane railing. Nevertheless, both failure mechanisms occur at the same order of earthquake magnitude caused by natural earthquakes which is an earthquake with horizontal peak acceleration between a_H = 0,05g - 0,06g m/s^2 this corresponds with a return period of approximately 2500 years and a Rigther local magnitude of $M_L \approx 5,1$ which its epicentre is located directly below the Euromax terminal. This indicates that both quay walls have the same order of resistance against earthquake. However, the consequences of the diaphragm quay wall failure and probably also for the combined walls will be much higher compared to that of the caisson. Seismic failure of the diaphragm quay wall will always result in a total destruction of the quay wall while seismic failure of the caisson quay wall can be repaired. For this reason, the caisson quay wall is a better solution against earthquakes compared to the diaphragm wall.

10.4 Recommendations

Based on the findings from this report some recommendations can be given for future researches.

- During the seismic hazard analysis only natural earthquakes are investigated for the Euromax terminal. Research also needs to be performed for human induces earthquakes like explosions and other hazards causing the ground to shake.

- Cone penetration tests which are used in determining the liquefaction susceptibility of soil layers where taken before the Euromax quay wall was constructed. Changes in the soil near the Euromax terminal are expected due to the construction and the usage of the quay wall. New cone penetration tests for this area will give more accuracy of the soil strata. Hence, more accurate liquefaction susceptibility could be determined.

- In this thesis two types of quay walls have been analyzed during seismic loading. Seismic analyses should be performed for more types of different quay walls to determine which type could resists earthquake the best and is therefore is the most suitable in earthquake regions.

- Seismic behaviour of the quay wall is based on a single real measured accelerogram per earthquake acceleration. In order to get a more reliable behaviour of quay walls during an earthquake, different earthquake accelerograms with the same peak ground acceleration but another earthquake source is needed.

- It appeared that the duration of the horizontal peak acceleration influences the impact on a quay wall. Further investigation of this phenomenon is recommended due to the fact that this will directly influences the stability and stresses of the quay wall.

- The dynamic behaviour of quay wall could not be determined accurately due to the limitations of the finite element method Plaxis which does not incorporate the gradual softening of the soil during cyclic loading and excess pore generation behaviour due to cyclic loading. Improvements of finite element program Plaxis should be made by solving the limitations mentioned above.